THE Marquardt CORPORATION

15 JULY 1965

REPORT 6095

COPY NO. 12

(Title--Unclassified)

DESIGN STUDY AND EVALUATION OF A MULTIFUEL ENGINE FOR A SPACE POWER SYSTEM

Final Report for
Phase II, Modification II

UNCLASSIFIED

UNCLASSIFIED

(Title -- Unclassified)

DESIGN STUDY AND EVALUATION OF A MULTIFUEL ENGINE FOR A SPACE POWER SYSTEM

Contract NAS 9-857
Phase II, Modification II

Project 287

PREPARED BY

M. Arao

B. R. Chandler

APPROVED BY

E. K. Burnett
General Manager
Aerospace Equipment Department

CHECKED BY

J. R. Kessler
Manager, Secondary Power Projects

UNCLASSIFIED

THE Marquardt CORPORATION
VAN NUYS, CALIFORNIA

MAC A1158

CONTENTS

CONTENTS (Continued)

ILLUSTRATIONS

ILLUSTRATIONS (Continued)

ILLUSTRATIONS (Continued)

TABLES

I. SUMMARY

This report describes the accomplishments of a seven-week program which was conducted to demonstrate the feasibility, performance, and endurance of a modified hypergolic ignition engine (Marquardt Model SPU-2A-3) operating on gaseous hydrogen and oxygen. The work reported herein was accomplished under NASA Contract NAS 9-857, Phase II, Modification II between 19 April and 4 June 1965.

The basic engine was designed to cope with the thermal and mechanical stresses for operation with hypergolic propellants. This design provided adequate capability for the Marquardt test engine to satisfactorily operate on other rocket propellant combinations. Slight modifications to the injector system and addition of a starting ignition source were required for use with gaseous hydrogen and oxygen propellants.

The demonstrated "multifuel" capability provides new possibilities for the NASA Space Power Programs. The demonstration has formulated a family of space power engines, the commonality of which assures low cost qualification programs for future space power applications.

II. INTRODUCTION

A. Current Program

This feasibility program was conducted with a principal objective of obtaining the high efficiency achievable with the reciprocating piston engine. This program included use of propellants at stoichiometric O/F (oxygen to fuel) ratios up to 8:1 and high volumetric expansion ratios of from 23:1 to 38:1. In addition, the wide range of power delivery, including overspeed and overload, was demonstrated repeatedly without damage.

Only slight modifications to permit operation with gaseous oxygen and hydrogen were required as follows:

1. The injection timing was changed.

2. The diameters of the injector valve orifices were increased from 0.060 to 0.090 inch.

3. An ignition source (a glow plug) was installed in the combustion chamber.

The engine was set up initially to operate on the highest efficiency Otto or constant volume combustion cycle. Combustion roughness accompanied by high pressure "spikes" in excess of 9000 psi resulted and this mode of operation was abandoned in favor of the Diesel or constant pressure combustion cycle. Smoother combustion and a significant decrease in pressure spikes were noted with the Diesel cycle. However control of combustion anomalies was obtained by keeping the O/F ratios high or by maintaining the exhaust pressure above 5.5 psia.

Ignition by glow plug was determined by test to be more positive and allowed repeated starts in contrast to operation with the easily "poisoned" catalysts which first were tested. A standard model aircraft engine glow plug gave completely satisfactory performance. In the majority of the test runs, the current was turned off after a few minutes of operation and the engine continued to run without this ignition source.

Oil cooling of the piston was discontinued during the latter phases of the program. The basic piston of composite structure developed during the hypergolic engine program was retained. However, the piston ring detail and the placement of the piston rings on the piston was changed for operation without auxiliary oil cooling to the underside of the piston crown. The benefits from operating without oil flow to the piston were as follows: carbon clogging of the injectors was eliminated, the oil consumption was lowered, and the heat losses were reduced.

Lubrication of injector valves with propellant compatible duPont PR143 oil resulted in high reliability. Except for periods of violent pressure spike (detonation) operation, injector valve wear was practically nonexistent.

The remainder of the engine was pressure and splash lubricated with a compounded mineral oil (Brayco No. 443). No wear of consequence was noted on any part although engine speeds to 6500 rpm were attained on several occasions.

Engine speed, power, and O/F variations were easily made by control of propellant injection pressures. The injection pressures ranged from 300 to 600 psi for H_2 and 450 to 1280 psi for O_2 corresponding to a speed range of 600 to 6800 rpm and a power range of 0.5 to 3.86 HP.

A specific propellant consumption of 2.44 lbs/HP-hr was obtained with an O/F ratio of 4.6 and an engine output of 3.86 HP at 5200 rpm. This consumption was attained with H_2 injector timing of 22.5° BTC to 10° ATC and O_2 injector timing of 20° to 35° ATC. A total of 191 minutes of engine operation was accumulated with a continuous run of 43.3 minutes.

The results of a study made to compare the performances of candidate H_2-O_2 power systems for extended missions in space are summarized in Appendix A.

B. Background

The Marquardt Independent Research Program for the development of a bipropellant internal combustion reciprocating engine for use in space power systems has been in effect since 1957. Until November 1962, these activities were supported entirely by The Marquardt Corporation. At this time, a formal contract was negotiated with NASA to conduct a feasibility study for development of a reciprocating engine for use in space power systems. A chronological summary of the space power unit activities to date follows:

An analytical program for investigation of an optimum prime mover using high energy rocket propellants was initiated by Marquardt in 1957. The internal combustion reciprocating engine was selected on the basis of offering the highest efficiency and lowest development costs for the effective power range.

The feasibility of the bipropellant reciprocating engine was demonstrated in 1958 using a modified, single cylinder, American Marc Diesel engine rated at 6 HP. The propellant combination of RFNA oxidizer and UDMH fuel was used. These demonstration tests supplied the following information:

1. The results of the analytical program were verified by demonstration of an engine developing useful power.

2. The influence of operating criteria on engine efficiency, injector timing, injector dwell, O/F ratios, and BMEP was determined.

3. The limitations of structural materials, processes, and mineral lubricants operating with the selected propellants were determined.

Engine operation at high speed (to 6000 rpm) with bipropellants was investigated in 1960. A Dooling 0.61 cu in. model racing engine was modified with an electronic injection system utilizing a high frequency response electromagnetic shaker actuating a pair of slide valves. Tests of this engine were not made to verify the feasibility of the high speed engine. However, the technology of the high speed injector valve system was applied to the Marquardt pulse rocket program.

A McCulloch chain saw engine was modified in 1961 with two mechanically actuated injector valves for operation with gasous hydrogen and oxygen. The mode of operation selected was the Otto cycle with both propellants admitted simultaneously. Conclusions derived from this program were as follows:

1. A spark plug ignition system is prone to early fouling due to condensation and cooling of propellants.

2. A widely adjustable injector valve timing system is required to investigate optimum operating conditions.

A hypergolic ignition engine based on a BMW motorcycle engine was fabricated and tested in 1962. This engine (designated SPU-1) utilized propellant compatible materials except for the crankshaft and connecting rods. A Bosch injection system was duplicated in stainless steel and an exhaust poppet valve was located in the cylinder head. The purpose of this effort was to determine problems associated with use of propellant compatible materials and also to critically examine the parameters affecting engine performance in order that the feasibility engine planned for the NASA contract program would benefit from these technological advantages.

In November 1962, work was begun under a NASA contract for a program to prove the feasibility of a hypergolic bipropellant engine. An engine (designated SPU-2) was built which incorporated all advancements including propellant compatibility where necessary and a short dwell, high speed injection system that would permit operation within the Otto cycle mode at engine speeds in excess of 6000 rpm. The displacement of the engine was 2 cu in. and the nominal rating was 4.5 HP at 4500 rpm.

In 1963, the NASA SPU-2 engine was redesigned to improve the propellant injector valve and the piston was altered to permit increased endurance and performance.

A feasibility demonstration was successfully conducted in 1964 with the hypergolic engine. The resulting specific propellant consumption was 6.4 lbs/HP-hr and the endurance was 6 hours and 40 minutes.

The NASA engine was redesigned in 1965 for minimum lubrication requirement by use of ball and roller bearings in critical areas. In addition, the engine was fabricated with materials which were completely compatible with the propellants. Two engines plus spares were made. These engines were designated as the SPU-3 and SPU-3-1 engines.

The NASA contract SPU-2A-1 engine was modified (and redesignated as the SPU-2A-3 engine) during the period April to June 1965 to demonstrate its multifuel capability using gaseous hydrogen and oxygen as propellants. This report presents the accomplishments of this program.

III. DESCRIPTION OF MULTIFUEL ENGINE

A. General Description

The engine used for operation with gaseous hydrogen and oxygen is a modified SPU-2A-1 engine identified as the SPU-2A-3 test engine. The external configuration of the SPU-2A-3 engine (See Figure 1) is identical to that of the SPU-2A-1 hypergolic ignition engine. The basic specifications for the SPU-2A-3 multifuel engine are summarized in Table I.

TABLE I

BASIC SPECIFICATIONS FOR THE SPU-2A-3 MULTIFUEL ENGINE

Type:	Water cooled, single cylinder, reciprocating engine
Operating cycle:	2-stroke cycle
Propellant admission:	1 Fuel injector valve 1 Oxidizer injector valve
Exhaust:	Piston controlled cylinder port
Ignition:	Electrically heated glow plug
Displacement:	2.43 cu in.
Bore and stroke:	1.38 by 1.625 ins.
Expansion ratio:	23 to 1
Envelope:	14 by 17 by 10 ins.
Weight:	30 lbs
Rated power:	4.5 HP at 4500 rpm
Maximum allowable power:	6.0 HP at 6000 rpm
Lubrication:	Pressure with dry sump

Most of the components of this engine are fabricated from corrosion resistant materials. The remaining engine components are fabricated from suitable materials consistent with high quality automotive engineering practice. Where applicable, well established, high efficiency, reciprocating engine design features within the present state of the art were used in formulating the design. The specific goals sought for establishment of the design were as follows:

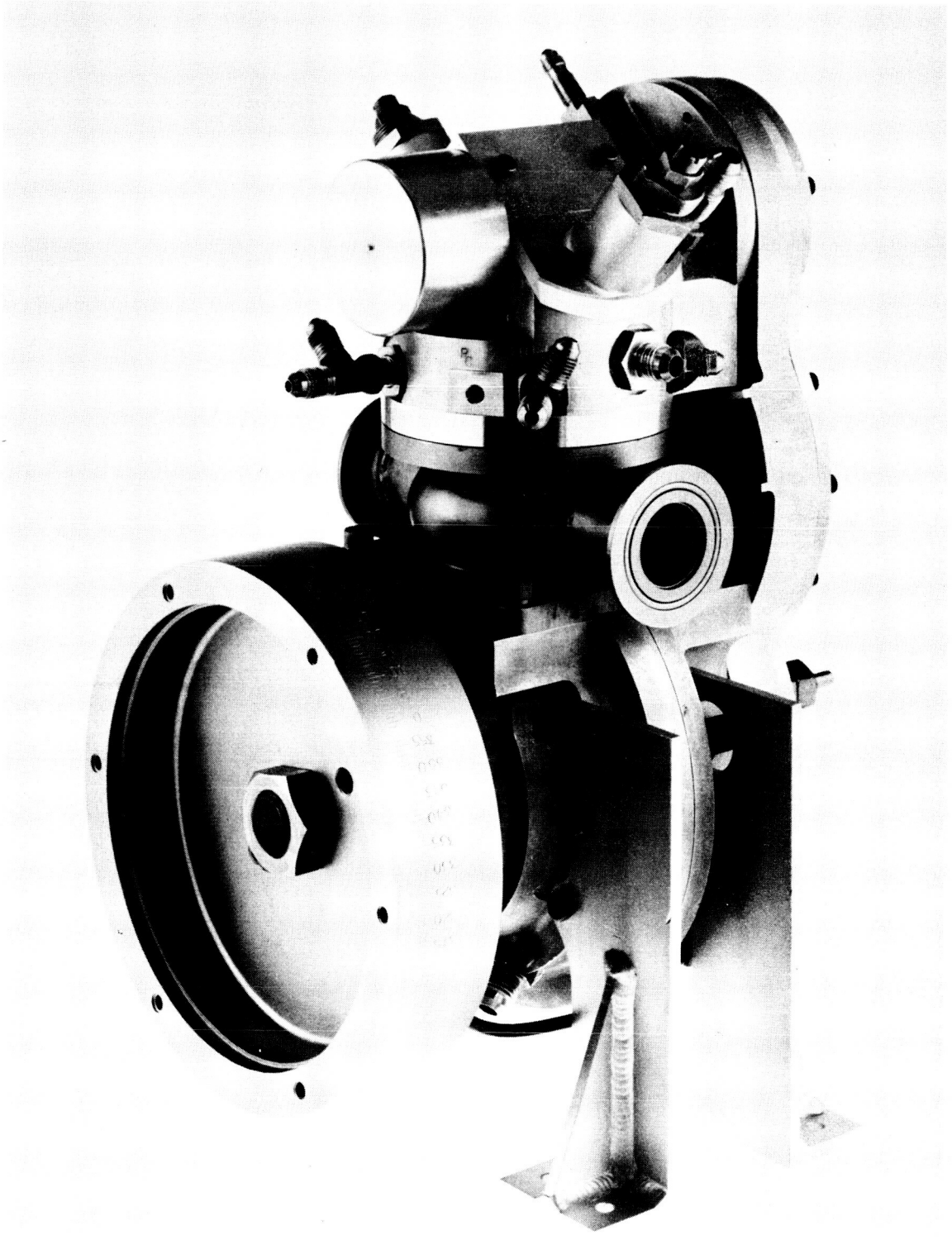

FIGURE 1. View of the SPU-2A-3 Space Power Unit

T5134-20

1. Minimum fabrication of new components

2. Completely adjustable propellant injection periods and timing

3. High overall engine efficiency, i.e., low specific propellant consumption

4. High engine and component reliability

Since the primary engine design target was to obtain design information and parametric test data for the hydrogen and oxygen fueled, reciprocating space power generating system, certain subsidiary components considered secondary in importance and contributing to added cost and delay to the program were not included. These components include an oil pump, the propellant pumps, a water circulation pump, and the starting system. These functions were provided to the engine from the test facility and external control and instrumentation were utilized for control and data recording.

B. Propellant Injection System

A modification of the unique dual poppet, mono seat, short duration valve concept which was developed during the Phase I and Phase II programs for development of the hypergolic ignition reciprocating engine was used in the gaseous hydrogen and oxygen engine. The valve modification consisted of altering the seat design of the inner and outer valve components. These valves normally had conical seats. This design was changed to a flat faced valve configuration for oxygen and hydrogen operation. This modification produced a higher gain characteristic of the valve which allowed more hydrogen and oxygen to enter the engine for a given pressure difference. In addition, this configuration eliminated the concentricity problems associated with conical seats and eliminated the need for extremely tight valve body clearances. The valves were previously fitted to clearances of 40 to 70 millionths of an inch to minimize valve leakage. These clearances were increased to 100 millionths of an inch. In addition to the change in the configuration of the valve seats, provisions were made to lubricate the valve components continuously during engine operation. The inertness of the duPont PR 143 oil made lubrication of these components feasible during operation. Valve lubrication is achieved by using the overboard drain ports previously required in the hypergolic ignition engine to supply pressurized lubricants directly to the valve stems. Direct lubrication of the valve stems in conjunction with additional teflon seal rings around the stems provided zero leakage of the gaseous oxygen and hydrogen into the valve chamber and significantly improved the durability of the valve.

The SPU-2A-3 engine utlizes the camshaft configuration design of the SPU-3 hypergolic ignition engine. This configuration features individual valve cams indexed with keys to a common shaft. The configuration allows each propellant injector to be timed independently with respect to dwell and start of injection. The fully adjustable camshaft assembly is shown in Figure 2. The durability and the relative simplicity of achieving timing changes were amply demonstrated during the testing of the engine.

C. Piston and Piston Rings

The piston design and ring configuration used in the SPU-2A-3 engine during the major portions of the engine testing is shown in Figure 3. This design consists of an N155 alloy crown and a D132 cast aluminum skirt section. The top ring assembly is carried in a groove machined in the crown material. Two additional ring assemblies are carried in the aluminum skirt at and slightly below the skirt crown interface. The ring assemblies themselves are of unique design, being composed of a three-piece interlocking configuration having two outer rings and a backup inner ring. This configuration offers the following major advantages:

1. Positive end gap sealing
2. Low leakage at high pressures
3. Low wall tension
4. Positive constraint of ring ends (cannot spring into exhaust ports, thus reducing possibility of breakage)
5. Elimination of ring pins
6. Improved mechanical strength.

The lower two ring assemblies have an L-shaped cross section. The top ring has a conventional rectangular cross section. All rings were fabricated from cast iron. Further discussion of the piston assembly is presented in Section V-B of this report.

D. Lubrication

The crankcase and crankshaft assembly of the SPU-2A-3 engine is designed for maximum strength and durability commensurate with a test engine configuration. The single throw crankshaft is supported in two sleeve bearings machined in the aluminum crankcase section. The connecting rod also utilizes a sleeve bearing. Oil is fed to the main bearings, to the rod bearing, and to the piston pin bearing under pressure by the facility oil pump. The cylinder

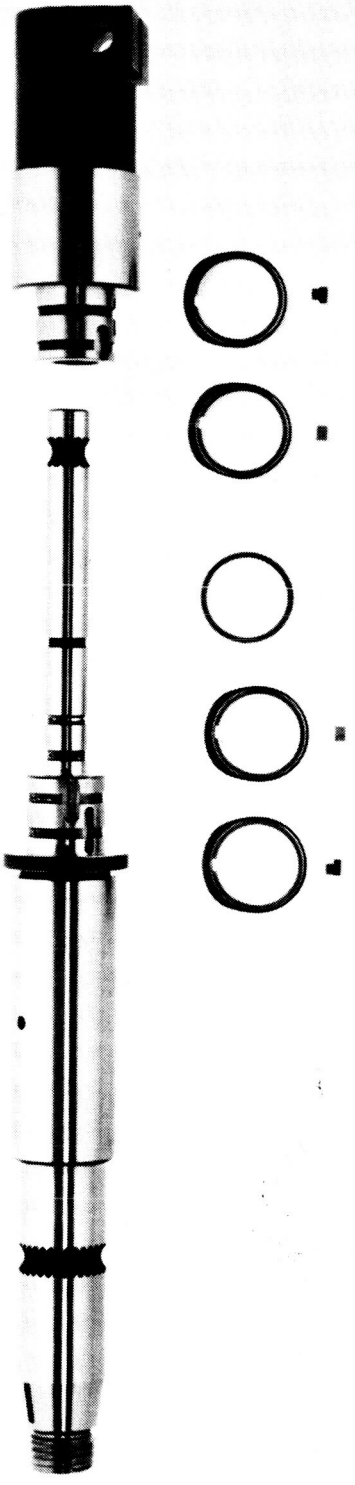

T5134-18

FIGURE 2. Fully Adjustable Camshaft Assembly for the SPU-2A-3 Engine

T5149-11

FIGURE 3. Piston and Piston Rings after 17 Minutes of Operation in the SPU-2A-3 Engine

and piston assembly are lubricated by splash oil from the connecting rod and piston pin bearing. The camshaft and rocker arm assemblies located in the cylinder head are also lubricated by pressurized oil from the facility pump. The lubricant used for all engine testing to date has been Brayco No. 443 medium (SAE 30) lubricating oil.

E. Ignition

Three types of engine ignition were investigated during the course of the test program. These ignition sources are categorized as follows:

1. Ignition by catalytic action

2. Glow plug ignition

3. Compression ignition

The ignition method which finally was chosen was glow plug starting and warm up and semi-compression ignition operation. A "VECO" (Henry Engineering Co., Burbank, Calif.) model airplane glow plug unit was fitted in the cylinder head adjacent to the hydrogen valve port. The plug was energized electrically during startup and it was de-energized when stable operating conditions were achieved. The engine then operated on a semi-compression ignition condition. This condition is assumed, since it is probable that the glow plug remained hot as a result of the heat of combustion and that it would assist with the initiation of combustion under most operating conditions.

IV. ENGINE TEST PROGRAM

A. Test Program Philosophy

Tests were conducted with the SPU-2A-3 engine to verify the concept feasibility, performance, and endurance of this engine. The tests were divided into three sections as follows:

1. Cylinder head component development tests - cold
2. Cylinder head component development tests - hot (burning propellants)
3. Engine operation development tests

The cylinder head cold tests were conducted to determine the injector valve calibration (pressure differential versus flow at various rpm and dwell conditions) and the suitability of the material under a normal propellant environment. This procedure afforded evaluation of the valve assembly without jeopardizing other engine components.

The cylinder head hot tests were conducted to establish the ignition characteristics at high differential pressures.

The engine development tests established the performance characteristics of the engine. Primary emphasis was placed on determining the specific propellant consumption (SPC).

B. Engine Tests

Full scale engine testing began on 7 May 1965 and continued intermittently until 4 June 1965. During this period, the basic operating cycle of the engine was changed from the Otto cycle to a dual cycle. The dual cycle can be defined as a partial constant volume and partial constant pressure (Diesel) cycle. This mode of operation was selected in order to suppress violent detonation and achieve reasonable performance with assured component reliability. As the testing progressed, it became apparent that this precaution was probably unnecessary but the depletion of funding precluded proving this contention.

A total of 3.19 hours of engine operation was accumulated during the test period. These tests are summarized in Table II.

1. Otto Cycle Operation and Test Results

The Otto internal combustion engine cycle was initially chosen for the hydrogen-oxygen engine. This mode of operation was successfully proved with the hypergolic propellant engine. Performance calculations for the

TABLE II

RUN SUMMARY FOR H_2O_2 ENGINE TESTS

Test No.	Test Date (1965)	Injector Timing (degrees) O_2	Injector Timing (degrees) H_2	Injection Pressures (psi) O_2	Injection Pressures (psi) H_2	Expansion Ratio	SPC (lb/HP-hr)	BMEP (psi)	O/F	HP	Speed (rpm)	Exhaust Temp. (°F)	Exhaust Back Pressure (psia)	Run Length Hot	Run Length Cold	Reason for Run Termination	Comments
5149-10 Run No. 1	3 June	20° ATC-35° ATC	22.5° BTC-10° ATC	980	440	23:1	3.96	95	4.2	1.92	4000	1550	7.6	21 min 25 sec	--	Scheduled shutdown	Performance demonstration test. Glow plug leaking at seal. All components OK.
5149-10 Run No. 2*	3 June	20° ATC-35° ATC	22.5° BTC - 10° ATC	1000	480	23:1	3.29	178	4.5	2.52	2790	1430	5.6	29 min 5 sec	--	Scheduled shutdown	Performance documentation test. Investigation of exhaust back pressure effects. All components OK. Glow plug leaking at seal.
5149-11 Run No. 3	4 June	20° ATC - 35° ATC	22.5° BTC - 10° ATC	870	520	23:1	3.11	105	3.6	2.36	4450	1460	10.8	37 min 25 sec	--	Scheduled shutdown	Performance documentation test. Modified glow plugs to achieve satisfactory seat seal. All components OK.
5149-11 Run No. 4	4 June	20° ATC-35° ATC	22.5° BTC - 10° ATC	870	480	23:1	--	--	--	--	--	2300	9.5	3 min 20 sec	--	T_{ex} over-temperature indicated	High P_{ex} & lean O/F at start caused excessive exhaust temperature resulting in glow plug failure. All components OK. Changed plug.
5149-11 Run No. 5	4 June	20° ATC-35° ATC	22.5° BTC - 10° ATC	450	450	23:1	--	--	--	--	--	--	9.0	3 min	--	Rotation reversal	Engine rotation reversal experienced while making an O/F change at low speed. All components OK. Rotation reversal caused O_2 to inject first, failing glow plug.
5149-11 Run No. 7	4 June	20° ATC - 35° ATC	22.5° BTC-10° ATC	900	450	23:1	--	--	--	--	--	--	9.0	2 min	--	Loss of combustion	Engine ignition loss during low speed O/F change. Too lean.
5149-11 Run No. 8	4 June	20° ATC-35° ATC	22.5° BTC-10° ATC	1280	480	23:1	2.44	144	4.6	3.86	5150	1180	1.4	43 min 22 sec	--	Scheduled shutdown	Performance documentation test at high rpm (6600) & low P_{ex} (0.6 psia), investigation of detonation combustion operation. Very severe operating conditions caused partial failure of top piston ring. All other components OK.

* Oil cooling to piston discontinued.

TABLE II (Continued)

Test No.	Test Date (1965)	Injector Timing (degrees) O_2	Injector Timing (degrees) H_2	Injection Pressures (psi) O_2	Injection Pressures (psi) H_2	Expansion Ratio	SPC (lb/HP-hr)	BMEP (psi)	O/F	HP	Speed (rpm)	Exhaust Temp. (°F)	Exhaust Back Pressure (psia)	Run Length Hot	Run Length Cold	Reason for Run Termination	Comments
5149-6 Run No. 8	7 May	1°-20° ATC	44° BTC -2° ATC	1050	600	36:1	--	--	6.0	3.0	1400 - 5500	1400	5.0	7	6.6	Piston failure	Sensitive to O_2 injection pressures. Smooth running obtained only at high O_2 pressures of 1050 psi. Difficult to control engine to specific conditions of speed and power. Chamber pressure spikes to 5,000 psi.
5149-7 Run No. 3	19 May	5° BTC - 5° ATC	55°-16.5° BTC	2300	450	36:1	--	--	--	--	--	--	--		14.3	Piston ring failure	Engine would not start. Intermittent ignition obtained with chamber pressure spikes to 9,000 psi. Violent spikes finally destroyed piston rings. Upon disassembly, following revisions made: Glow plug transfer port enlarged 200%, starting speed increased from 600 rpm to 700 rpm, O_2 valve housing leak repaired (Note: Valve itself O.K.).
5149-8 Run No. 5	24 May	30°-46° ATC	20° BTC-29° ATC	1275	375	23:1	3.68	134	5.07	2.14	3150	370	3	17.25	24	Scheduled shutdown	Ignition not obtained until glow plug energized with three times normal voltage. Engine ran smoothly and with good control. Engine would not continue running with glow plug de-energized. Piston was cooled with jet of oil. Disassembly disclosed good condition of all parts except O_2 valve housing leakage again. O_2 valve itself in good condition.
5149-9 Run No. 3	28 May	20°-ATC -35° ATC	21° BTC-11.5° ATC	1200	500	23:1	4.04	119	5.7	1.92	3200	1350	6	10 min	11 min	Scheduled shutdown for inspection and change timing	Run satisfactory except combustion roughness noted, appeared to be preignition. Shut down to check for O_2 leak and reset timing.
5149-9 Run No. 4	28 May	10°-25° ATC	31° BTC - 1.5° ATC	1020	340	23:1	4.2	154	18.0	1.64	2100	570	5.3	16 min 17 sec	19 min 22 sec	Scheduled shutdown to change timing and inspect engine	High O_2 flows indicated. Found inner O_2 valve to be leaking allowing long dwell ignition. Lube oil noted in GH_2 valve and on face of O_2 valve. Face of inner valve slightly oxidized possibly from oil/O_2 reaction

hydrogen-oxygen engine indicated that the Otto cycle was superior to other engine cycles because it affords the following advantages:

1. Minimum specific propellant consumption
2. High specific power
3. High thermal efficiency
4. High expansion ratio capability
5. Minimum surface area exposed to combustion
6. Minimum heat rejection

Since the propellant consumption of an engine varies inversely with the thermal efficiency of the engine cycle and since the ideal thermal efficiency of an Otto cycle is a function only of the expansion ratio, the hydrogen-oxygen engine was fabricated with an expansion ratio of 36 to 1. This ratio had been used for the hypergolic propellant engine and the crankshaft assembly and other components had been stressed for the resulting high pressures. Additionally, the small surface area of the combustion chamber for a 36 to 1 expansion ratio was desirable to minimize heat rejection.

Two major problem areas were encountered, namely, combustion efficiency and improper mixing. The time required for the hydrogen and oxygen mixtures to react when mixed and ignited was also a cause for concern. The rate of pressure rise during combustion is quite important in an internal combustion Otto cycle engine. If it is too slow, as might be experienced with the stratification of propellants, the efficiency of the conversion of heat into useful work would be impaired. If the pressure rise is too rapid, shock and rough operation will occur. Therefore, the method of admitting the propellants into the cylinder and the timing of the admission is very critical.

Unlike the normal reciprocating engine in which a fuel and air mixture is inducted into the cylinder or a Diesel engine in which air is inducted and the fuel is injected to obtain combustion, the SPU-2A-3 hydrogen-oxygen engine injects the fuel during the compression stroke and the oxygen is injected at approximately top center. Combustion starts with oxygen injection. The duration (dwell) of the oxygen injection and the injection pressure control the chamber pressure and the duration of combustion.

For the initial engine tests, the injector valves were timed as follows:

GH_2		GO_2	
Start	44° BTDC	Start	1° ATC
End	2° ATC	Stop	20° ATC
Dwell	46°	Dwell	19°
	Overlap 1°		

Since the reaction rate and the ignition delay characteristics for the propellants were not firmly established for the SPU-2A-3 engine, the timing of the oxygen valve was set to start after top center to insure rotation in the proper direction.

The original oil system was modified to provide a jet of oil to the underside of the piston for cooling. The oil was transferred through the connecting rod and ejected from an orifice in the top of the rod to the underside of the piston.

Following initial starting difficulties, engine operation was achieved for a period of 7 minutes during the first test. The starting problems were primarily a result of insufficient heating of the glow plug igniter. This particular problem of hard starting continued throughout most of the test program until sufficient experience was obtained and enough data had been accumulated to define the problem. The model airplane engine glow plugs used for the ignition system normally are limited to 1.5 to 2.0 volts. Under normal conditions, the glow elements will burn out if the 2.0 volt limit is exceeded. However, the conditions within the SPU-2A-3 engine were not normal because the cooling action of the hydrogen caused a "quenching" of the glow plug element and voltages as high as 6.0 volts were required to achieve ignition. This problem and its solution are discussed fully in Section V-A of this report.

The initial engine test run indicated a sensitivity to oxygen injection pressure and dynamometer loading. The engine operated unstably at approximately 2000 rpm with a partial load and would rapidly accelerate to 5500 rpm if any increase was made in the oxygen injection pressure or if the dynamometer load was decreased. The proper combinations of O/F ratio, propellant flow rates, and load were not achieved prior to a piston failure, which terminated further operation. During the engine test run, rough combustion with greater than 5000 psi pressure spikes was indicated on the oscilloscope indicating chamber pressure with ignition occurring at 22° $\pm$ 10° ATC. Although the

engine did not operate as expected, the indicated performance of over 3.0 HP at 5500 rpm was indicative of the capabilities of the engine.

For the second series of tests, the injector valve timing was adjusted as follows:

GH_2		GO_2	
Start	55° BTC	Start	5° BTC
End	16.5° BTC	End	4.8° ATC
Dwell	38.2°	Dwell	9.8°
		Null period	11.5°

These timing values were selected on the basis of flow rates and indicated ignition delay during the previous engine test.

Self-sustaining engine operation was not achieved during the second test series, although exhaust temperatures as high as 600°F were recorded. A typical photograph of a cylinder pressure versus crank angle diagram is shown in Figure 4. Unfortunately, randomly occurring detonations were experienced but they could not be successfully photographed. These detonations were audible over the facility intercom system. Peak pressures were recorded on the instrumentation provided for this specific parameter and values in excess of 9000 psi were indicated. Further testing of the engine in the Otto cycle mode was suspended following an inspection of the engine because the violent detonations had shattered all three piston ring assemblies. No other damage was sustained by the engine.

The piston ring assemblies were replaced and the engine was set up for dual cycle operation.

2. Dual Cycle Operation and Test Results

Because the reasons for the erratic operation and the violent detonation experienced with Otto cycle operation were not clearly understood or completely documented, dual cycle operation was initiated. As previously stated, the dual cycle is a partial constant volume and partial constant pressure cycle. Initially the constant pressure, or Diesel cycle, was stressed to assure engine operation with maximum reliability. The injector valves were timed so as to achieve ignition later than 30° ATC. It was calculated that the pressure rise characteristics under this mode of operation would partially match the increasing cylinder volume and thus they would approach constant pressure conditions.

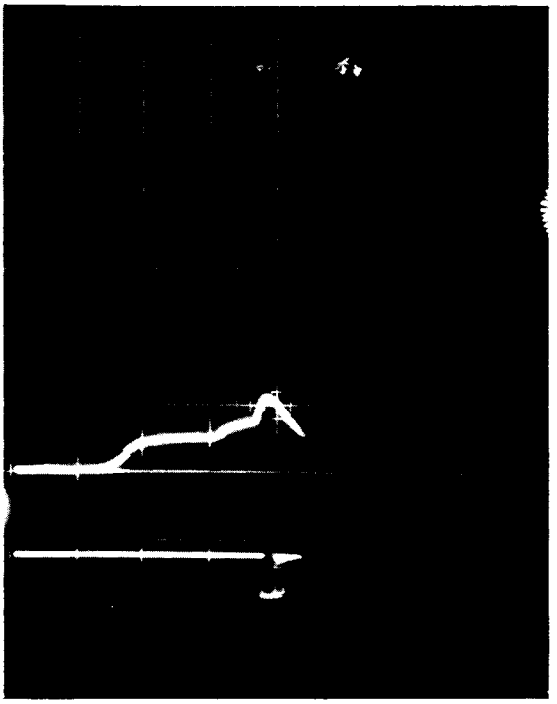

rpm = [illegible]

P_{f_i} = 300 psi

P_{o_i} = 800 psi

P_{ex} = 4.5 psia

O/F = 2.5

FIGURE 4. Typical Otto Cycle, SPU-2A-3 Engine, Cylinder Pressure vs. Crank Angle Diagram, Test 5149-7, Run No. 3

This procedure proved successful. Engine operation for 17.25 minutes was achieved during the first test run. No problems with controllability were experienced. However, the propellant flow rates were higher than anticipated and they exceeded the limits of the instrumentation provided for these parameters. During subsequent testing, the range of the propellant flow meters proved to be the limiting factor for engine power output.

This range limitation was not critical, but it did prevent documentation at engine design rated power conditions (i.e., 4.5 HP at 4500 rpm).

A total of 3.0 hours of engine testing was achieved during the dual cycle test program. During this period, various injector valve timing adjustments were made and engine performance was documented. The injector valve settings which were evaluated are summarized in Figure 5. In general, the performance of the engine improved and its specific propellant consumption decreased as the timing of the oxygen injector valve was moved toward top center (i.e., Otto cycle operation).

Two factors tended to obscure this trend during the early dual cycle tests: the engine was sensitive to exhaust back pressure (i.e., the lower the pressure the more likelihood of detonation) and the lower seal of the oxygen injector housing was inadequate. The effect of the inadequate seal was to allow some oxygen to enter the cylinder during the compression stroke and cause preignition when hydrogen injection started. This effect can be clearly observed in the cylinder pressure versus crank angle photographs for Test 5149-8, Run No. 5, Data Points Nos. 2 and 3 and also for Test 5149-9, Run No. 3, Data Point No. 3. These photographs are presented in Appendix B as part of the complete data point summary presentation for all of the dual cycle engine tests.

Because detonation and rough engine operation were experienced at all injector timing conditions, a decision was made to fix the timing at one setting and evaluate the effects of exhaust pressure, glow plug voltages, and O/F ratios on these conditions. The valve timing selected was as follows:

GH_2	GO_2
Start 22.5° BTC	Start 20° ATC
Stop 10° ATC	Stop 35° ATC
Dwell 32.5°	Dwell 15°
Null Period 10°	

A schematic diagram of the engine cycle with the above injection timing is shown in Figure 6.

SPU-2A-3 INJECTOR TIMING SUMMARY
DUAL CYCLE OPERATION

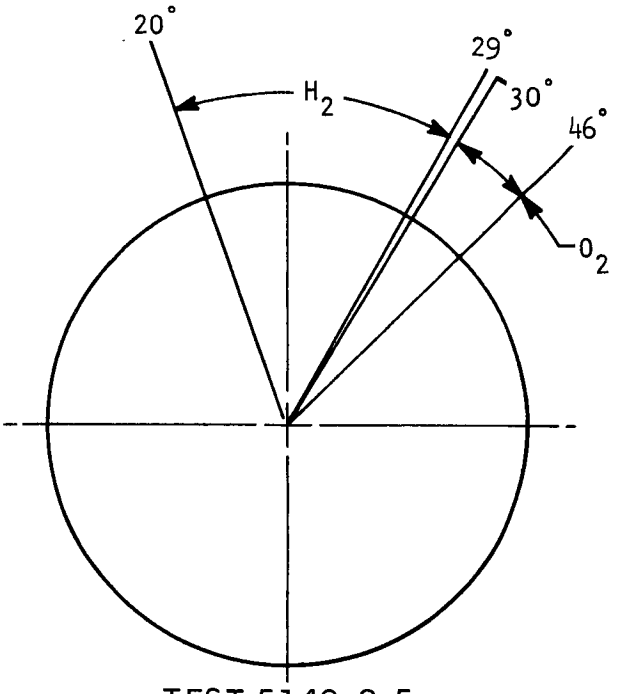

TEST 5149-8-5

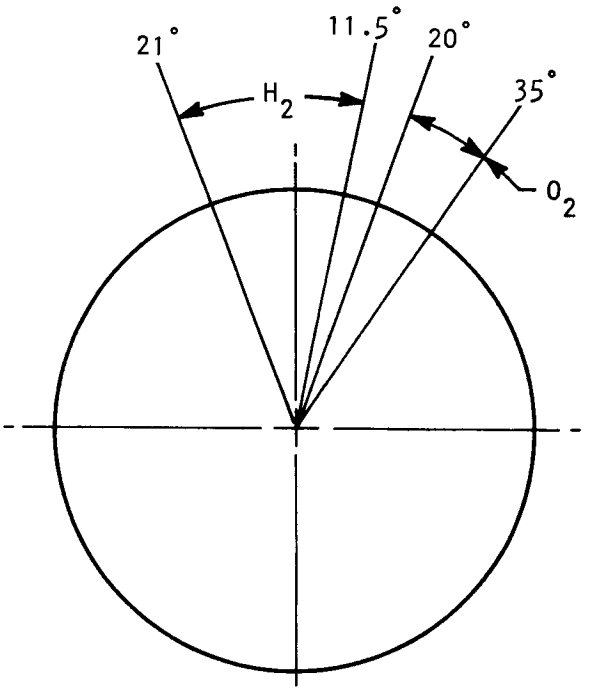

TEST 5149-9-3

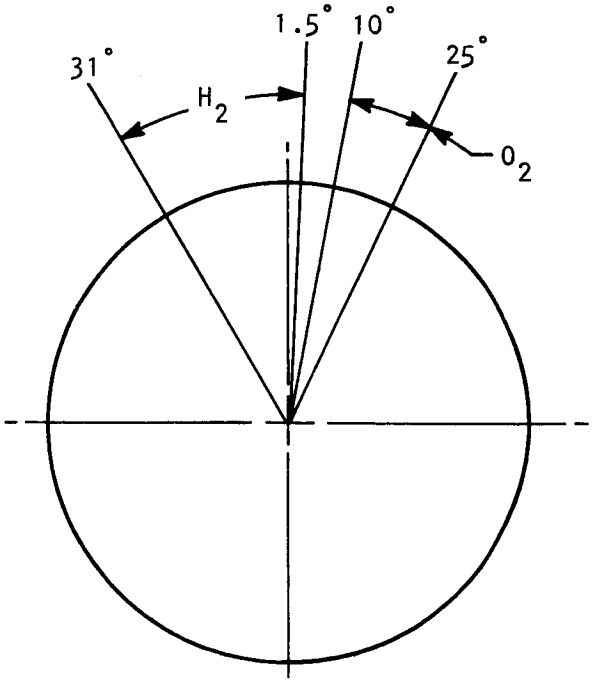

TEST 5149-9-4

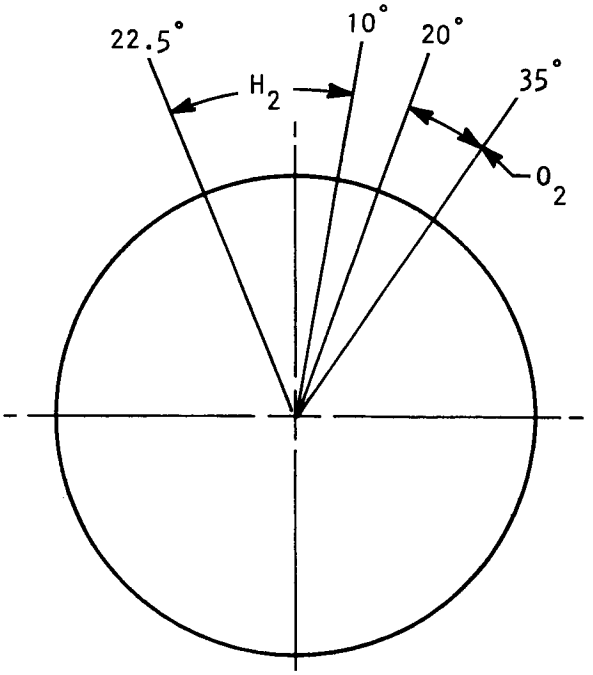

TEST 5149-10-1 & -2
TEST 5149-11-1 THROUGH -8

OPERATING CYCLE H_2-O_2 ENGINE WITH LATE O_2 INJECTION

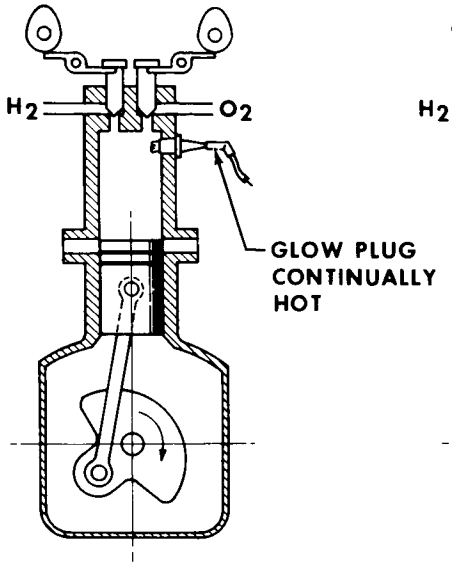

1-2
RESIDUAL COMPRESSION
130° BTC - 23° BTC

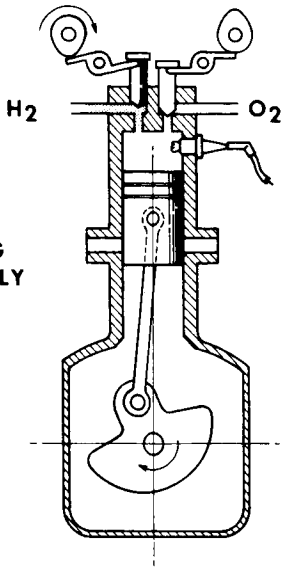

2-3-4
H_2 INJECTION PHASE
23° BTC - 10° ATC

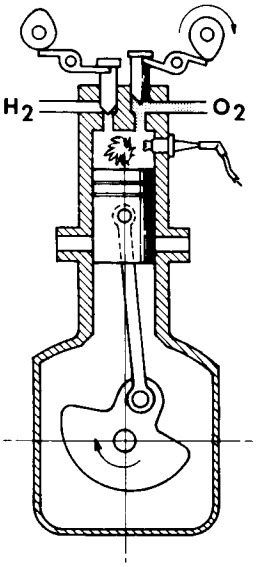

4-5
O_2 INJECTION AND COMBUSTION PHASE
20° ATC - 35° ATC

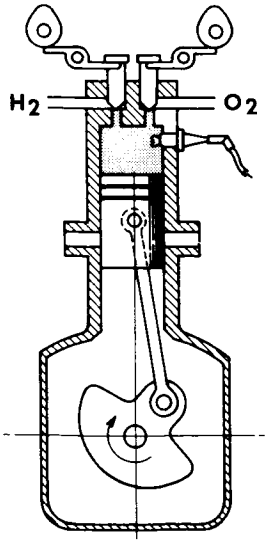

5-6
EXPANSION PHASE
40° - 130° ATC

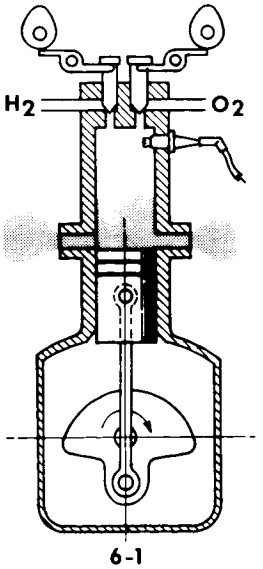

6-1
EXHAUST PHASE
130° ATC - 130° BTC

INDICATOR DIAGRAM
LATE O_2 INJECTION

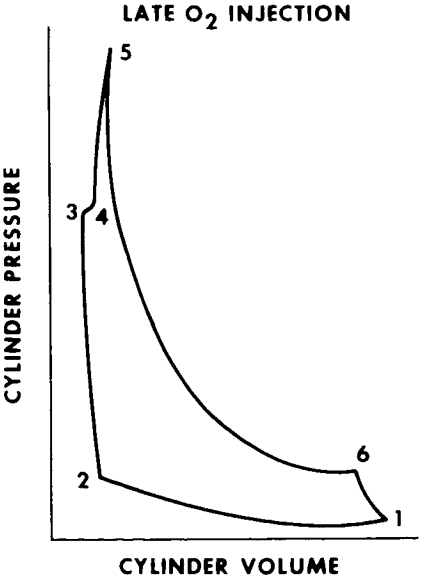

FIGURE 6

The ensuing engine tests showed that smooth engine operation was obtained at exhaust pressures between 10 and 7 psia, that detonation operation occurred between 4.5 and 0.5 psia, and that random rough running and detonation occurred between 7 and 4.5 psia. The performance of the engine was adversely affected at the higher exhaust pressures, as expected, and it improved as the exhaust pressures approached 4.5 psia. These conditions are shown in Figure 7. The rapid decay in performance above 10 psia was a result of high compression pressures which rapidly decreased the amount of hydrogen injected, which resulted in an increase in O/F ratio. Power output could be maintained constant at any exhaust pressure conditions by increasing the hydrogen injection pressures. However, the specific propellant consumption was adversely affected by increasing exhaust pressure.

The effect of varying the voltage supplied to the glow plug was noticeable only during starting. A power of approximately 40 watts was required to assure prompt starting of the engine. Once the engine had achieved thermal stability, the application of power to the glow plug was not required except below O/F ratios of 2.0 and below 1.5 HP at low rpm. At these conditions, the combustion chamber cooled too rapidly to keep the glow plug element hot. No experiments were made with glow plugs of various heat ranges because suitable plugs were not available. It is believed that glow plugs having more heating element surface area and operating at a higher temperature in a more suitable location within the combustion chamber would greatly assist in eliminating detonation. This conclusion is based upon sustained detonation operation during the final engine test, during which it was obvious that an ignition delay was the cause of detonation. In every case wherein smooth combustion was obtained, ignition occurred approximately within 1° of the start of oxygen injection. In the case of detonation operation, ignition delays of 5° to 10° from the start of oxygen injection were noted. This phenomenon is illustrated in Figure 8. This graph is a pressure versus cylinder volume plot derived from Test 5149-11, Run No. 8, Data Point No. 8 (See Appendix B) and it shows superimposed detonation and non-detonation combustion. These data were taken during a slow transition from high exhaust pressure (i.e., greater than 7 psia) to low exhaust pressure (i.e., 0.6 psia). The previously presented Figure 7, if viewed in terms of decreasing P_{ex}, would indicate a cooling condition for the glow plug and a requirement of a higher O/F condition to achieve ignition at low exhaust pressures. A hotter glow plug having greater heated surface area located in a more suitable region of the combustion chamber should alleviate, or eliminate completely, the ignition delay and the resulting detonation.

The best performance of the engine was achieved during the final test run. This test lasted approximately 43 minutes and covered a broad range of engine operation. Approximately 15 minutes of this test period was at very low exhaust pressure conditions of 0.6 psia. The maximum performance of the engine, within the limitations imposed by the propellant flowmeter ranges, was documented during this period. This performance is presented in Figures 9 to 15. These graphs present the following parameters as a function of engine speed:

SPU-2A-3 ENGINE
EFFECT OF INCREASING P_{ex} ON rpm, HP, AND T_{ex}

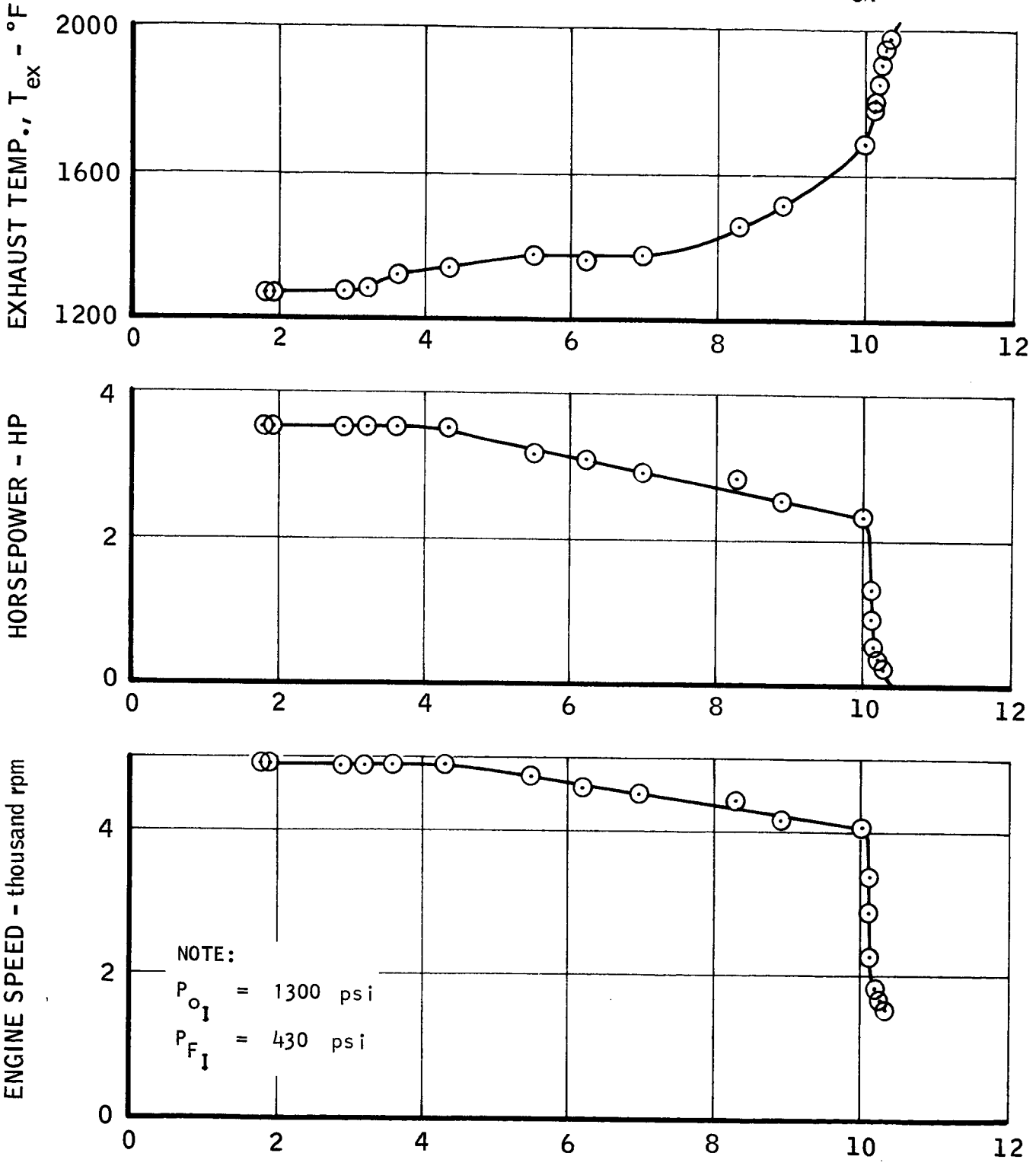

SPU-2A-3 ENGINE
CHAMBER PRESSURE vs. CYLINDER VOLUME
TEST 5941-11, RUN No. 8, DATA POINT NO. 8

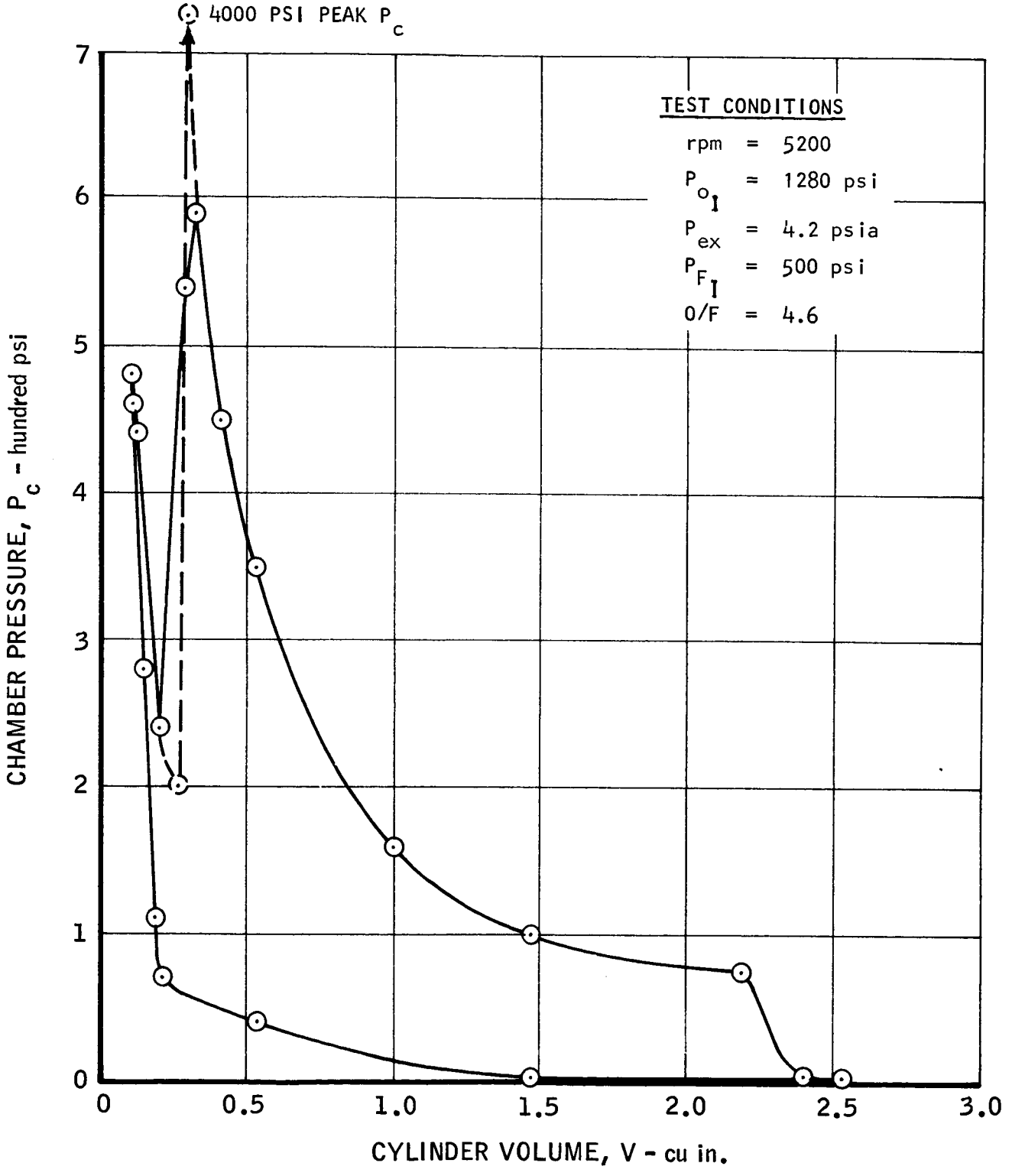

FIGURE 8

SPU-2A-3 ENGINE
HORSEPOWER vs. ENGINE SPEED

TEST 5149-11, RUN No. 8

VALVE TIMING

GH_2 - 22.5° BTC to 10° ATC

GO_2 - 20° ATC to 35° ATC

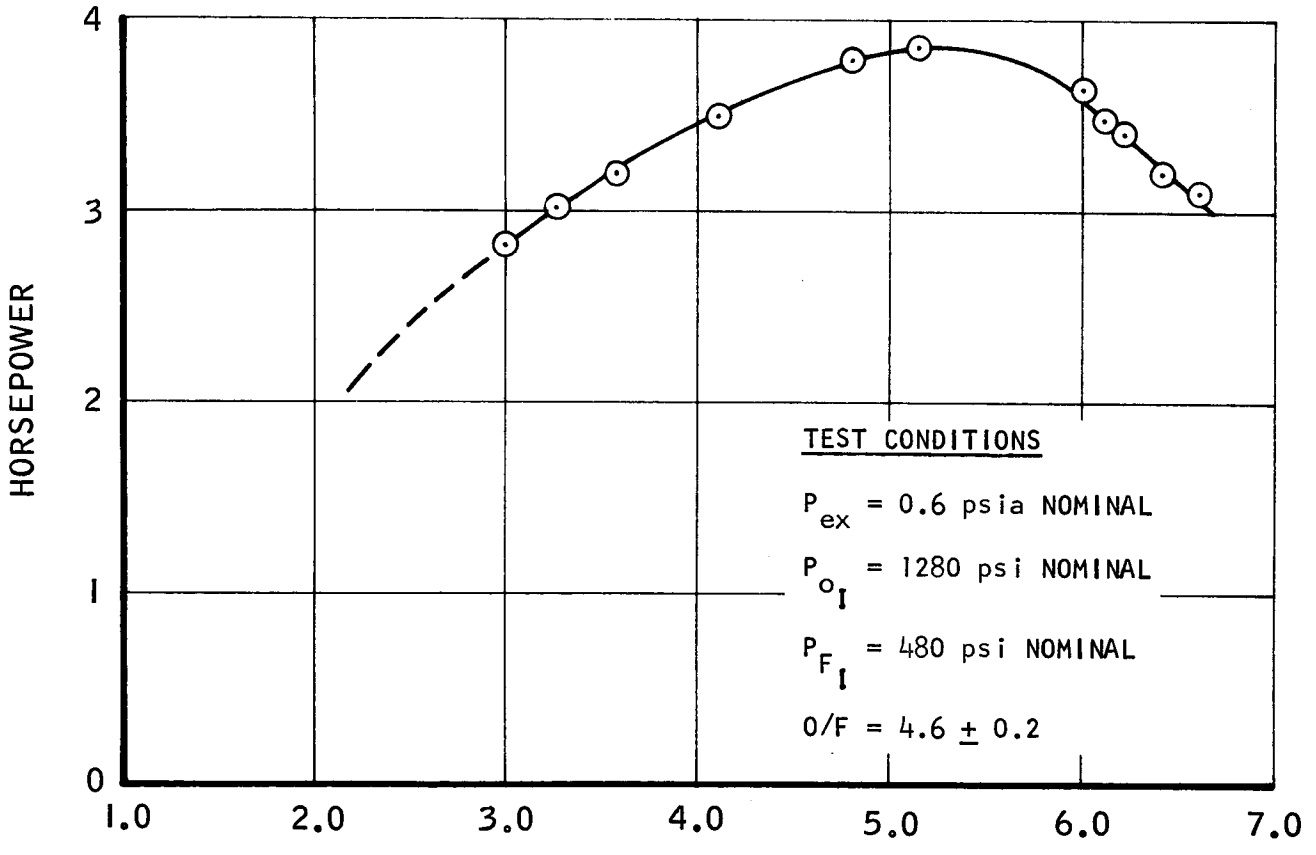

SPU-2A-3 ENGINE
SPECIFIC PROPELLANT CONSUMPTION vs. ENGINE SPEED
TEST 5149-11, RUN No. 8

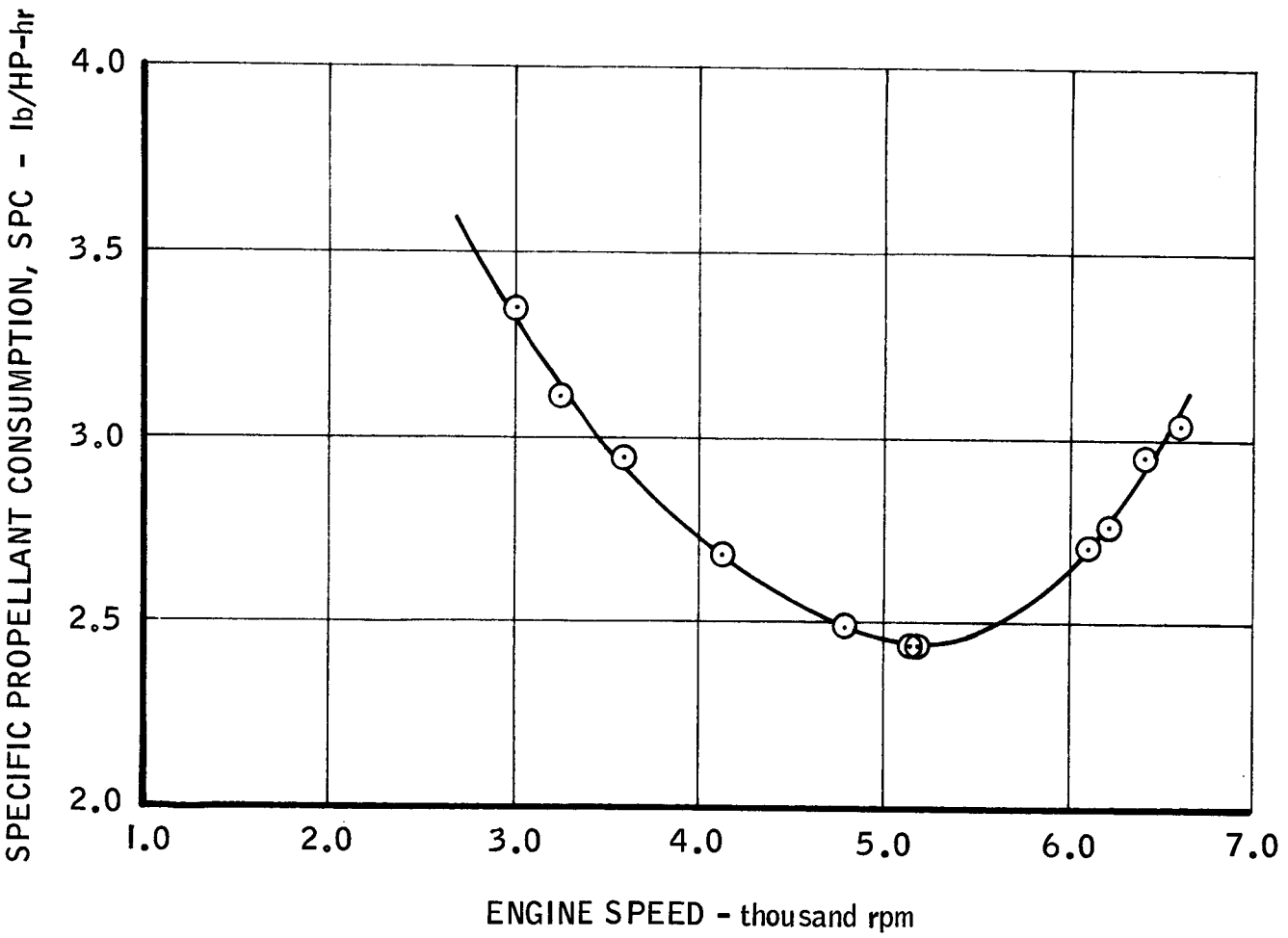

FIGURE 10

SPU-2A-3 ENGINE
TORQUE vs. ENGINE SPEED

TEST 5149-11, RUN No. 8

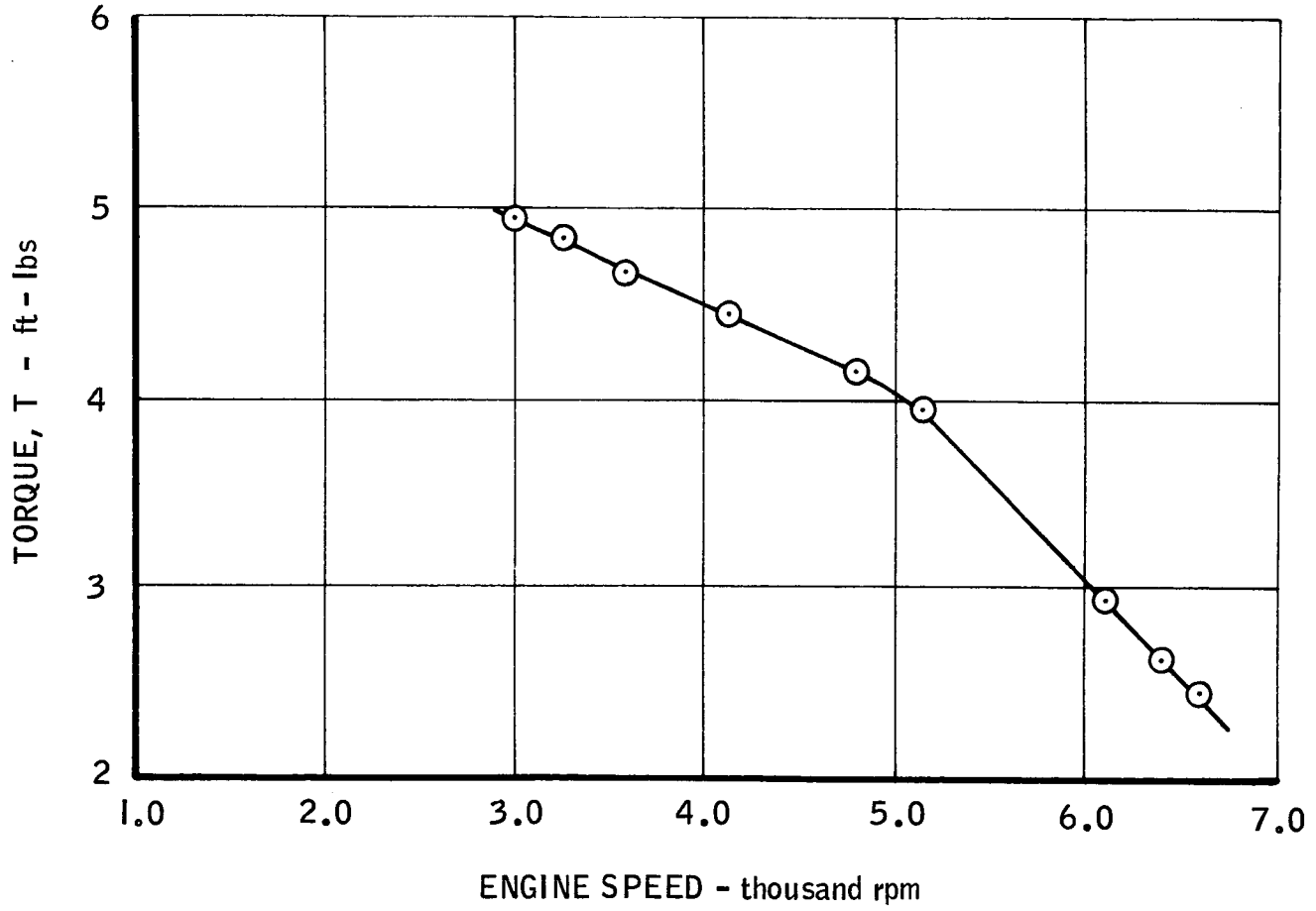

FIGURE 11

SPU-2A-3 ENGINE
BRAKE MEAN EFFECTIVE PRESSURE vs. ENGINE SPEED

TEST 5149-11, RUN No. 8

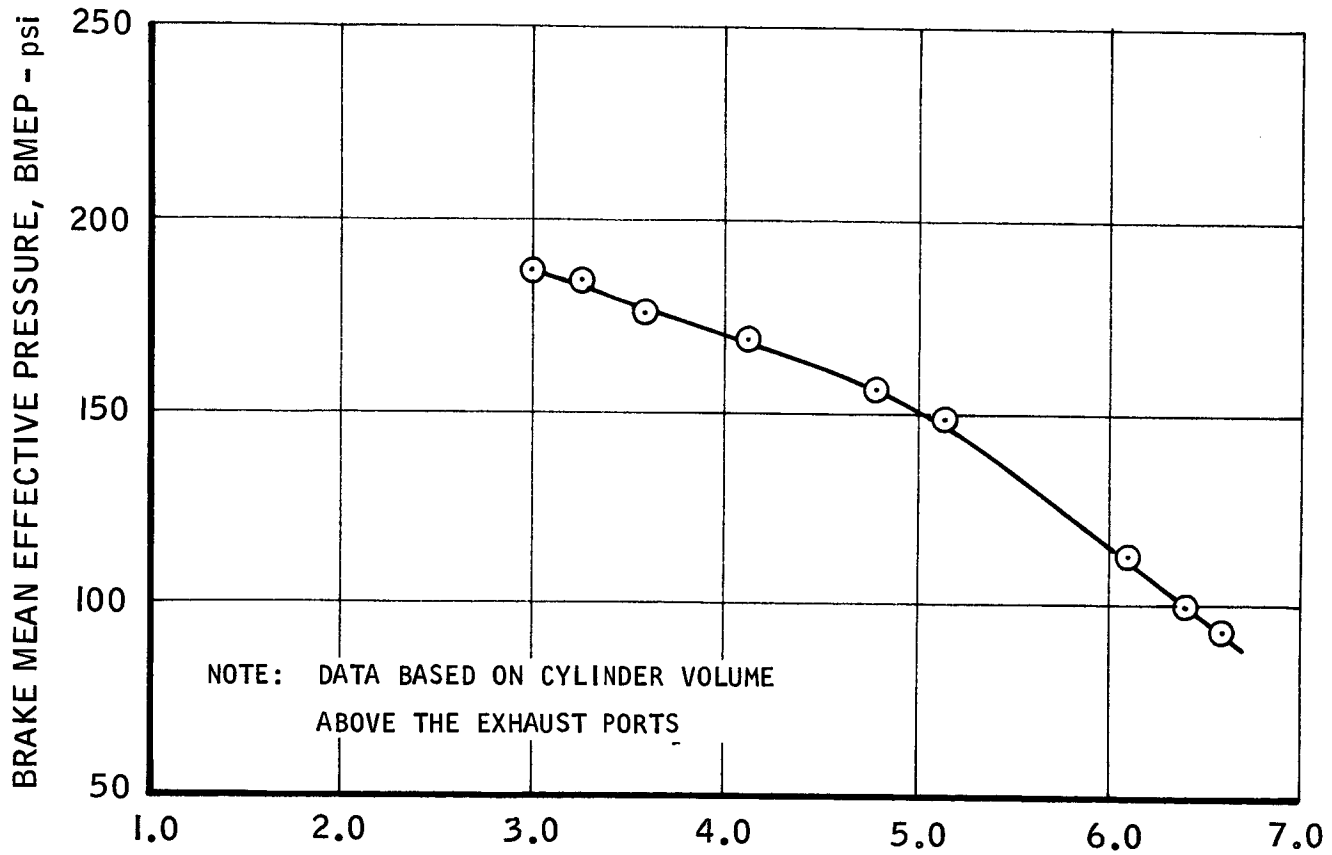

FIGURE 12

SPU-2A-3 ENGINE
EXHAUST TEMPERATURE vs. ENGINE SPEED

TEST 5149-11, RUN No. 8

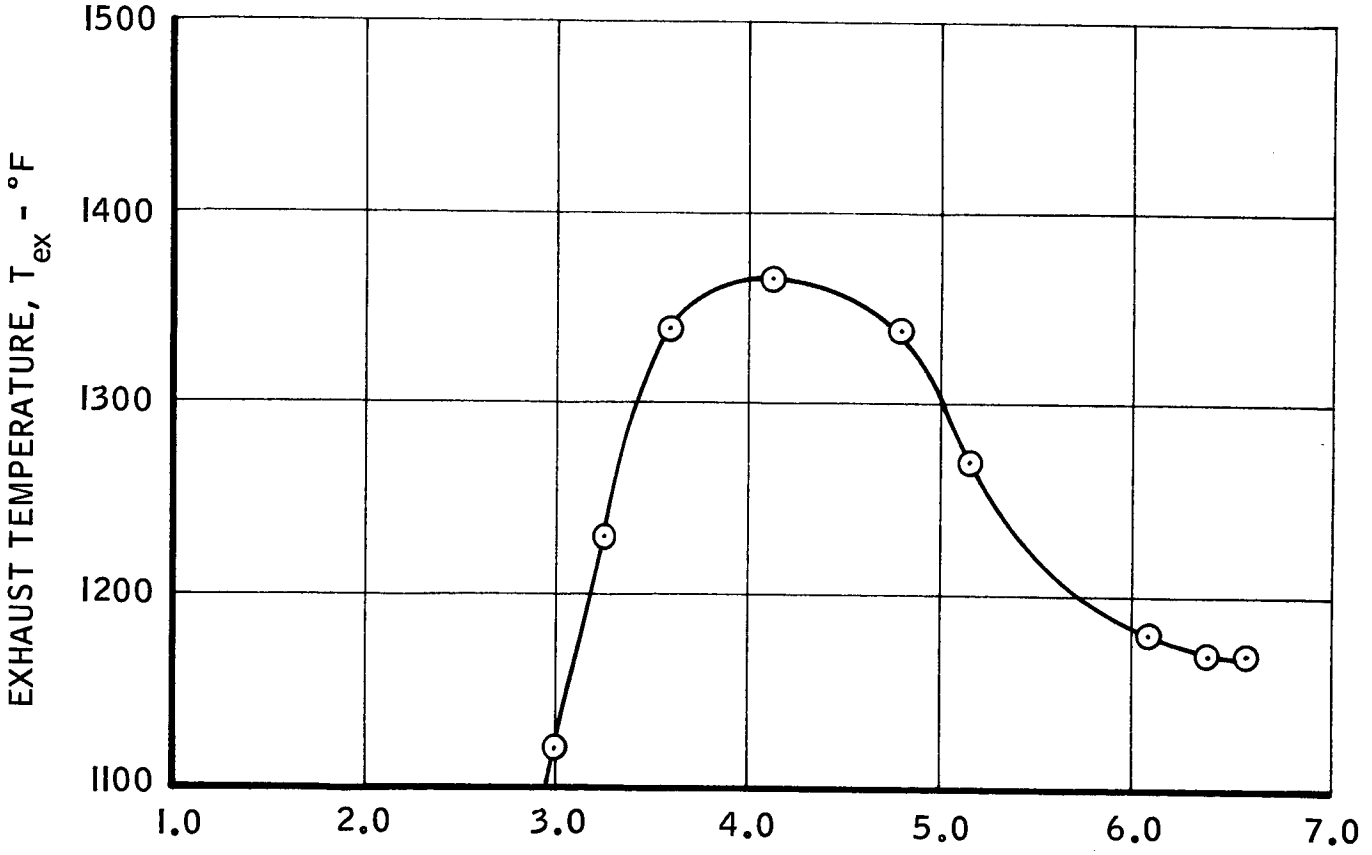

SPU-2A-3 ENGINE
THERMAL EFFICIENCY vs. ENGINE SPEED

TEST 5149-11, RUN No. 8

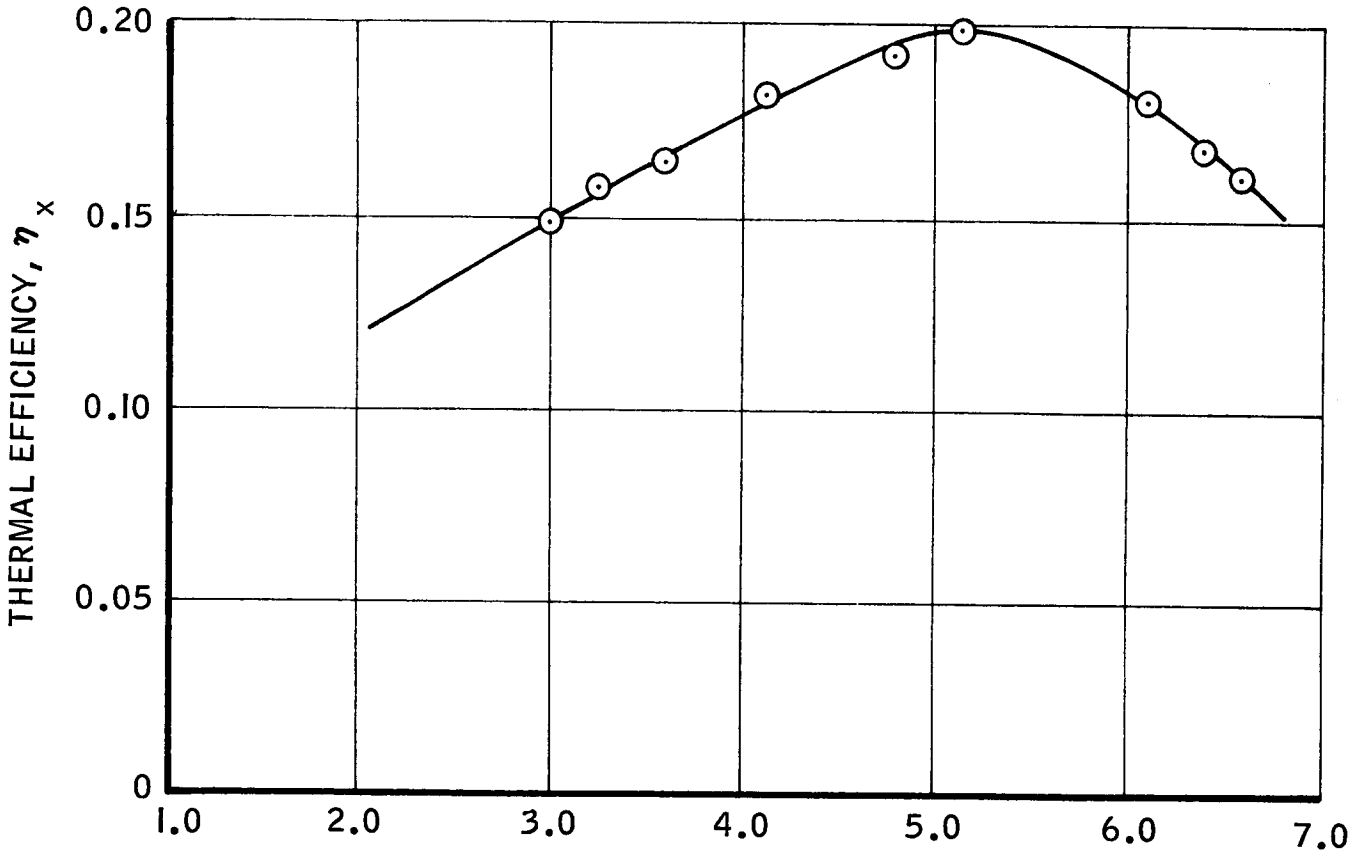

SPU-2A-3 ENGINE
MECHANICAL EFFICIENCY vs. ENGINE SPEED

TEST 5149-11, RUN No. 8

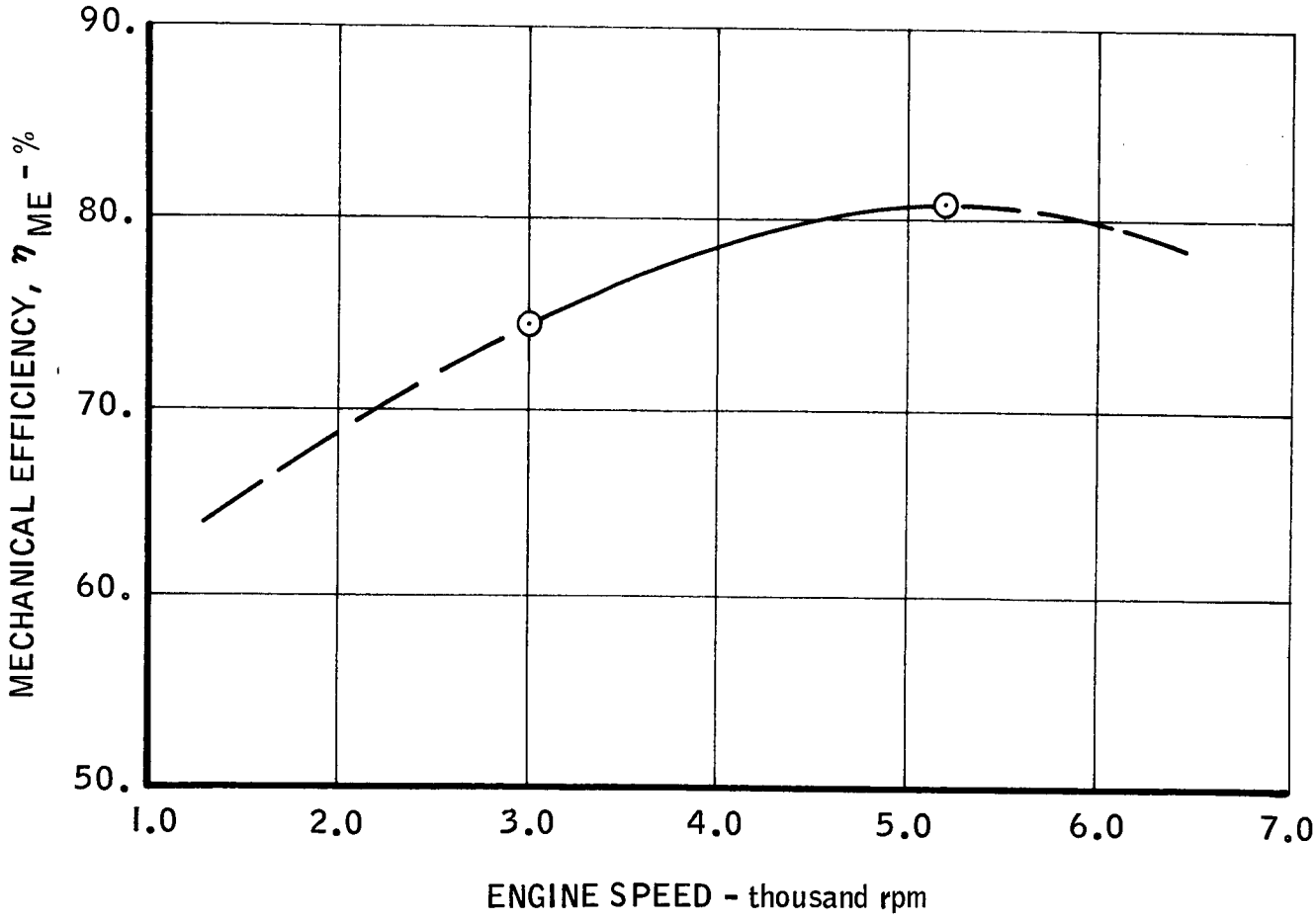

FIGURE 15

1. Horsepower
2. Specific propellant consumption
3. Torque
4. Brake mean effective pressure
5. Exhaust temperature
6. Thermal efficiency
7. Mechanical efficiency

The test conditions for these data were as follows:

1. Exhaust pressure, P_{ex} = 0.6 psia
2. Oxygen injection pressure, P_{O_I} = 1280 psi
3. Fuel injection pressure, P_{F_I} = 480 psi
4. O/F ratio = 4.6 ± 0.2

The valve timing was as follows:

GO_2	GH_2
Start 20° ATC	Start 22.5° BTC
End 35° ATC	End 10° ATC
Dwell 15°	Dwell 32.5°
Null Period 10°	

These data show that the engine produced a maximum power output of 3.85 HP at 5150 rpm with a minimum specific propellant consumption of 2.43 lb/HP-hr. The corresponding brake mean effective pressure (BMEP) was 142 psi, the mechanical efficiency was 81%, and the overall thermal efficiency was 20%.

During the low exhaust pressure period, the engine was operating in a sustained detonation combustion condition. The magnitude of the detonation spikes was approximately 4000 psi. Since those pressure levels were approximately half of the previously experienced detonation pressure levels of 9000 psi, the engine was allowed to operate at these conditions in order to obtain structural integrity data.

A typical plot of chamber pressure versus cylinder volume for low exhaust pressure conditions is presented in Figure 16. These data clearly show the pressure loss resulting from the delayed oxygen injection and the rapid pressure rise of the delayed ignition condition. It can also be seen from these data that the exhaust port area is a great deal larger than necessary for low exhaust pressure conditions. The exhaust porting was sized to achieve maximum cylinder scavenging to minimize recompression power losses. This design parameter was achieved with satisfactory results. On the basis of these data, future engines can be designed with smaller exhaust ports with subsequent reductions in piston ring stresses.

A plot of mechanical efficiency as a function of brake mean effective pressure is shown in Figure 17. These data were derived from the pressure versus volume curves (presented previously, Figures 8 and 16), and they are within the range of expectation for a small displacement engine such as the SPU-2A-3 engine.

Figure 18 is a summary plot of specific propellant consumption versus horsepower. Data for this graph were taken from several test runs having the same injector timing and which were at an O/F condition of 4.6 ± 0.2. This graph shows a steady decrease in specific propellant consumption with increasing horsepower. The previously presented performance plots (Figures 9 to 15) showed that maximum power output and minimum specific propellant consumption occurred in the 5000 rpm range. At this speed range, the propellant mixing conditions and the turbulence during combustion appear to have been optimum for the combustion chamber design. Since the higher power levels were obtained at these rotational speeds, the lower specific propellant consumption would reflect these conditions. Because the propellant flow meters were inadequate for power conditions above 3.8 HP, a minimum obtainable specific propellant consumption could not be demonstrated. Extrapolation of these data from Figure 18 indicate a specific propellant consumption of 1.8 lb/HP-hr at the rated power condition of 4.5 HP would be obtained with the engine configuration which was tested.

C. Summation of Engine Test Program

The test program was concluded on 4 June 1965 because of funding depletion. During the period from 26 April until 4 June 1965, a total of 7.64 hours of running time was accumulated with the engine components of which 3.12 hours was hot running time. Figure 19 is a plot of accumulated running time as a function of calendar time. The last 2.45 hours of engine operation were obtained without malfunction or replacement of components. During the final 2 hours of operation, no attempt was made to operate the engine "softly". It was deemed desirable to establish structural integrity and component reliability as well as performance within the short test time span which was available. The three major problem areas of hard starting, preignition, and detonation were explored, documented, and explained.

SPU-2A-3 ENGINE
CHAMBER PRESSURE vs. CYLINDER VOLUME
TEST 5149-11, RUN No. 8, DATA POINT No. 8

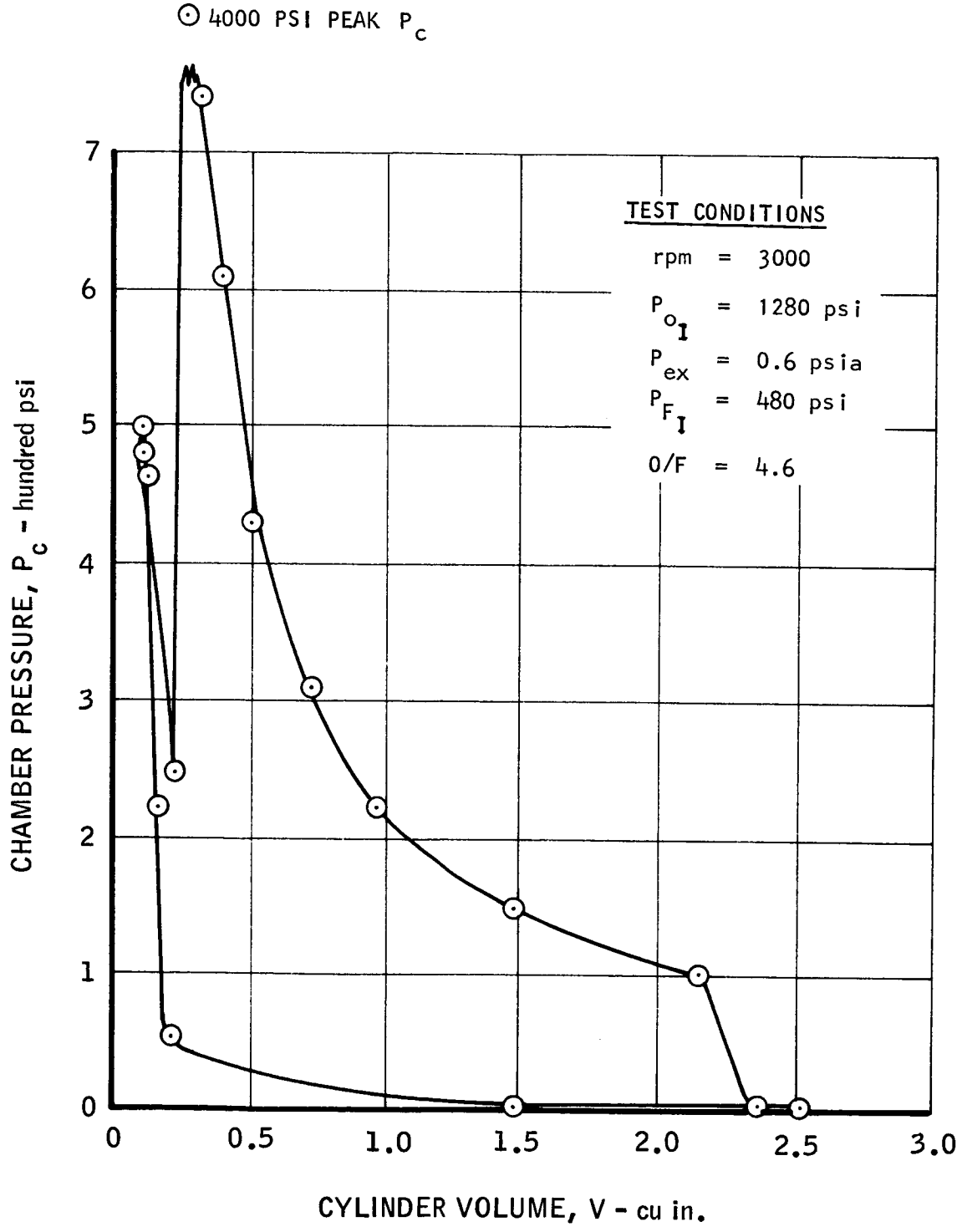

FIGURE 16

SPU-2A-3 ENGINE
MECHANICAL EFFICIENCY vs. BRAKE MEAN EFFECTIVE PRESSURE

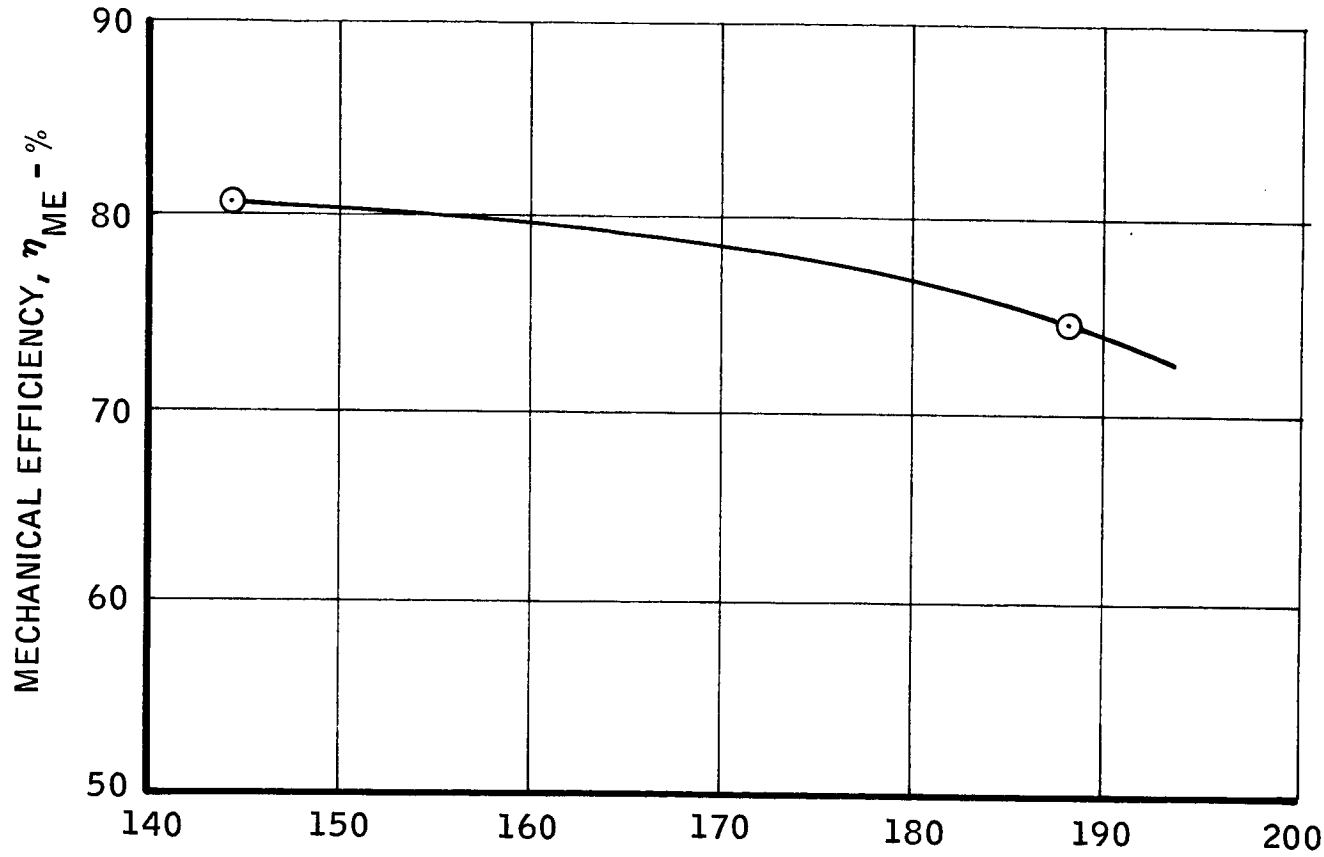

287-70

FIGURE 17

SPU-2A-3 ENGINE
SPECIFIC PROPELLANT CONSUMPTION vs. HORSEPOWER

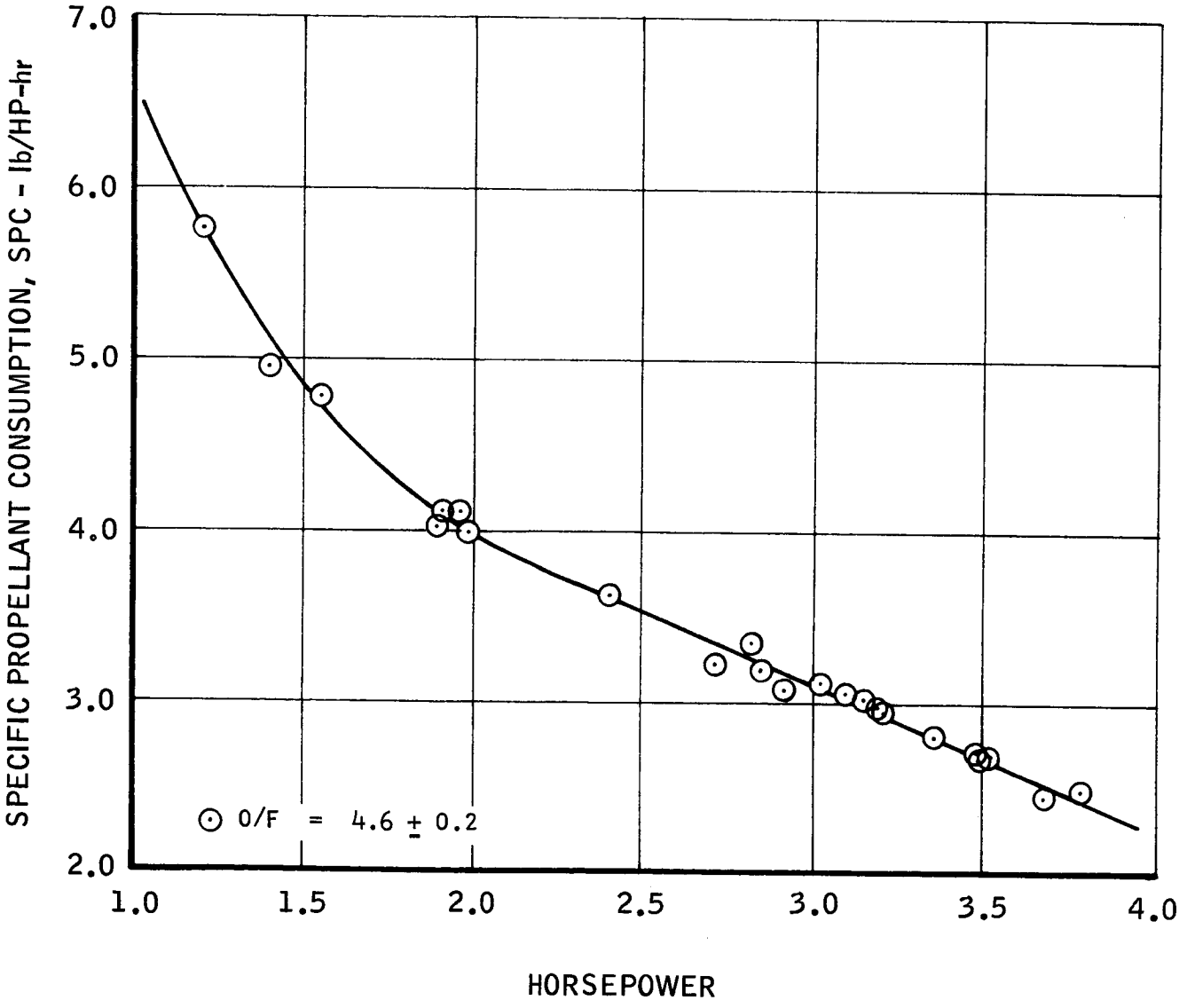

FIGURE 18

SPU-2A-3 ENGINE -- ACCUMULATED RUN TIME

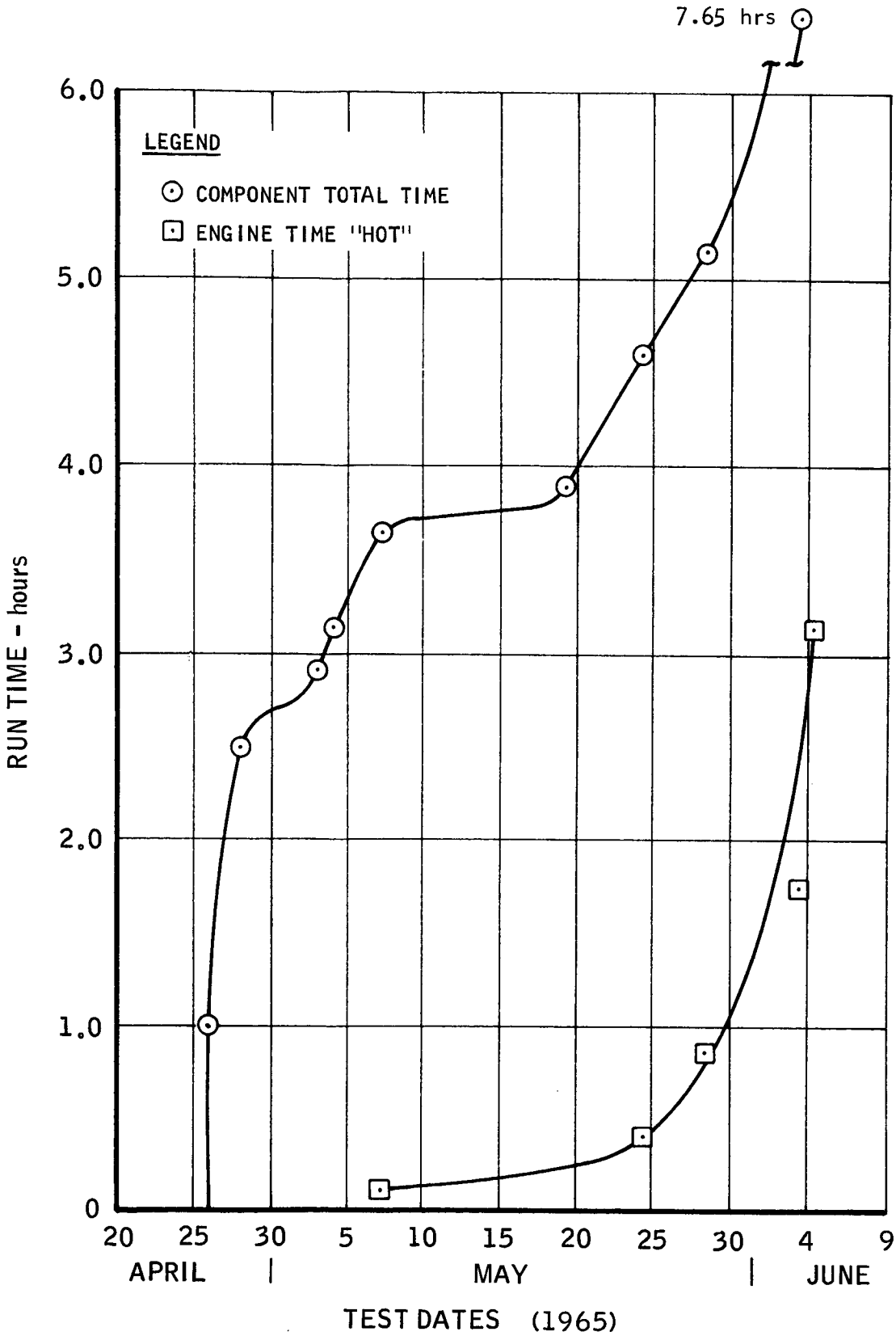

FIGURE 19

V. COMPONENT DEVELOPMENT

A. Cylinder Head Development Testing

Component testing was initiated on 26 April 1965 with the successful accumulation of 1 hour of dynamic operation with the oxygen valve. Engine speeds up to 4000 rpm and injection pressures up to 1000 psi were demonstrated without measurable changes in timing, leakage, or physical condition. The same operating conditions and results were obtained with the fuel injector valve on the following day. Figure 20 shows the setup for this component test.

At the completion of these "cold" tests, the ignition tests were initiated. The valves were timed to give a 15° overlap period and the activated platinum catalyst screens were installed. With the cylinder head assembly operated at a steady 2000 rpm, traverses in oxygen pressure from 50 psi to 1350 psi and in hydrogen pressure from 100 psi to 1000 psi were made without successfully achieving ignition. At the high differential pressure conditions, the catalyst screens were partially displaced from their retainer. Several palladium pellets were then placed in the combustion chamber and retained with a new set of platinum screens and the test was repeated. The results were the same. Although it was recognized that the conditions within the engine cylinder would be far more conducive to achieving ignition with catalytic elements than the conditions of the evaluation test, it was decided to discontinue the catalyst igniter tests and to evaluate the glow plug system.

Initially, a model airplane engine glow plug was mounted on a simple bracket in front of the combustion chamber opening and it was energized with a 1.5 volt battery. Results were immediate and successful. The glow plug installation for these tests is shown in Figures 21 and 22. The cylinder head was then modified to accept a glow plug internally. The location which was selected was based upon the capability of the existing cylinder head to accept the installation without interfering with other existing holes rather than choosing the optimum location within the combustion chamber. This installation was then evaluated to establish combustion limits and characteristics. It was immediately noted that the injection pressures required to obtain steady combustion were significantly higher than the pressures which were required with the plug mounted externally. This was not an unexpected condition because the plug was shrouded and located deep within the combustion chamber adjacent to the hydrogen injection port. Additionally, the effects of atmospheric oxygen were minimized.

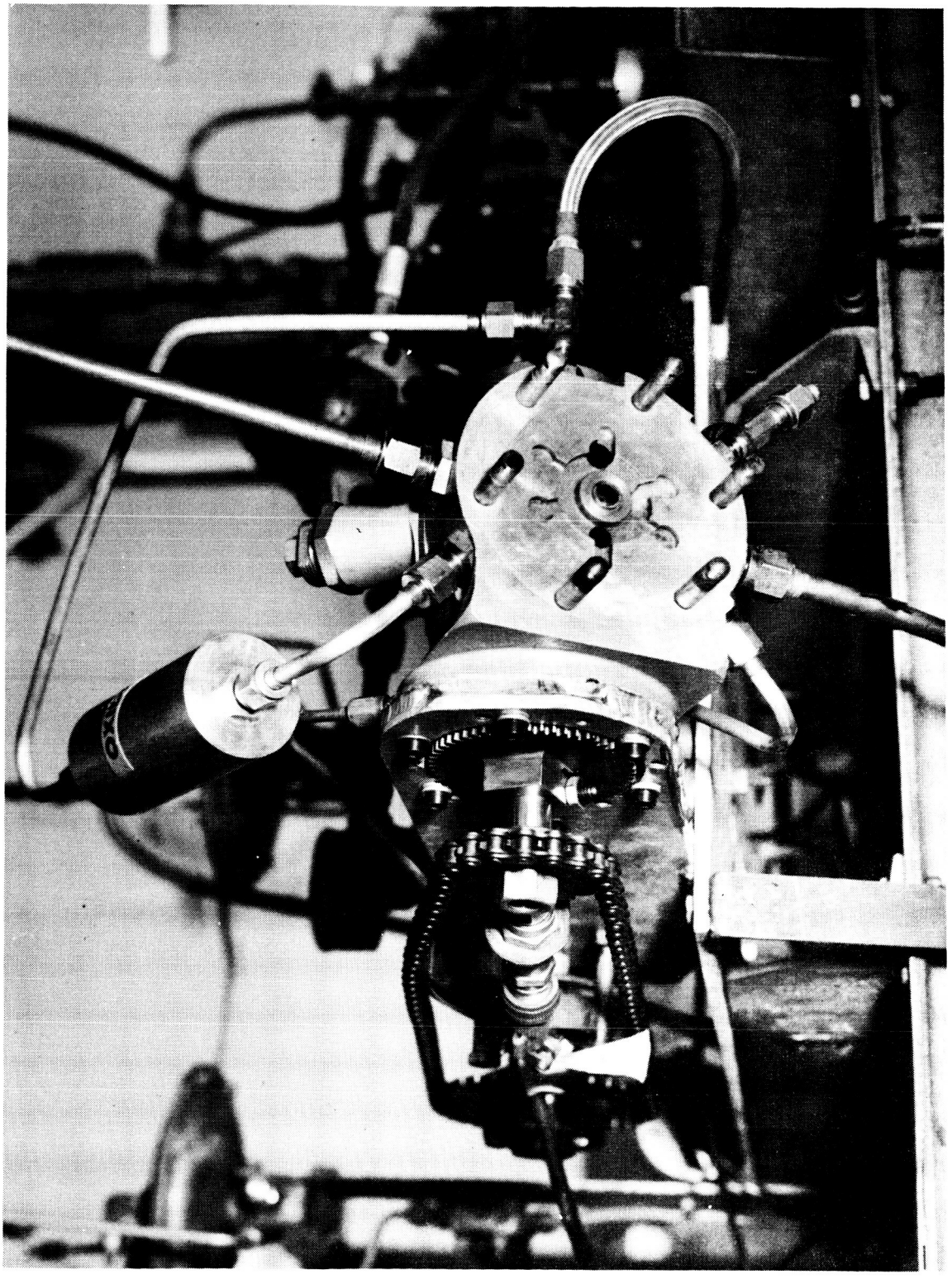

T5149-2

FIGURE 20. Setup for Development Testing of the Cylinder Head for the SPU-2A-3 Engine

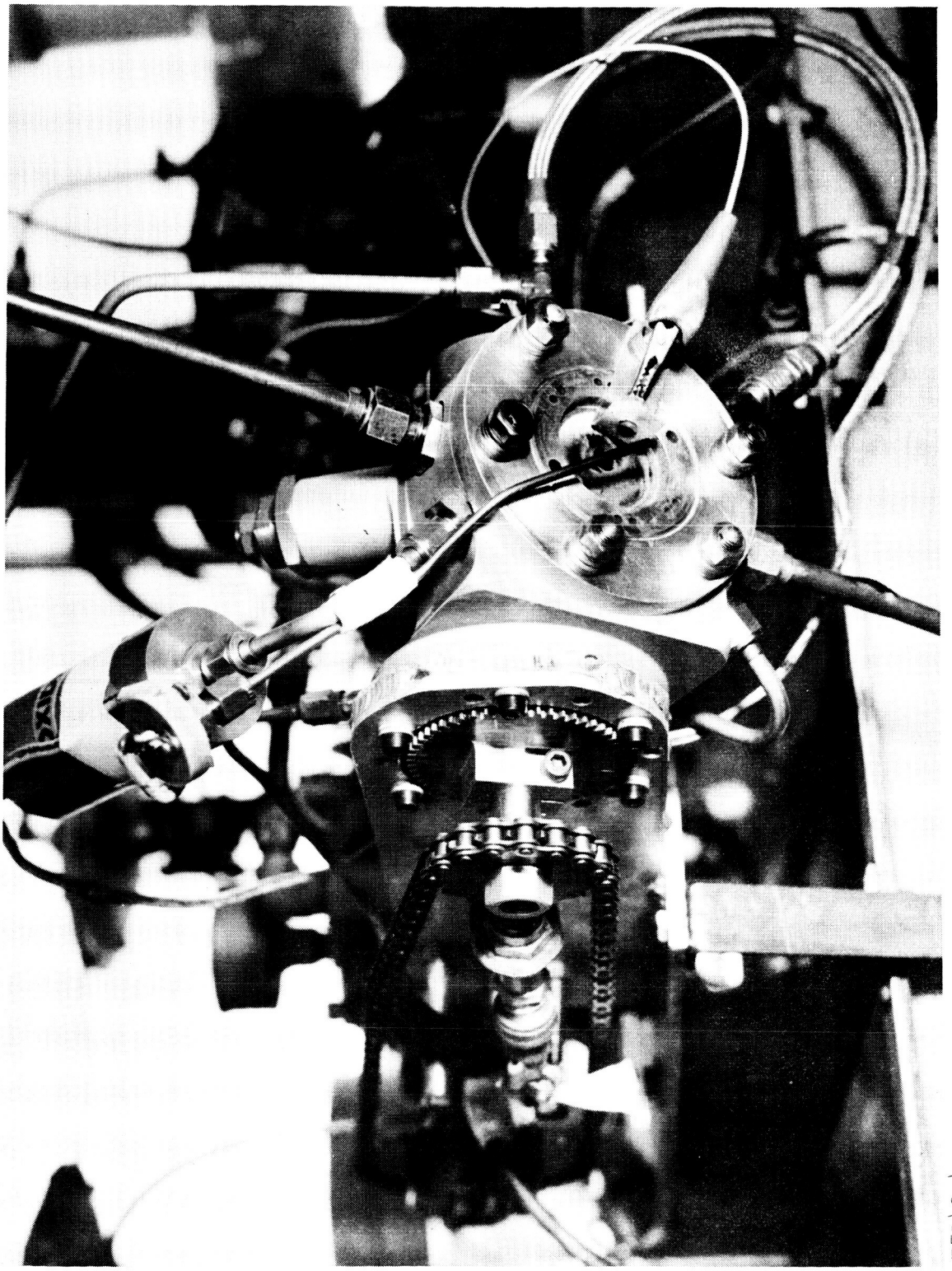

T5149-4

FIGURE 21. View of Setup for Open Face Combustion Test of the SPU-2A-3 Engine with glow Plug Igniter

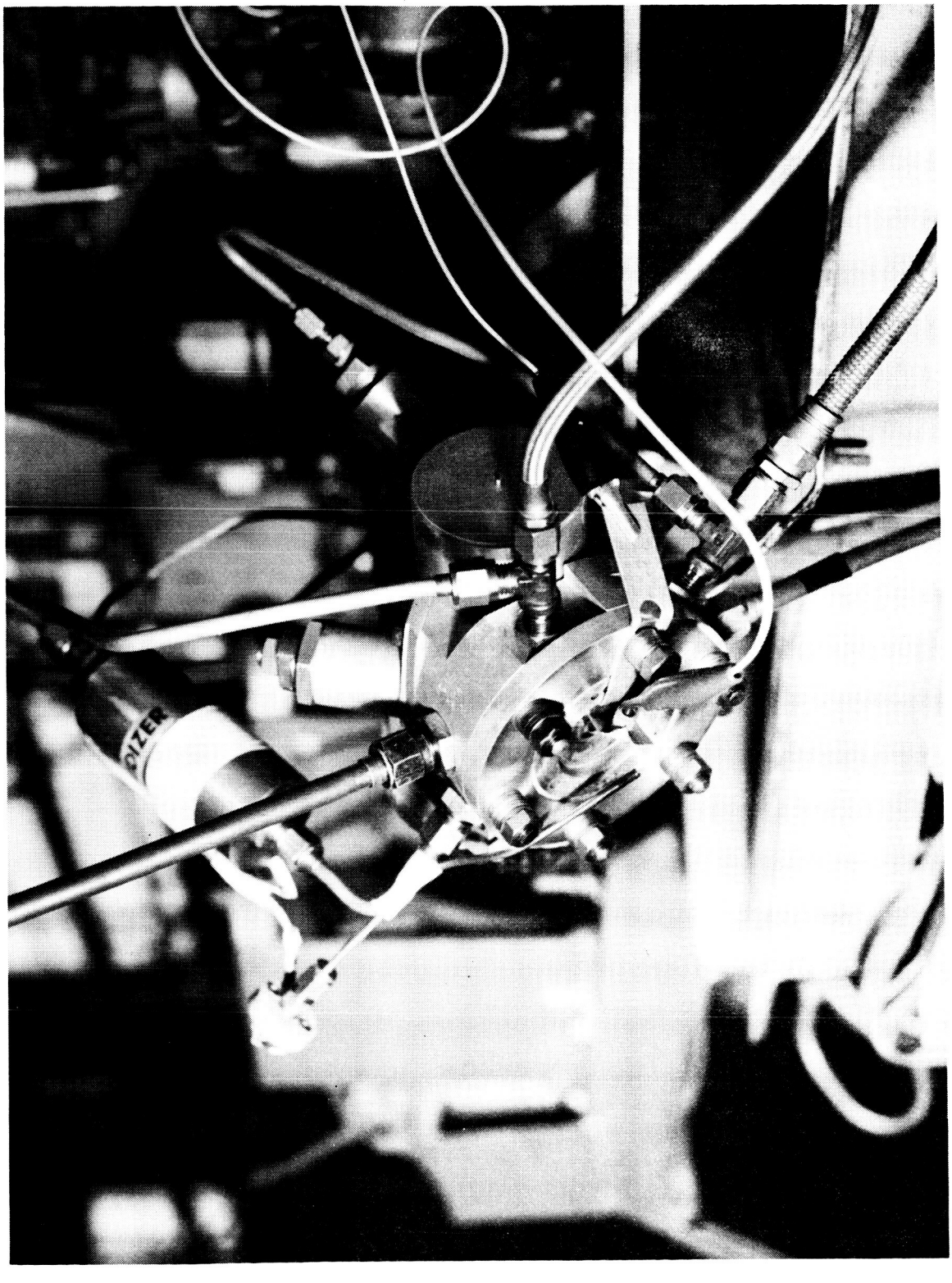

FIGURE 22. Closeup of Setup for Open Face Combustion Test of the SPU-2A-3 Engine with Glow Plug Igniter

T-5149-5

A total of 3.12 hours of engine operating time was accumulated with the injector valve system during these tests. Rotational speeds in excess of 4000 rpm were sustained for significant periods at various injection pressures. Throughout the component test program, neither changes in timing, dwell, or injection characteristics nor measurable wear of any component were noted. The loss rate of the duPont PR143 injector valve lubricant was insignificant during this test period.

B. Development of Piston and Piston Rings

Following the first test run, the engine was disassembled for inspection and for repair of components. Inspection of the piston indicated that the top ring had failed because of excessive heating of the aluminum ring land. The high temperatures caused a section of the ring land to deflect under the ring. The unsupported ring was then broken up in small segments as it crossed the exhaust port openings. Figures 23 and 24 show two views of the piston failure. Secondary effects of the piston failure were noted in the cylinder bore and cylinder head. Melted aluminum was deposited on the surface of the cylinder bore. These deposits are shown in Figure 25. No actual damage was sustained by the cylinder bore because the deposits were only on the surface and they were removed by chemical means without further rework being necessary.

The cylinder head plate is shown in Figure 26. The effects of the broken ring segments that were trapped between the piston crown and the head disk are very apparent.

All other engine components were in excellent condition and they were reinstalled following cleaning. The injector valves and actuation mechanism showed no signs of wear at any point and they maintained their prerun adjustments without measurable changes.

Following careful evaluation of the mode of piston failure, the piston was redesigned. The major changes were to extend the N-155 crown down to the top of the second ring and to carry the top ring completely in the high temperature material. Only one part had to be fabricated (the new crown) because the skirt section was easily modified to accept the new component. The piston design proved to be very successful and it required no further modification or replacement during the remainder of the test program.

In addition to the piston assembly, a new cylinder head spacer was fabricated. A minor modification was made to this component to compensate for the reduction in heat transfer of the top piston ring to the piston. This modification allowed direct contact between the coolant and the outer cylinder wall at the top of the cylinder.

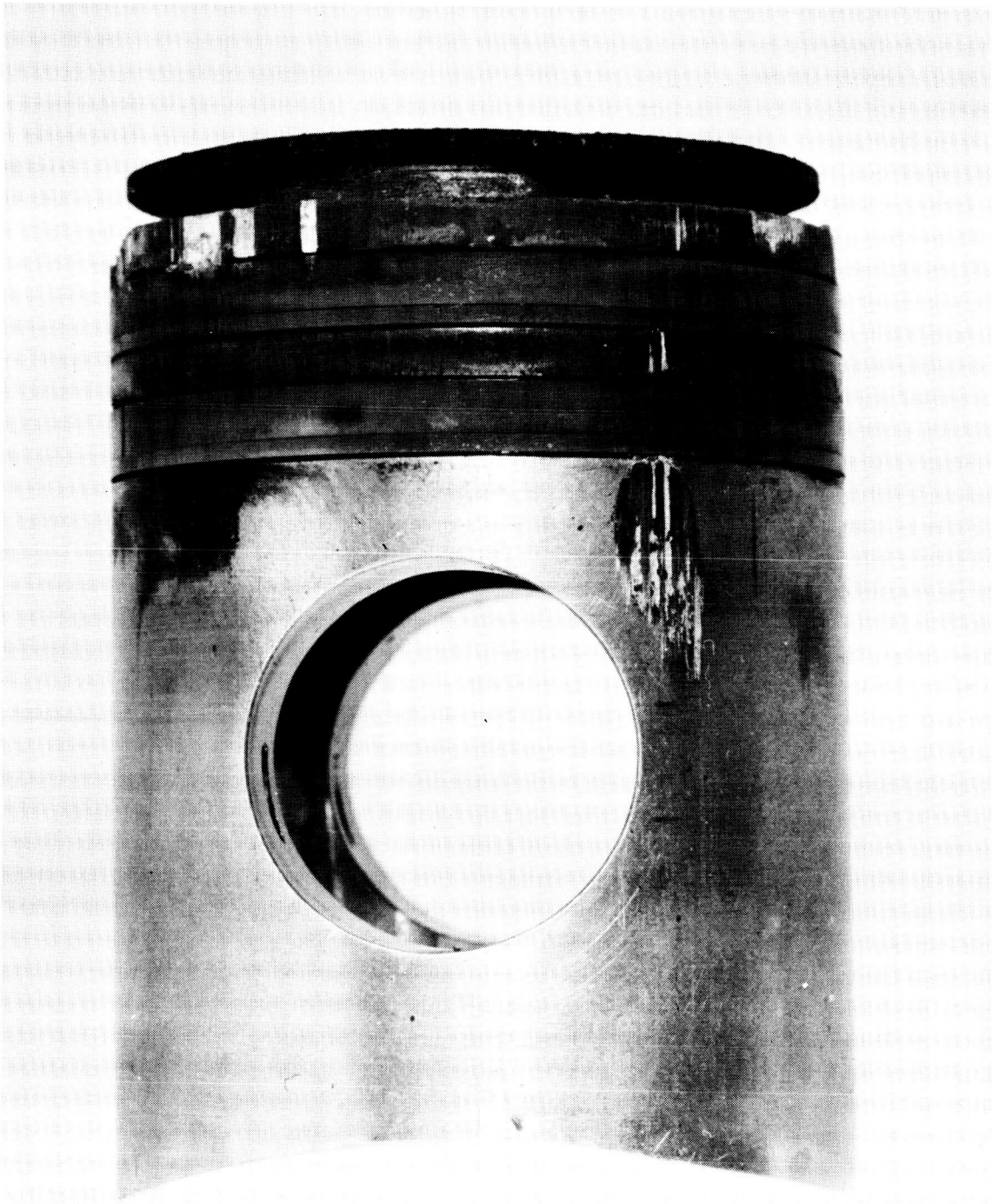

FIGURE 23. SPU-2A-3 Piston Following 13 Minutes Operation, Test 5149, Run No. 8

T5149-7

T5149-6

FIGURE 24. SPU-2A-3 Piston Following 13 Minutes Operation, Test 5149-6, Run No. 8

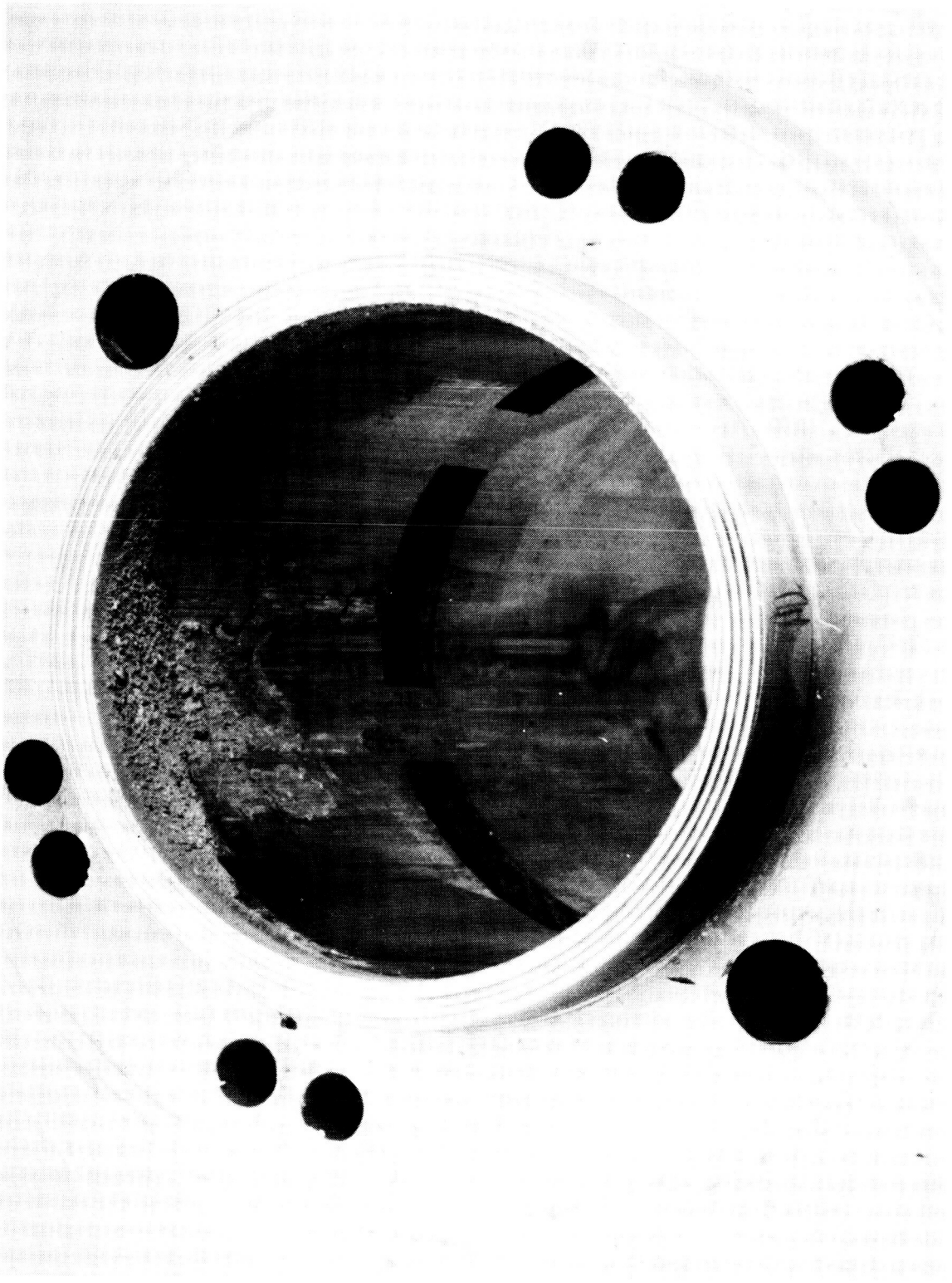

T5149-8

FIGURE 25. SPU-2A-3 Cylinder Bore Following 13 Minutes Operation, Test 5149-6, Run No. 8

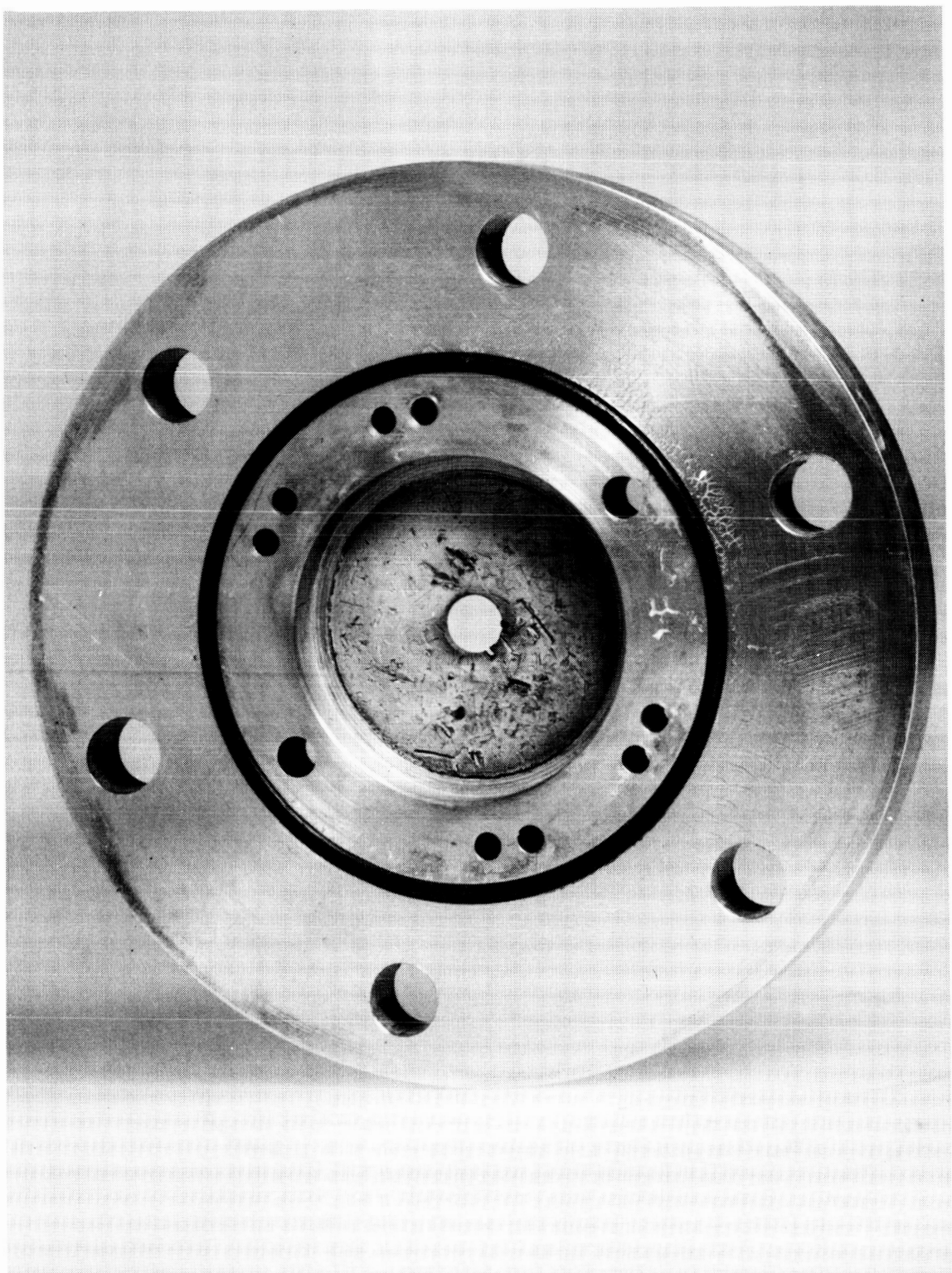

T5149-9

FIGURE 26. SPU-2A-3 Cylinder Head Plate Following 13 Minutes Operation, Test 5149-6, Run No. 8

VI. ANALYSIS OF TEST DATA

A. Propellant Flow Measurements

The O_2 flow is a sonic process and thus flow is constant regardless of engine speed for a constant supply pressure. The available line volume for flow damping is more effective in O_2 service than in H_2 service because of the higher density and the lower sonic velocity of O_2. Although the O_2 flow is pulsing, the accuracy of the rotometer is considered quite accurate. As a further check, the flow conditions were calculated using the proper dwell and supply pressure of the O_2. Using a discharge coefficient, C_d, (sometimes called contraction factor) of 0.60, a flow rate of 9 pph was calculated. Using a C_d of 0.516, the calculated O_2 flow equals the measured 7.75 pph value. These data are shown in Figure 27. A C_d value between 0.5 and 0.6 is estimated to be the proper order for the dual concentric valve, since it should be lower than that normally associated with a single sharp edged orifice which produces a C_d value between 0.7 and 0.8 with sonic flow. In summary, the O_2 flow measurements are regarded as realistic. If error exists, the measurements should be on the high side and hence should give conservative results.

The H_2 flow process is quite different than the O_2 flow process. The clearance volume plus a small admission volume are filled with H_2 each stroke. Thus the H_2 flow characteristics are like those one expects from positive displacement machinery, namely, flow increases directly with rpm. At high engine speeds, the volumetric efficiency may decrease, thus altering the linear flow-speed relation.

Two indicator diagrams were analyzed to determine the H_2 flow. A 3000 and a 5200 rpm run were studied. The following data were obtained:

Run	H_2 Pressure (psi)	Total Volume at 10° ATDC (cu in.)	Speed (rpm)	WH_2 (pph)
5149-11-8-12	480	0.104 (Hot)	3000	1.43
5149-11-8-8	500	0.104 (Hot)	5200	2.54

As expected, the indicator cards show H_2 flow increasing with speed.

Comparison of the flows determined from the indicator diagrams with the measured values is warranted. Throughout the test run, where these data were obtained, the speed varied between 3000 and 6000 rpm, while the measured H_2 flow remained constant at 1.69 pph.

SPU-2A-3 ENGINE
COMPARISON OF MEASURED AND CALCULATED PROPELLANT FLOW

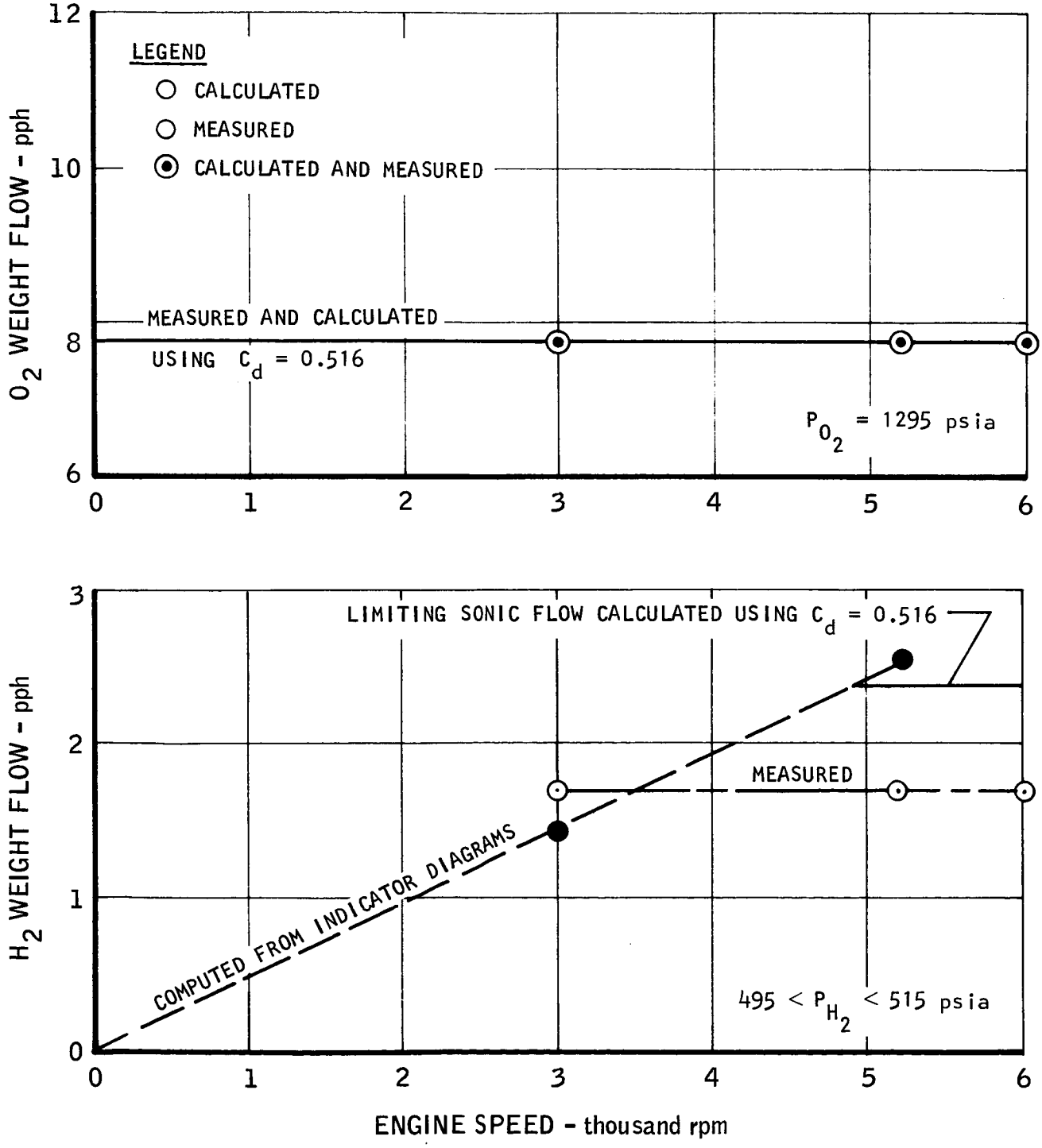

287-58

FIGURE 27

The limiting (or maximum) H_2 flow which can be injected into the engine is obtained when the engine speed is sufficiently high to require sonic flow in the H_2 injector valve. The same discharge coefficient ($C_d = 0.516$) as the one correlated to the O_2 flow was used. Since the H_2 and O_2 valves are identical (except for dwell) there is good reason to expect similar values for C_d for the H_2 and O_2 injectors.

Figure 27 also summarizes the H_2 flow data. This plot shows the flow values computed from the indicator data, the sonic limit calculated, and the measured flow test data. The measured flow is higher than the indicator value at 3000 rpm and lower at 6000 rpm.

The characteristic flow-speed relation for 500 psi H_2 is a linearly rising curve to 4950 rpm and a constant H_2 flow of 2.37 pph at speeds in excess of 4950 rpm.

Possible explanations for the discrepancy between the theoretical and measured H_2 flow include the following:

1. Adverse line dynamics caused by pulsing flow.

2. H_2 expulsion back through the H_2 injector valve during admission. This is caused when the cylinder is filled to the H_2 regulated supply pressure before the piston reaches TDC. As the piston rises, the H_2 pressure in the cylinder exceeds the supply pressure and some H_2 may be expelled through the H_2 valve. This phenomenon would tend to introduce back pulsations which may cause the ball in the Rotometers to assume a lower equilibrium position and thus indicate lower flow.

3. Differential thermal contraction of clearance volume. In computing the clearance volume during hot conditions, it was assumed that the piston was at 400°F, the connecting rod at 300°F, and the cylinder at 300°F. If the piston and/or rod were at temperatures higher than those assumed or if the cylinder temperature were lower than that assumed, the clearance volume would diminish and the flows calculated from the indicator information would be reduced. The sonic limit shown in Figure 27 would not change, however, since expansion in the valve is negligible.

In summary, the H_2 flow measurements do not correlate well with theory and may be as much as 40% low at speeds in the 5000 to 6000 rpm range. Flow measurements in the 3000 rpm vicinity appear reasonable.

B. Rationalized Propellant Flow Characteristics

Based on the correlations of the previous section, Figure 27 shows the best interpretation of the propellant consumption during the testing. The H_2 flow is proportional to engine speed up to the sonic flow limiting condition, and the O_2 flow is constant with engine speed.

Based on the plots of Figure 27 and the measured power and engine speed data of Run 5149-11-8, BSPC and O/F versus engine speed are shown in Figure 28. For comparative purposes, the performance using measured propellant consumption is indicated.

The rationalized data yield slightly higher BSPC values than do the measured data. The most important difference is in the O/F trends. For the measured data, the value of O/F is a constant 4.6. For the rationalized data, the value of O/F decreases with speed to 4950 rpm and is constant as speed increases above 4950 rpm.

To further substantiate the rationalized propellant flow, a calculation was made to determine the ratio of gas constants for the 3000 and 5200 rpm runs. These were calculated at conditions just prior to blowdown, using indicator data.

Using the equation of state,

$$PV = w R T$$

Where

w = Unit change = $W/60 \cdot n$

in which

W = Propellant flow, lbs/HP-hr

n = rpm

and

$T = \gamma \cdot T_{ex}$, °R

Thus,

$$R = \frac{60 P V n}{WT}$$

and the gas constant ratio, R_a/R_b is

$$\frac{R_a}{R_b} = \left(\frac{P_a}{P_b}\right)\left(\frac{n_a}{n_b}\right)\left(\frac{T_b}{T_a}\right)\left(\frac{W_b}{W_a}\right)$$

SPU-2A-3 ENGINE
COMPARISON OF MEASURED AND RATIONALIZED PROPELLANT CONSUMPTION AND O/F RATIO

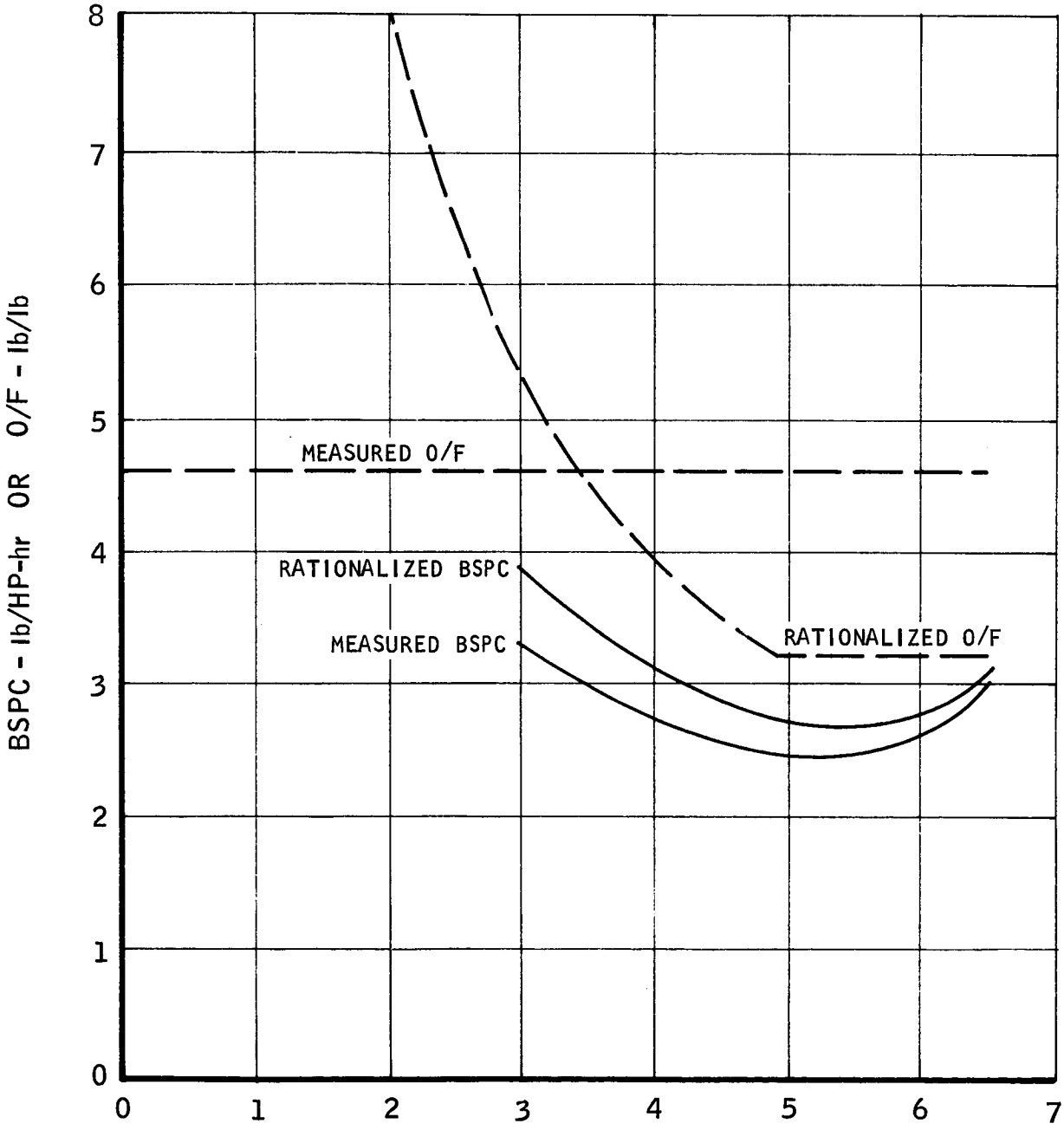

287-59

FIGURE 28

Using measured test data where propellant flows for 5200 and 3000 rpm are equal,

$$\frac{R_{5200}}{R_{3000}} = \left(\frac{P_{5200}}{P_{3000}}\right)\left(\frac{3000}{5200}\right)\left(\frac{T_{3000}}{T_{5200}}\right)$$

$$= \left(\frac{95}{115}\right)\left(\frac{5200}{3000}\right)\left(\frac{1980}{2150}\right)$$

$$= 1.32$$

Using rationalized data where $W_{3000} = 9.2$ pph and $W_{5200} = 10.32$ pph,

$$\frac{R_{5200}}{R_{3000}} = (1.32)\left(\frac{9.2}{10.32}\right)$$

$$= 1.17$$

Assuming complete combustion, theory indicates MW = 2 (1 + O/F), since O/F varies for the rationalized data case.

At 3000 rpm,

$$MW = 2\,(1 + 5.35)$$

$$= 12.7\ \frac{lb}{lb\ mole}$$

and

$$R_{3000} = \frac{1544}{12.7}$$

$$= 122\ \frac{ft}{^\circ R}$$

At 5200 rpm,

$$MW = 2(1 + 4.6)$$

$$= 11.2\ \frac{lb}{lb\ mole}$$

and

$$R_{5200} = \frac{1544}{11.2}$$

$$= 138 \frac{ft}{°R}$$

Thus for the rationalized data case

$$\frac{R_{5200}}{R_{3000}} = \frac{138}{122}$$

$$= 1.13$$

The correlation is very good (1.13 vs. 1.17) for the rationalized data case. Instrumentation errors and combustion inefficiencies could easily account for the discrepancy.

C. Combustion Efficiency

The combustion efficiency was estimated using the following method:

$$\eta_c = \frac{Q_{released}}{Q_{theoretically\ available}}$$

The actual heat release is

$$Q_{rel} = Work + Q_{rej\ to\ coolant} + Q_{ex}$$

and the theoretical heat added is

$$Q_{th} = 6440\ \dot{W}_{O_2}$$

Therefore

$$\frac{Q_{rel}}{lb\ prop.} = \frac{Work}{W_{pr}} + \frac{Q_{rej}}{W_{pr}} + \frac{Q_{ex}}{W_{pr}}$$

$$= (1 + Q/HP) \frac{2545}{BSPC} + C_p T_{ex}$$

Where

$$\frac{Q}{HP} = \frac{\text{Heat rejected}}{\text{Power output}}$$

and

$$\frac{Q_{th}}{\text{lb prop.}} = \frac{6440}{1 + F/O}$$

Thus

$$\eta_c = \left(\frac{1 + F/O}{6440}\right)\left(\frac{(1 + Q/HP)\ 2545}{BSPC}\right) + C_p\ T_{ex}$$

The following tabulation illustrates the heat balance and combustion efficiency characteristics at 3000 and 5200 rpm using measured propellant flow:

Speed (rpm)	Q/HP	BSPC (lb/HP-hr)	C_P (Btu/lb-°R)	T_{ex} (°R)	η_c
3000	2.06	3.19	0.885	1580	0.734
5200	1.61	2.43	0.885	1640	0.790

Using the rationalized propellant flow data, similar results are obtained, as shown in the tabulation below:

Speed (rpm)	Q/HP	BSPC (lb/HP-hr)	C_P (Btu/lb-°R)	T_{ex} (°R)	η_c
3000	2.06	3.34	0.885	1580	0.685
5200	1.61	2.67	1.16	1640	0.89

The principal conclusion is that combustion efficiency increases with engine speed. This is undoubtedly attributable to increased turbulence resulting in better mixing. Another conclusion can be drawn if the rationalized data are used. At the higher speeds, the O/F ratio is reduced which reduces the amount of O_2 injected per cycle. The greater excess of H_2 then provides greater probability of all the O_2 reacting with a stoichiometric amount of H_2.

Although high combustion efficiency is desirable, it is equally important that combustion occur early (near TDC) in the cycle. For instance, combustion occurring during exhaust blowdown produces no work--only heat rejection.

Analysis of the indicator diagrams indicated pronounced late burning throughout the 3000 rpm expansion. A lesser degree of late burning was noticed for the 5200 rpm case. The consistent pressure spikes at 3000 rpm indicated rapid combustion early in the cycle with a large percentage of the available oxidizer reacting. The temperatures during expansion were higher for the 5200 rpm case than for the 3000 case. Since initial combustion appeared better at 3000 rpm there was indication that the major portion of the energy was lost to the cylinder heat and to the piston before expansion began.

D. Indicator Diagram Analysis

The 5200 rpm test indicator diagram was plotted on log-log paper (See Figure 29) to analyze the expansion, compression, and filling processes. The analysis utilized the slope of the process line to determine whether heat addition, heat rejection, leakage, flow restriction, etc. were present. The negative slope, n, of the expansion and compression processes is the indicator. The value of n then is the polytropic constant.

For expansion processes,

$n < \gamma$ Indicates heat addition or leakage into the cylinder (Where γ = Specific heat ratio)

$n = \gamma$ Indicates isentropic expansion or $Q_{in} = Q_{out}$

$n > \gamma$ Indicates leakage from the cylinder, flow restriction, or heat rejection

For compression processes,

$n < \gamma$ Indicates heat rejection or leakage from the cylinder

$n = \gamma$ Indicates isentropic expansion or $Q_{in} = Q_{out}$

$n > \gamma$ Indicates heat addition or leakage into the cylinder

SPU-2A-3 ENGINE
INDICATOR DIAGRAM AT 5200 rpm

(RUN 5149-11-8-8)

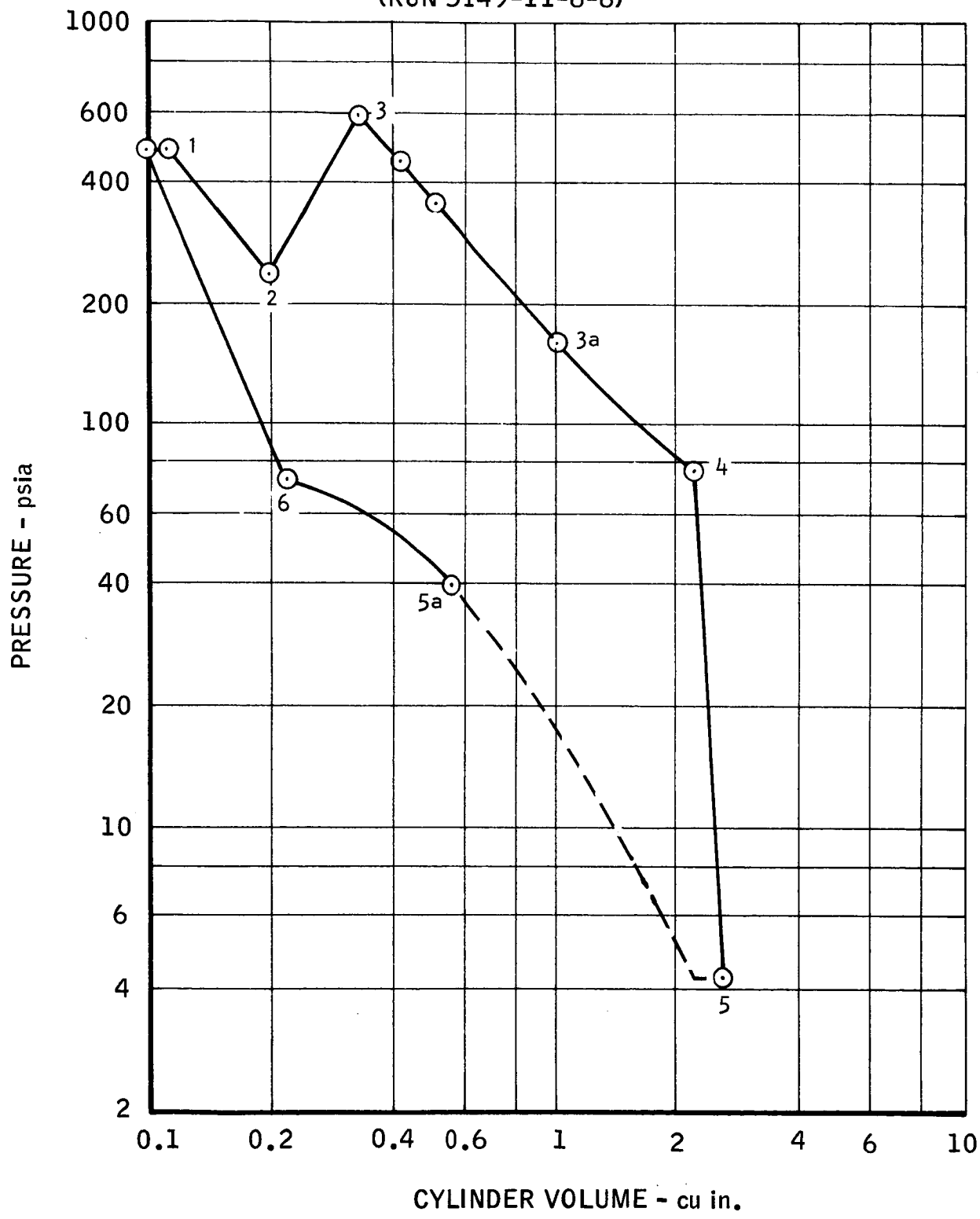

FIGURE 29

The following tabulation summarizes the conclusions drawn from Figure 29:

Process	n	Comments
1 - 2	1.1	Leakage not noticeable. High cyclic heat transfer from walls to H_2.
2 - 3	-1.86	Rapid O_2 injection and combustion heat release. Probable high heat rejection to cylinder.
3 - 3a	1.18	Nearly isentropic expansion or heat addition due to late burning only slightly higher than the heat transfer to the walls.
3a - 4	Approx. 1.0	Late burning indicated as constant gas temperature is implied in this range. A leaking O_2 valve could cause this condition.
4 - 5	--	Exhaust porting is too large as indicated by too rapid a blowdown which reduces BMEP.
5 - 5a	Approx. 1.6	Data difficult to plot accurately, but cyclic heat transfer to the gas, probably from the piston, is indicated. Inlet H_2 or O_2 valve leakage could also cause this increase in n.
5a - 6	Approx. 0.6	Reduction in n could be caused by leakage from the cylinder or cyclic heat transfer from the gas to the walls. It is probable that the TDC location is not accurately known.
6 - 1	2.42	Cylinder filling with H_2 appears satisfactory. No "wire drawing" is indicated.

Comparison of the two expansion curves plotted in Figure 30 leads to the following conclusions. The rapid decay in pressure with an indicated value of n of approximately 20 is indicative of excessively large heat rejection. Correlation with the measured exhaust gas temperatures indicates lower gas temperature during the late expansion for the lower speed case.

E. Heat Rejection Analysis

In a piston engine, the ratio of heat rejection to power is

$$\frac{Q}{HP} = \left(\frac{h\, A_s\, \Delta T}{P_m\, L\, A\, N}\right)\left(\frac{550}{2545}\right)$$

SPU-2A-3 ENGINE
EXPANSION AT 3000 AND 5200 rpm

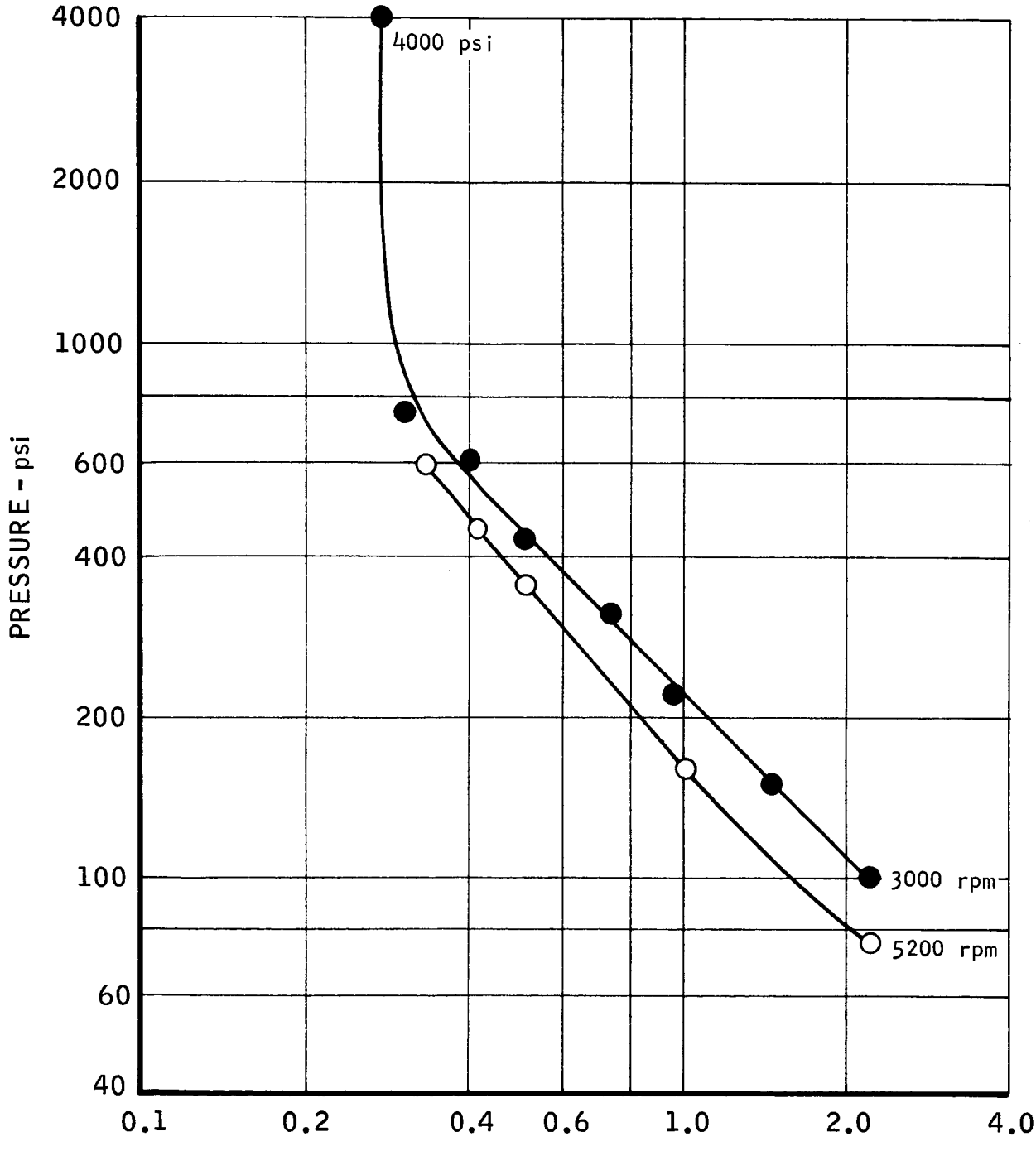

287-61

FIGURE 30

Where

ΔT = Mean temperature difference between the gas and the cylinder walls, °F

D = Bore, ft

L = Stroke = C_2 D, ft

A = $0.785\ D^2$, sq ft

N = $V/2\ L$, revolutions/second

h = Film coefficient, (Btu/hr ft^2 °F) · (1/3600)

A_s = $0.785\ D^2 + \pi\ D\ L$, sq ft

C_2 = Stroke/Bore

P_m = BMEP, lbs/ft^2

V = Piston speed, ft/sec

Making the substitution as noted above, the original equation may be rewritten as

$$\frac{Q}{HP} = \frac{H\ D^2\ (0.785 + C_2\ \pi)\ \Delta T\ (550)}{P_m\ L\ 0.785\ D^2\ (\frac{V}{2\ L})(2545)}$$

$$\frac{Q}{HP} = \frac{C_1\ H\ \Delta T}{P_m\ V}$$

Where

$$C_1 = \frac{(0.785 + C_2\ \pi)\ 2\ (550)}{(0.785)\ (2545)}$$

$$= 0.55\ (0.785 + C_2\ \pi)$$

Assuming two similar engines producing the same power at the same speed. (i.e., V, B, and P are equal for Cases a and b)

$$\frac{Q_a}{Q_b} = \frac{h_a \Delta T_a}{h_b \Delta T_b}$$

The film coefficient for air/hydrocarbon products as suggested by Taylor and Taylor* can be calculated from the expression

$$\frac{h D}{k} = 10.4 R_e^{0.75}$$

Where

R_e = Reynolds number = $\frac{\rho V D}{\mu}$

k = Gas normal conductivity

Applying the usual turbulent flow Prandtl number correction yields

$$\frac{h D}{k} = 10.4 R_e^{0.75} P_r^{1/3}$$

Solving for h and simplifying,

$$h = 10.4 \, k/D \, R_e^{0.75} P_r^{1/3}$$

$$h = 10.4 \rho V C_P \left(\frac{k}{C_p \mu}\right) \left(\frac{\mu}{\rho V D}\right)^{0.25} P_r^{1/3}$$

$$h = \frac{10.4 \rho V C_P}{P_r^{2/3} R_e^{0.25}}$$

Where

C_P = Gas specific heat

* Taylor, C. F. and E. S. Taylor," The Internal Combustion Engine", International Textbook Co., J. Wiley & Co., New York, N. Y., 1961.

Using this expression in the Q ratio equation produces

$$\frac{Q_a}{Q_b} = \left(\frac{\rho_a}{\rho_b}\right)^{0.75} \left(\frac{C_{pa}}{C_{pb}}\right) \left(\frac{\mu_a}{\mu_b}\right)^{0.25} \left(\frac{P_{rb}}{P_{ra}}\right)^{2/3} \left(\frac{\Delta T_a}{\Delta T_b}\right)$$

Which can be expressed as

$$\frac{Q_a}{Q_b} = \left(\frac{R_a}{R_b}\right)^{0.25} \left(\frac{\mu_a}{\mu_b}\right)^{0.25} \left(\frac{T_b}{T_a}\right)^{0.75} \left(\frac{\Delta T_a}{\Delta T_b}\right) \left(\frac{\gamma_a}{\gamma_b}\right) \left(\frac{\gamma_b - 1}{\gamma_a - 1}\right) \left(\frac{P_{rb}}{P_{ra}}\right)^{2/3}$$

Consider two similar engines operating at an exhaust temperature of 2240°R.

With Case a	With Case b
$O/F = 5.3$	$O/F = 2.0$
$P_{ra} = 0.59$	$P_{rb} = 0.517$
$T_a = \frac{5490 + 2240}{2} = 3865°R$ (avg)	$T_b = \frac{3600 + 2240}{2} = 2920°R$ (avg)
$\Delta T_a = 3865 - 860 = 3005°R$	$\Delta T_b = 2920 - 860 = 2060°R$
$\mu_a = 614 \times 10^{-6}$ centipoise	$\mu_b = 467 \times 10^{-6}$ centipoise
$\gamma_a = 1.24$	$\gamma_b = 1.3$
$R_a = 122$	$R_b = 258$
$T_{ex} = 2240°R$ (assumed)	$T_{ex} = 2240°R$ (assumed)
$r_e = 36$	$r_e = 5$

Applying these factors yields

$$\frac{Q_a}{Q_b} = \left(\frac{122}{258}\right)^{0.25} \left(\frac{615 \times 10^{-6}}{466 \times 10^{-6}}\right) \left(\frac{2920}{3865}\right)^{0.75} \left(\frac{3005}{2060}\right) \left(\frac{1.24}{1.3}\right) \left(\frac{0.3}{0.24}\right) \left(\frac{0.517}{0.59}\right)^{2/3}$$

$$= (0.83)\ (1.31)\ (0.81)\ (1.46)\ (0.955)\ (1.25)\ (0.917)$$

$$= 1.4$$

Thus it appears that increasing O/F ratios increase the heat rejected by an engine operating at constant BMEP and rpm.

Since power increases directly with speed, BMEP is constant, and the heat rejection varies as $(\text{BMEP} \times n)^{0.75}$. Then

$$\frac{Q}{HP} \text{ varies as } \left(\frac{1}{n}\right)^{0.25} \left(\frac{1}{\text{BMEP}}\right)^{0.25}$$

For example, with constant O/F and BMEP,

$$\frac{(Q/HP) \text{ at } n = 5200}{(Q/HP) \text{ at } n = 3000} = (3000/5200)^{0.25}\ (188/144)^{0.25} = 0.932$$

Comparing this result with the test data at the same conditions,

$$\frac{(Q/HP) \text{ at } n = 5200}{(Q/HP) \text{ at } n = 3000} = 1.61/2.06 = 0.78$$

The trend is correct, but numerous effects such as combustion inefficiency, accuracy of measurements, etc., render a different numerical answer.

Summarizing, Q/HP increases as

1. O/F ratio increases

2. Speed decreases

3. BMEP decreases

F. Performance Improvement Trends

Figure 31 illustrates the BSPC and O/F improvement which can result from increases in expansion ratio. Increasing expansion ratio decreases BSPC and increases the permissible O/F ratio.

Figure 32 illustrates the effect of heat rejection on BSPC and O/F ratio. Increases in Q/HP degrade performance (BSPC) and increase the required O_2 flow. H_2 flow is not influenced by Q/HP. The higher expansion ratio case is more sensitive to the changes in Q/HP than is the lower expansion ratio case.

Figure 33 indicates the increases in BSPC and O/F caused by reduction in combustion efficiency. Combustion efficiency losses increase only the required O_2 flow, not the H_2 flow.

G. Vacuum Operation

Difficulty in starting and backfiring while operating at low back pressures may be attributed to one or more of the following reasons:

1. Recompression of residuals maintains a hot environment into which the incoming H_2 is injected. After H_2 injection, the mixture temperature is higher than when residuals are not present.

2. Residuals may contain free OH radicals which may act as a catalyst to the H_2 - O_2 reaction.

3. The hot piston dome, which aids in initiating combustion, may lose less heat to the cylinder walls during the recompression stroke when residuals are present.

4. Some turbulence may be generated in any residuals remaining in the cylinder during the "up stroke" which may ultimately add to the overall turbulence which vitally affects the combustion process.

5. Glow plug quenching may be reduced when hot residuals are present.

SPU-2A-3 ENGINE
EFFECT OF EXPANSION RATIO ON BSPC AND O/F RATIO

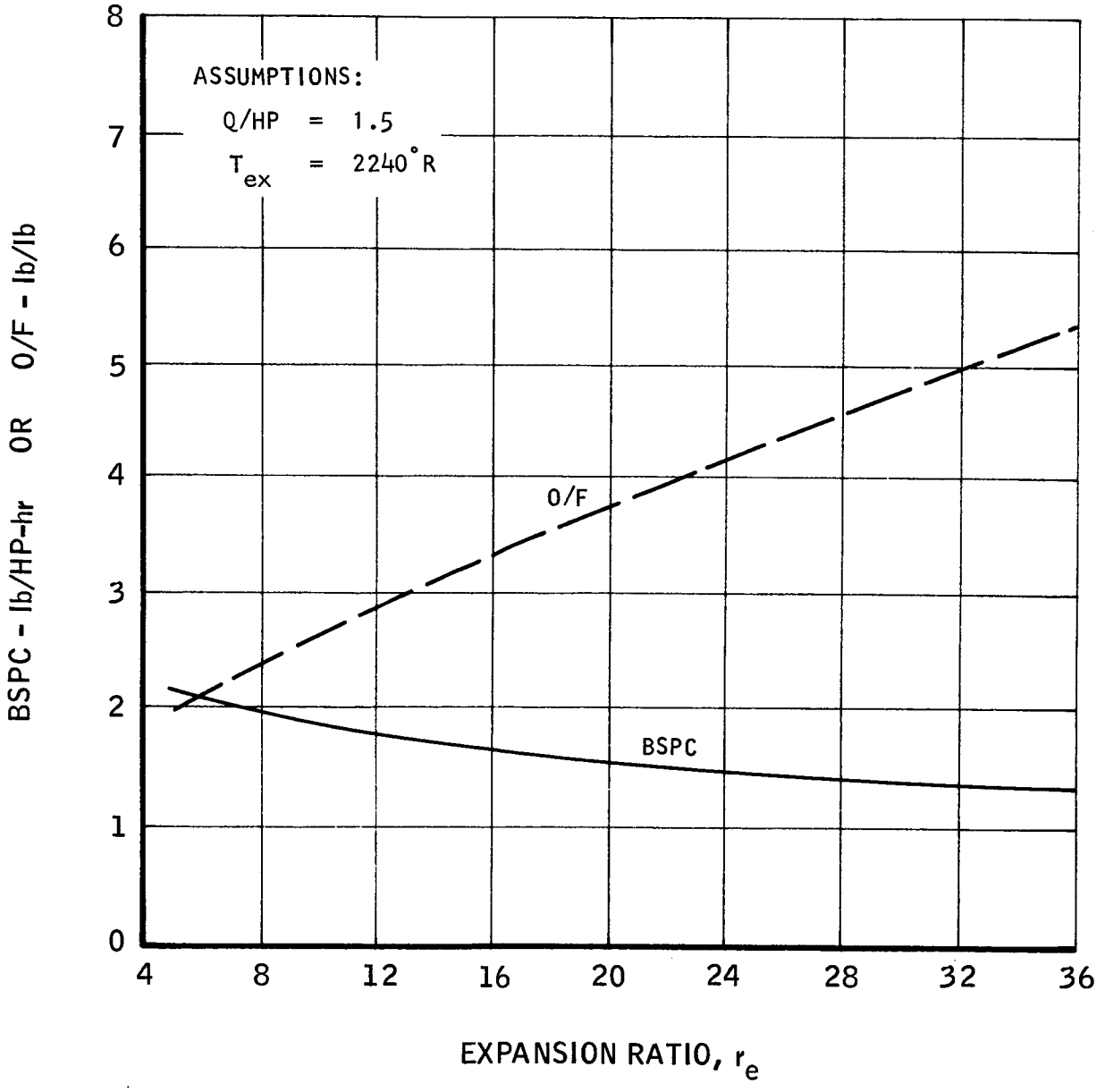

287-62

FIGURE 31

SPU-2A-3 ENGINE
EFFECT OF HEAT REJECTION ON BSPC AND O/F RATIO

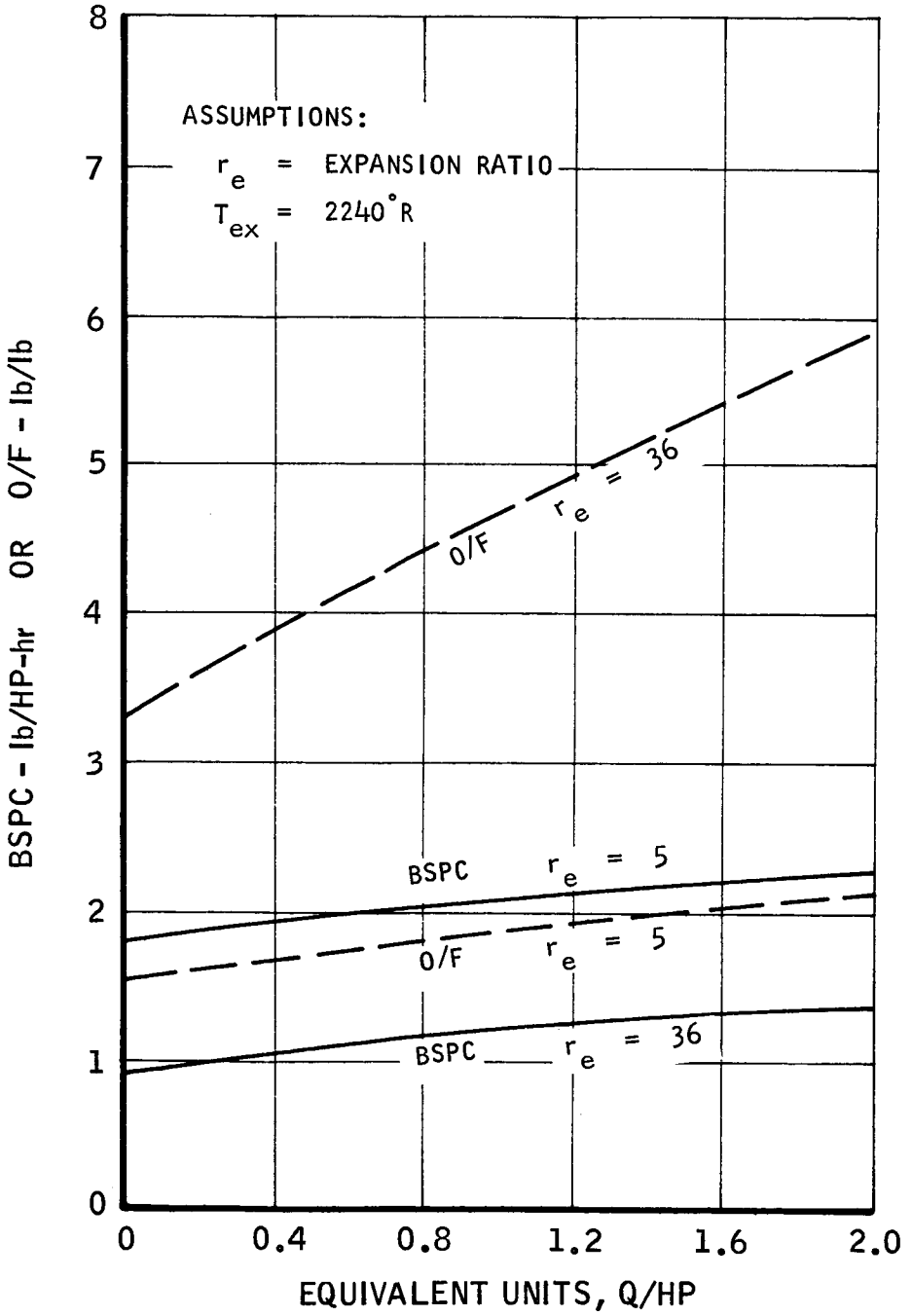

FIGURE 32

SPU-2A-3 ENGINE
EFFECT OF COMBUSTION EFFICIENCY ON BSPC AND O/F RATIO

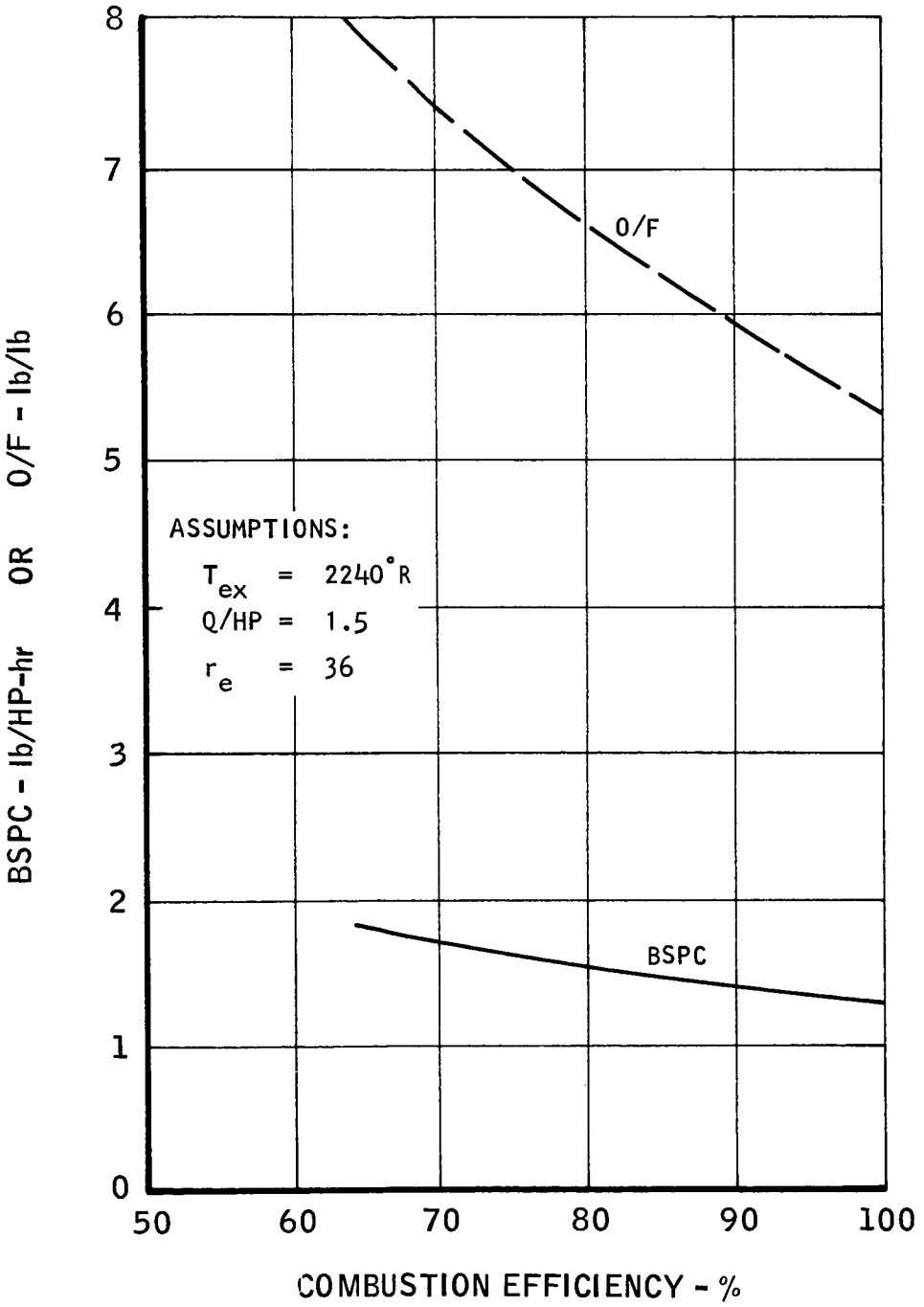

Limitation on experimental time and funding level precluded tests which would provide more insight into the combustion phenomena with low back pressures.

H. Conclusions

The following conclusions are evident from a review of the test data:

1. Measured BSPC is 50% higher than theoretical BSPC.
2. Heat rejection decreases as engine speed increases.
3. Heat rejection increases as O/F and expansion ratio increase.
4. Hydrogen flow measurements are not consistent with analysis of H_2 flow from indicator diagrams.
5. Combustion efficiency is on the order of 60 to 90%, the higher values being attained at higher speed.
6. Late combustion is evident at all engine speeds tested.
7. Leakage past the piston rings, valve ports, etc. did not appear to be significant.
8. Future testing should be conducted with the O_2 injection immediately following or slightly overlapping the H_2 injection, reduced piston cooling, and particularly with improved combustion chamber designs for greater turbulence. All these factors should reduce BSPC.
9. System studies indicate the superiority of H_2 - O_2 reciprocating engines with O/F ratios between 4 and 5 over turbines for durations in excess of 15 hours and over fuel cells for durations less than 160 hours.

VII. TEST FACILITY AND EQUIPMENT

A. General Description

The test facilities used for the hypergolic space power unit were modified and utilized for the SPU-2A-3 hydrogen-oxygen engine. A general view of the installation of the engine in the test facility is shown in Figure 34. A major addition was made to the existing test facilities to control and measure the flow rates of hydrogen and oxygen propellants. The major components of the facility are as follows:

1. The test stand with all necessary mounts for mechanical, electrical, and instrumentation components
2. An engine starting mechanism and power supply
3. An engine power absorption unit
4. A self-regulating engine cooling system
5. A temperature regulated oil supply and scavenging system
6. An exhaust ejector and altitude simulation system
7. A large volume, high pressure hydrogen and oxygen propellant system
8. A glow plug power supply and control system

B. Description of Test Facility Subsystems

1. Propellant Supply System

The test facility propellant supply system is shown schematically in Figure 35. This system is composed of high pressure gaseous hydrogen and gaseous oxygen supply tanks, an oxygen manifold pressure boost pump, a flow measuring system, and the necessary plumbing and control equipment to regulate the propellant supply to the engine. The propellant supply system also includes a very precise filtering system. Propellants entering the test engine are filtered to 1/2 micron absolute. The oxygen and hydrogen propellant storage is sufficient to allow engine operation in excess of 50 hours and can supply propellants at pressures up to 2200 psi.

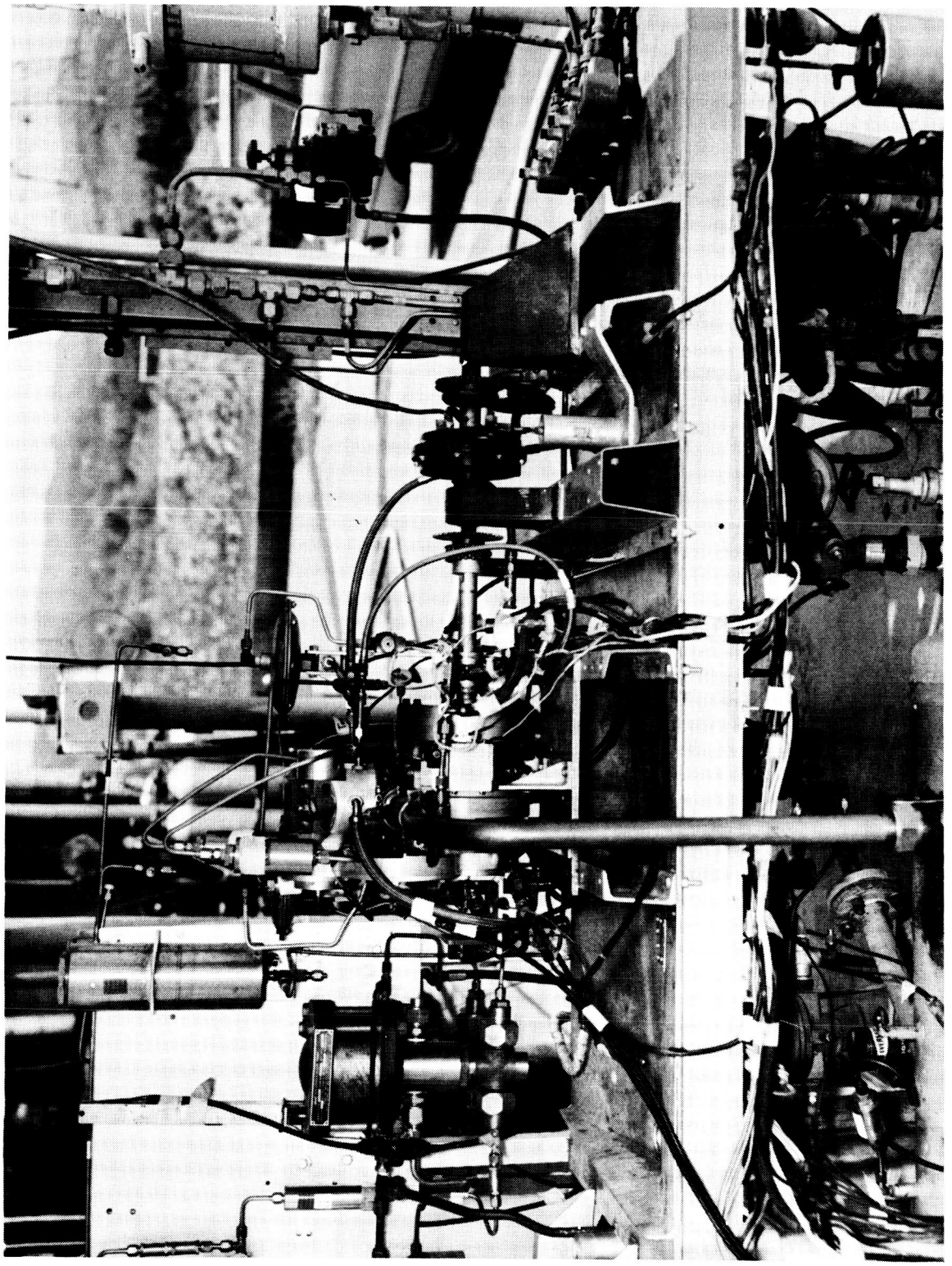

FIGURE 34. SPU-2A-3 Engine Installed in the Test Facility

T5149-15

SCHEMATIC OF THE PROPELLANT SYSTEM FOR THE SPU-2A-3 ENGINE TEST

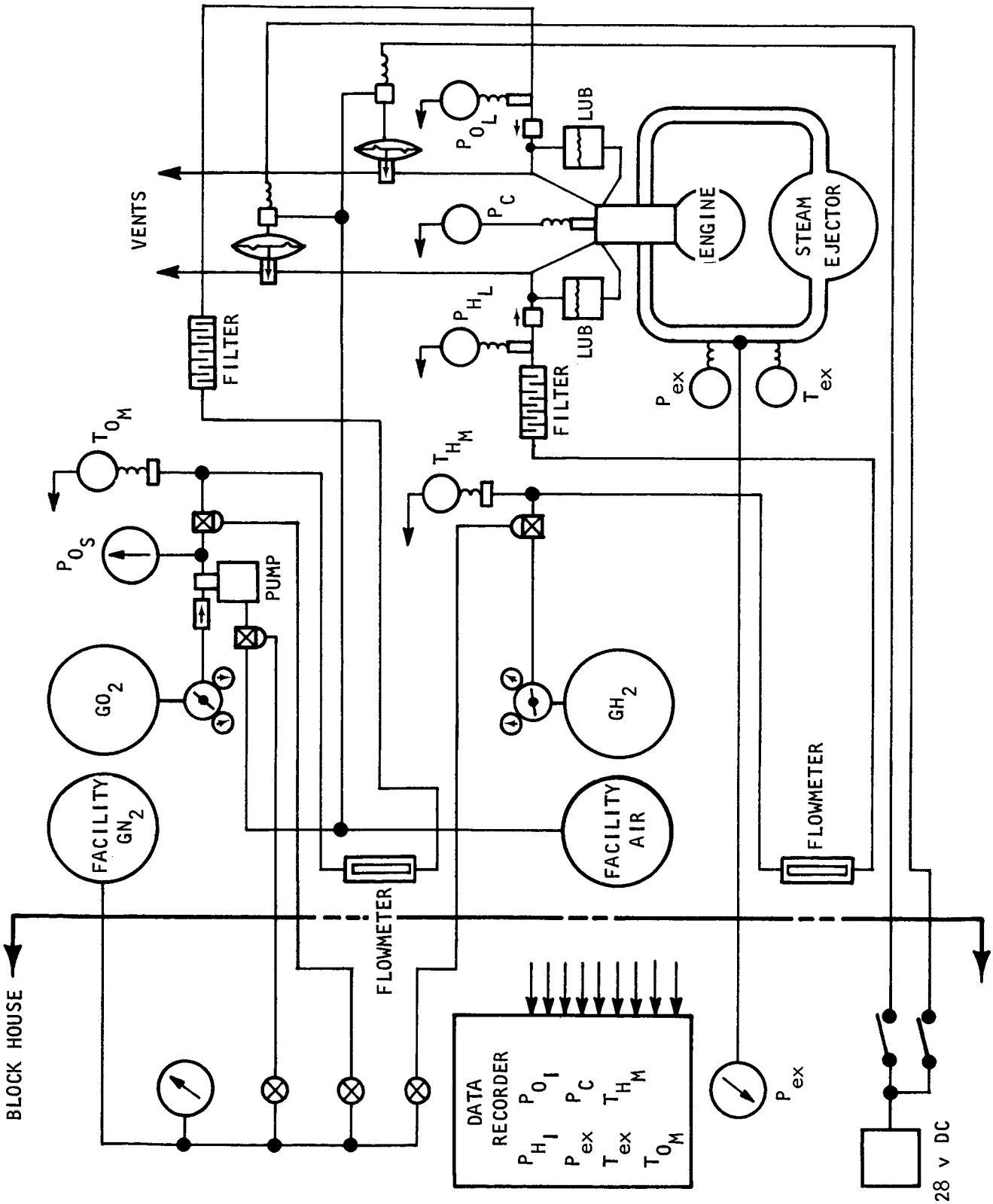

287-78

FIGURE 35

The exhaust products from the engines are removed by a two-stage steam ejector system. This system is capable of continuous operation at 0.5 psia when the SPU-2A-3 test engine is operating at maximum power and rpm.

2. Cooling System

A schematic diagram of the cooling system is presented in Figure 36. This system automatically regulates the inlet coolant temperature at any temperature between ambient temperature and 200°F. In addition to temperature regulation, the coolant flow rate is also adjustable over a broad flow range. The cooling system is activated during engine startup and it will maintain preset conditions of flow rates (0.1 to 5.0 gpm) and inlet temperatures (ambient temperature to 200°F for water). An automatic over-temperature warning system is provided. This system will actuate if the exit temperature exceeds a preset value (normally 170°F) and it will signal the inlet temperature regulator to reduce the inlet coolant temperature until the high exit temperature is corrected. Heat input to the coolant is accurately determined by the flow and temperature instrumentation.

3. Oil System

The oil system is composed of a tank complete with temperature control, a high pressure pump, a low pressure high volume scavenge pump, a 2 micron filter, a quantity gage, and the necessary plumbing and control components. This system is shown schematically in Figure 37. This system is capable of handling both petroleum and synthetic lubricants.

4. Drive System and Ignition System

The drive system is composed of the following major elements: a starting system, a torque absorption unit (dynamometer), a top center indicator, a crankshaft position indicator, and a glow plug activation system. A schematic diagram of the system is shown in Figure 38. The starting system is a 12 volt starting motor transmitting rotation via an overrunning clutch to the engine. The water dynamometer provides accurately controlled absorption of power of up to 15 HP and allows speeds up to 10,000 rpm. To facilitate engine testing, the dynamometer is precalibrated with fixed orifices in the dynamometer water inlet line. Several orifices were calibrated and arranged to form a valve tree. The location of this tree relative to the dynamometer system is shown in the schematic (Figure 38). The crankshaft position indicator is a rotary potentiometer which is capable of being driven at high speeds. This device is attached to the crankshaft of the test engine and when it is used in conjunction with the cylinder pressure transducer, a top center indicator, and oscilloscope it will produce indexed continuous diagrams of cylinder pressure versus crankshaft position. These data are recorded photographically for later reduction into pressure versus volume plots.

SCHEMATIC OF COOLING SYSTEM FOR THE SPU-2A-3 ENGINE TEST

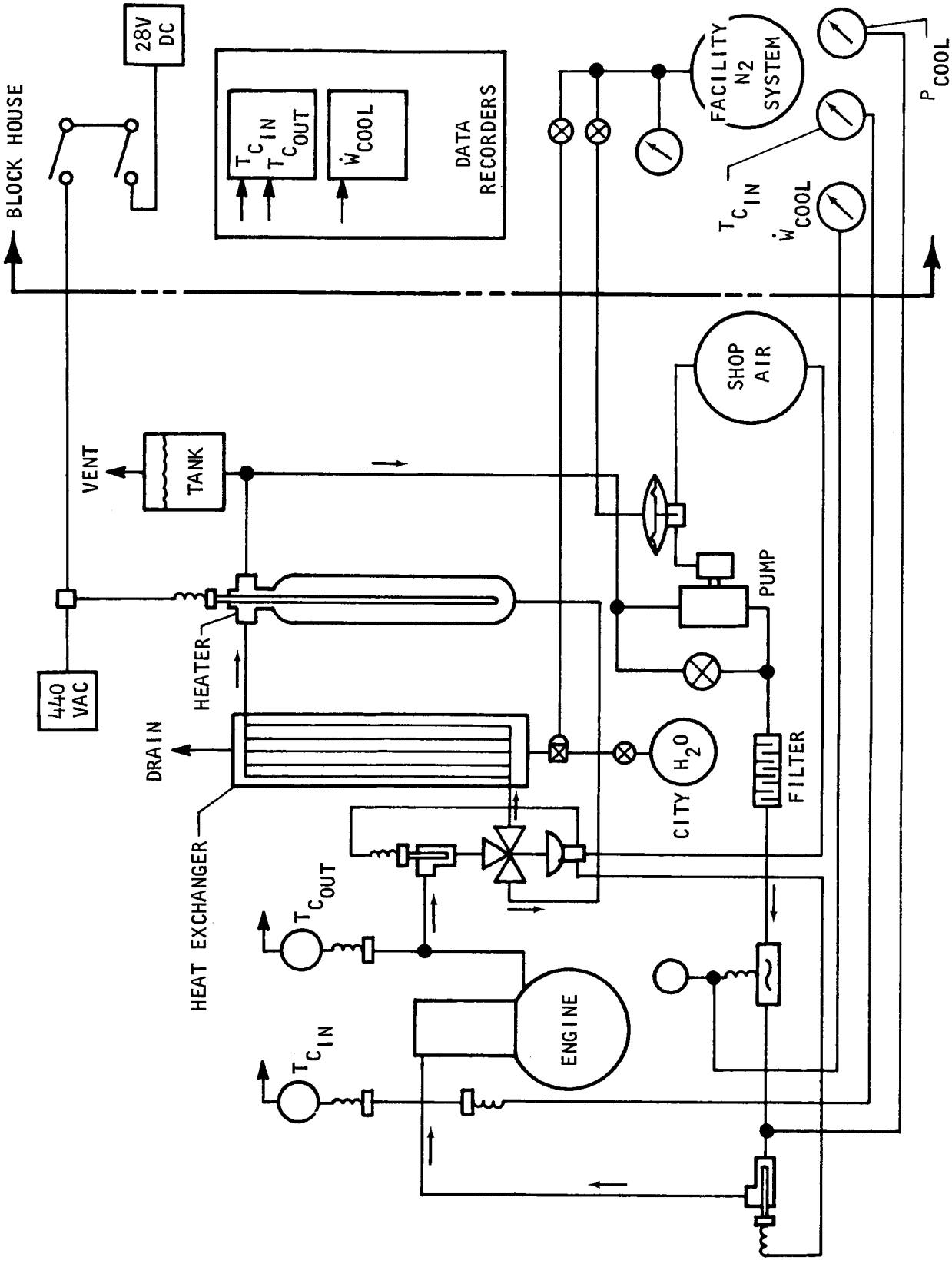

287-79

FIGURE 36

SCHEMATIC OF OIL SYSTEM FOR THE SPU-2A-3 ENGINE TEST

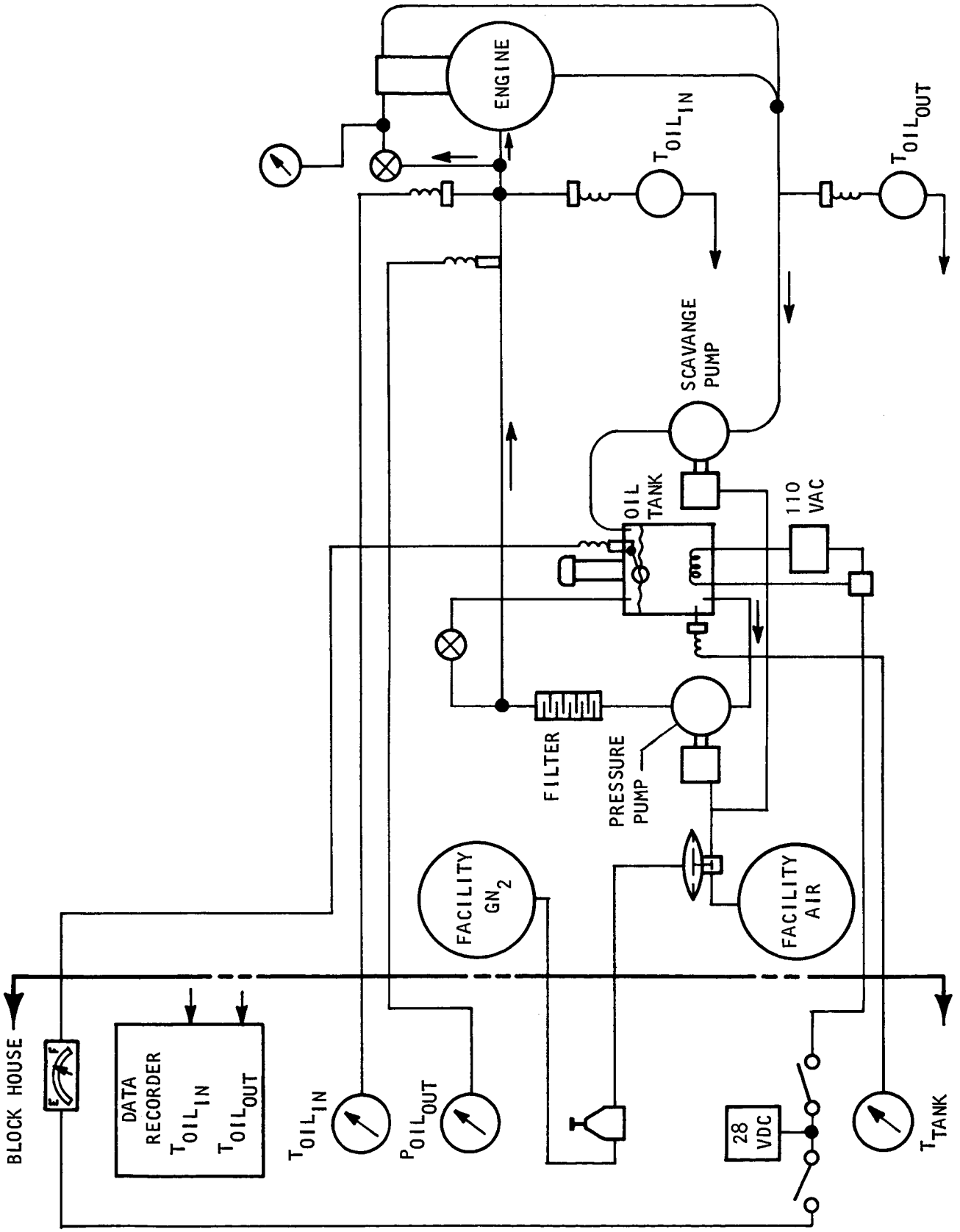

FIGURE 37

SCHEMATIC OF THE DRIVE SYSTEM FOR THE SPU-2A-3 ENGINE TEST

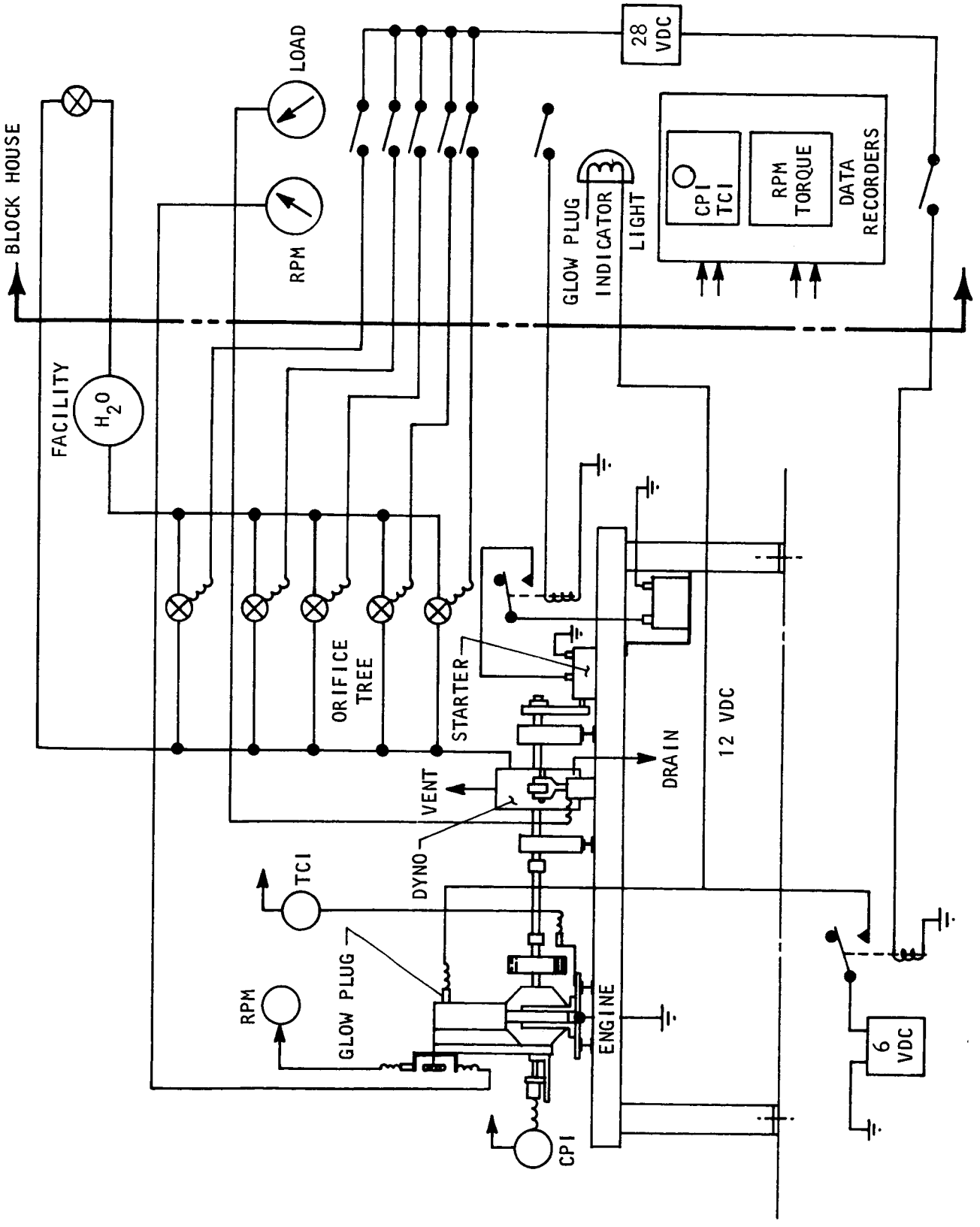

287-81

FIGURE 38

5. Instrumentation

The instrumentation provided to document engine performance is shown in Table III. The instrumentation list is divided into visual and recorded sections. The visual instrumentation operates continuously during engine operation to allow precise setting of engine run conditions and manual recording of performance parameters. The data recording system may be operated continuously during short engine test periods or intermittently, utilizing the random sampling technique, during long duration engine testing. The locations of each transducer necessary to produce the required data are shown in the various system schematics (Figures 35 to 38).

C. Component Test Capability

In addition to support, control, and documentation of full scale engine operation, the test facility provides the capability of testing engine components and subsystems. The basic facility is augmented with additional mounts and drive systems for dynamic injector valve development testing. The cylinder head assembly of the SPU-2A-3 engine can be mounted on the test pad and supplied with propellants from the facility propellant system and it can be driven at speeds up to 5600 rpm with a remotely actuated air driven motor system. The drive system is equipped with a torque limiter to preclude extensive damage to the test item components in the event of a component malfunction.

D. Facility Performance

The performance of the facility throughout the test program was excellent. All engine support systems performed without malfunction during both component testing and engine testing. The facility did impose one performance limiting factor on the engine, namely the propellant flowmeters. The meters were specially built Rotometers rated for 3000 psi service. Because of the physical characteristics of hydrogen, the Rotometer fabricated for these tests was calibration limited to a flow of 2.7 pph at an injection pressure of 1480 psi. Since the test engine operated at hydrogen injection pressures of approximately 500 psi, the usable range of the flowmeter was only 1.6 pph. This range was not sufficient to allow the engine to be operated at rated power. The short length and funding level of the test program did not afford sufficient time to obtain a flowmeter of adequate range.

Another limitation imposed by the flowmeters resulted from the fact that automatic recording of flow data could not be obtained from the Rotometers. This limitation precluded obtaining transient flow conditions or dynamic effects of the injector valves at any condition. Future test programs will require a more sophisticated flow measuring system.

TABLE III

SUMMARY OF SPU-2A-3 TEST INSTRUMENTATION

Parameter	Symbol	Range	Display Method	
			Recorded	Visual
Combustion chamber pressure	P_c	0 to 5000 psi	x	--
Crank position indicator	CPI	0 to 360°	x	--
Top center indicator	TCI	TC $\pm$ 0.5°	x	--
Engine speed	rpm	0 to 6000 rpm	x	x
Engine load	L	0 to 20 lbs	x	x
Facility GN_2 pressure	P_{N_2}	0 to 1000 lbs	--	x
Oxygen tank pressure	P_{O_t}	0 to 2500 psi	--	x
Oxygen supply pressure	P_{O_s}	0 to 2500 psi	--	x
Oxygen injection pressure	P_{O_i}	0 to 4000 psi	x	x
Hydrogen injection pressure	P_{h_i}	0 to 2000 psi	x	x
Exhaust manifold pressure	P_{ex}	0 to 1 atmos.	x	x
Oil manifold pressure	$P_{oil_{in}}$	0 to 75 psi	--	x
Cylinder head oil pressure	$P_{cyl_{in}}$	0 to 20 psi	--	x
Coolant pressure	P_{cool}	0 to 30 psi	--	x
Oxygen flow rate	W_O	0 to 10 pph	--	x
Hydrogen flow rate	$\dot{W}_h$	0 to 2.7 pph	--	x
Coolant flow rate	$\dot{W}_{cool}$	0.1 to 1.0 gpm	x	x

TABLE III (Continued)

Parameter	Symbol	Range	Display Method	
			Recorded	Visual
Exhaust temperature	T_{ex}	0 to 2000°F	x	--
Oxygen manifold temperature	T_{Om}	0 to 500°F	x	--
Hydrogen manifold temperature	T_{hm}	0 to 250°F	x	--
Oil inlet temperature	$T_{oil_{in}}$	0 to 250°F	x	--
Oil outlet temperature	$T_{oil_{out}}$	0 to 250°F	x	--
Oil tank temperature	T_{Tank}	0 to 250°F	--	x
Coolant inlet temperature	$T_{c_{in}}$	0 to 250°F	x	x
Coolant outlet temperature	$T_{c_{out}}$	0 to 250°F	x	--
Oil tank level	L_{o_t}	Empty to full	--	x

VIII. CONCLUSIONS

The multifuel capabilities of the Marquardt hypergolic engine have been conclusively demonstrated. The structural integrity of the engine as designed for hypergolic operation was proven to be adequate at extremes of engine operation including stoichiometric mixture ratios and extremely high chamber pressures. In addition, only a minimum of conversion for multifuel operation was required due to the versatility of the injection system which has proven equally efficient and reliable for gaseous propellant operation. The use of a glow plug was proven as a positive and reliable method of igniting the hydrogen-oxygen mixtures. The propellant compatible lubricant (duPont PR143) provided the necessary, safe lubrication for valve operation and added immeasurably to the reliability and life of these components.

IX. RECOMMENDATIONS

During the multifuel feasibility demonstration of the hypergolic engine, development was advanced sufficiently such that the specific propellant consumption, power output, and heat rejection meet the requirements of some space applications. The important area for immediate development is the upgrading of engine reliability and endurance. This requires a program of extended duration testing through the simulated mission power-time profile and continued improvement of components.

Concurrent with the endurance-reliability program of the basic engine, analytical and developmental efforts should be directed toward the formulation of a space suitable system using the multifuel engine as the nucleus. This would require investigation and space simulated testing and development of the following subsystems:

1. Lubrication system
2. Cooling system
3. Starting system
4. Power and speed control system
5. Generator and electrical control

These development and functional requirements are common with the hypergolic engine system. Therefore, the development costs could be shared by each program.

However, for the gaseous hydrogen-oxygen engine system, the following systems are unique and each must be developed in its own program:

1. Boil-off utilization system
2. Propellant pressurization pumps
3. Auxiliary ignition (Glow plug)
4. Exhaust pressure control

Although good performance in specific propellant consumption has already been obtained, it is possible to make substantial improvements by the following changes:

1. Advancing the timing of the oxygen injection toward top center
2. Removing the "deadband" between the end of the hydrogen injection and the start of oxygen injection
3. Creating turbulence in the combustion chamber for better mixing of gases
4. Increasing the expansion ratio
5. Repositioning the glow plug, i.e., removal of the long passage between the combustion chamber and the glow plug
6. Increasing the operating temperature of the engine

Most of these changes do not require physical alterations of components and could be immediately investigated at the onset of a development program.

Heat rejection in space is a difficult problem and any reduction in such is highly desirable. A program to accomplish this reduction would include an analytical effort and a test effort.

APPENDIX A

PERFORMANCE COMPARISON OF CANDIDATE H_2-O_2 POWER SYSTEMS FOR EXTENDED MISSIONS IN SPACE

A-I. SYSTEMS COMPARED

Optimistic and conservative assumptions were made for the following power systems for extended missions in space:

1. H_2-O_2 turbine (multiple re-entry)/alternator
2. H_2-O_2 regenerative internal combustion reciprocating engine/alternator
3. H_2-O_2 stoichiometric combustion reciprocating engine/alternator
4. H_2-O_2 high temperature (Apollo type) fuel cell

A-II. ASSUMPTIONS

1. Redundancy

   2 dynamic systems at rated power

   1 1/2 fuel cells at rated power

2. Propellant Tankage

   Supercritical tankage was assumed.

3. Radiator Aspects

   Considered as intergral with the fuel cell system with no additional weight penalty.

   Not required with a turbine system.

   Required with H_2-O_2 reciprocating engine systems.

4. Checkout and Temperature Conditioning

   Dynamic systems can be checked out prior to usage sufficiently with propellant to be vented (viz S/C boiloff).

APPENDIX A (Continued)

5. Specific Weights (5 HP Systems)

SPU Type	Without Redundancy (lbs/HP)	With Redundancy (lbs/HP)
Turbine SPC system	20	40
Reciprocating SPU system	25	50
Fuel cells	75	112.5
Radiator for reciprocating system		
When Q/hp = 0.5	10	Not required
Q/hp = 1.5	30	Not required

6. Specific Weights (20 HP Systems)

SPU Type	Without Redundancy (lbs/HP)	With Redundancy (lbs/HP)
Turbine SPU systems	16	32
Reciprocating SPU systems	20	40
Fuel cells	67	100.5
Radiator for reciprocating systems		
When Q/hp = 0.5	8	Not required
Q/hp = 1.5	24	Not required

APPENDIX A (Continued)

7. BSPC, O/F and Q/hp (Average Conditions)

SPU Type	BSPC (lb/HP-hr)	O/F	(Not regenerated)
Optimistic Assumptions:			
Turbine (η_T = 0.70, T_{in} = 2460°R)	2.24	1.66	0
Reciprocating SPU systems	1.3	5	0.5
Fuel cells	0.7	8	0*
Conservative Assumptions:			
Turbine (η_T= 0.45, T_{in} = 2460°R)	3.48	1.66	0
Reciprocating SPU systems	1.5	4	1.5
Fuel cell	0.85	8	0*

*Fuel cell heat rejection by radiator accounted for in specific weight.

8. Propellant Tankage Weights

SPU Type	O/F	W Tank/W Propellant
Turbine	1.66	$0.27 + 0.307\ \theta_w$
Reciprocating (Optimistic)	5	$0.173 + 0.231\ \theta_w$
Reciprocating (Conservative)	4	$0.185 + 0.247\ \theta_w$
Fuel cell	8	$0.150 + 0.210\ \theta_w$

Where θ_w is the storage time (prior to usage) in weeks.

APPENDIX A (Continued)

9. Average Power

The average power during operation is assumed to be 1/2 rated power.

A-III COMPARATIVE RESULTS

Figures A-1, A-2, and A-3 indicate the relative regions of superiority of the candidate space power systems for various conditions of storage and length-of-use time.

ENDURANCE OF TURBINE, STOICHIOMETRIC RECIPROCATING ENGINE, AND FUEL CELL USING CONSERVATIVE ASSUMPTIONS

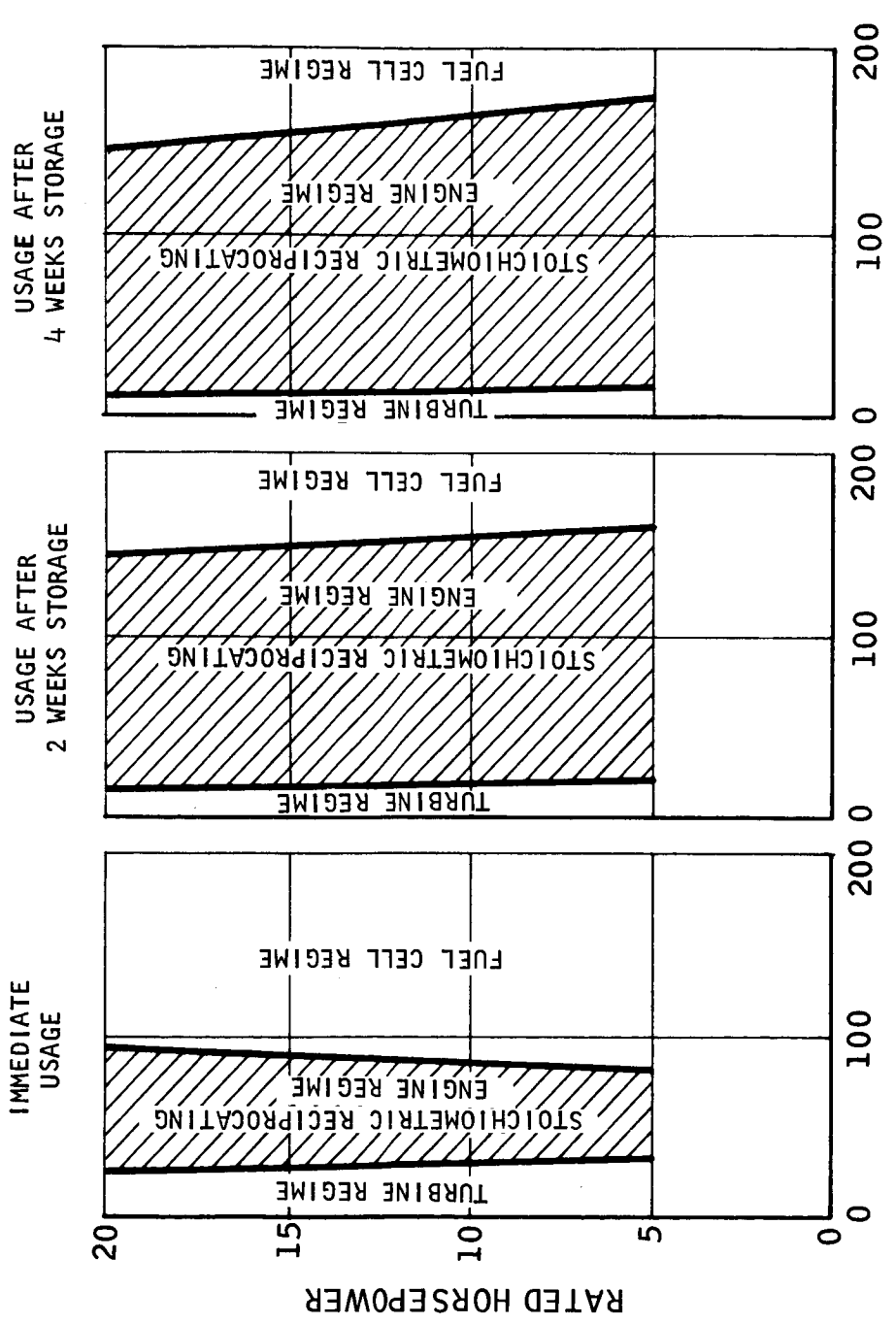

FIGURE A-1

ENDURANCE OF TURBINE, STOICHIOMETRIC RECIPROCATING ENGINE, AND FUEL CELL USING OPTIMISTIC ASSUMPTIONS

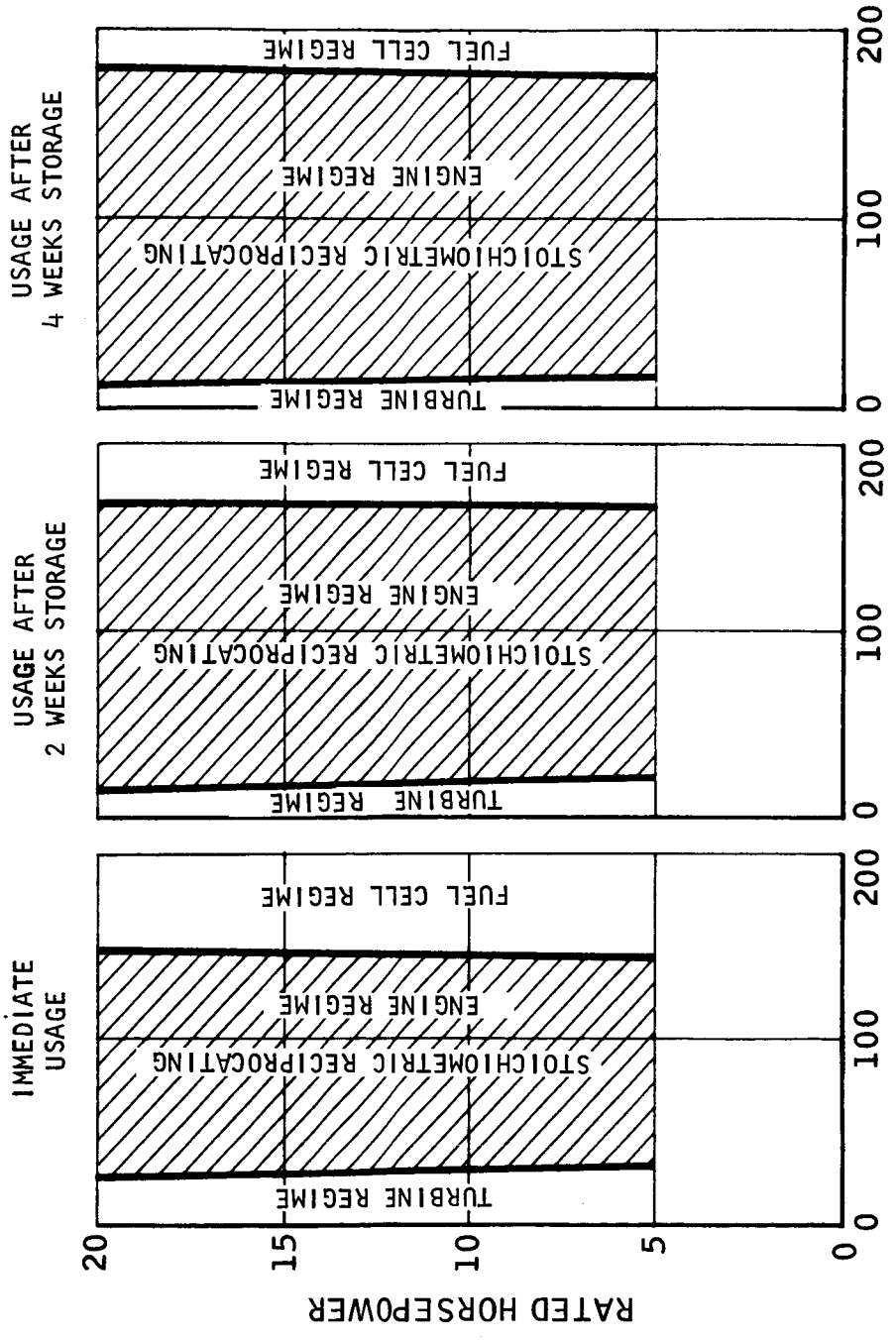

287-73 A

FIGURE A-2

ENDURANCE OF TURBINE, REGENERATIVE RECIPROCATING ENGINE, AND FUEL CELL USING OPTIMISTIC ASSUMPTIONS

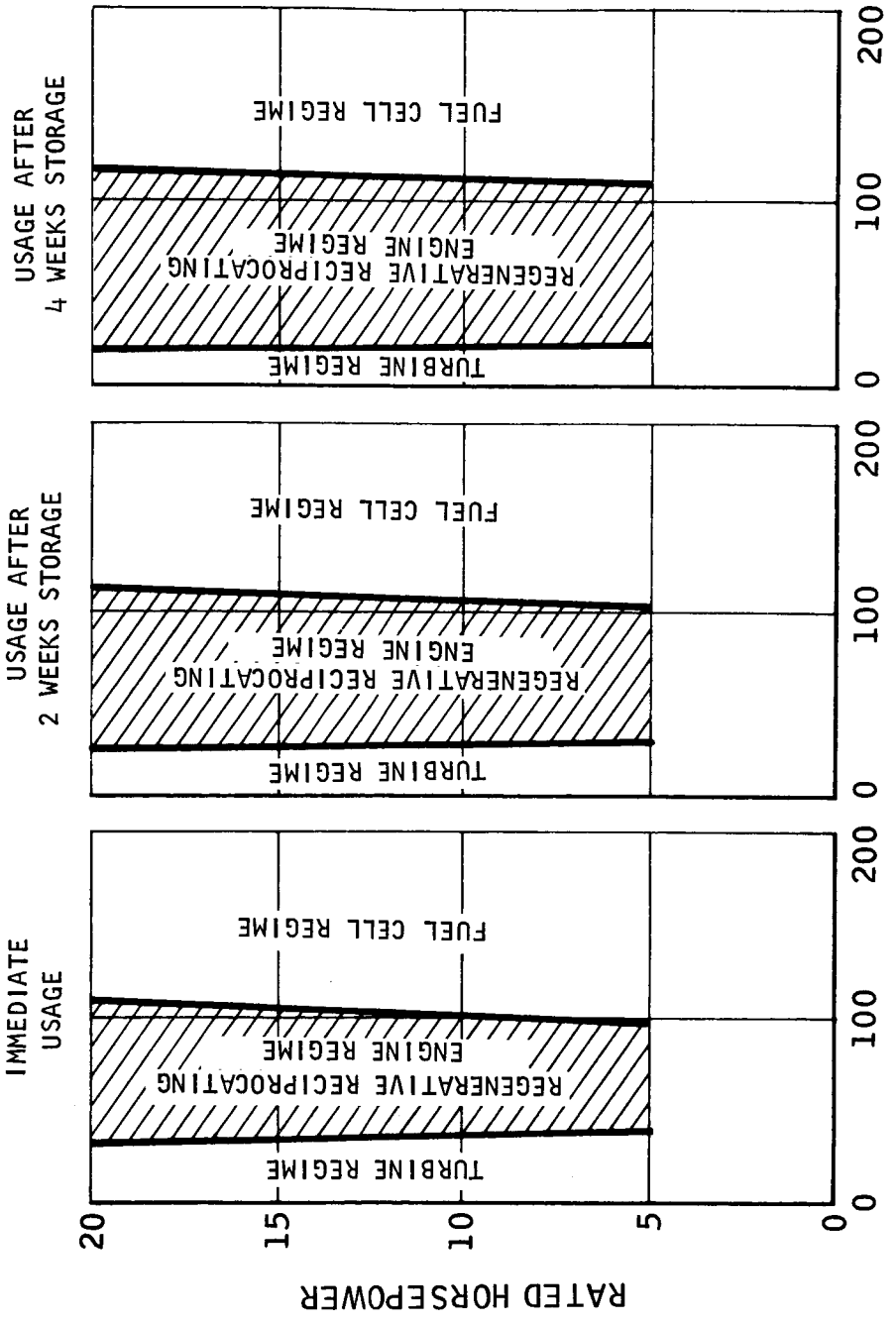

287-72 A

FIGURE A-3

APPENDIX B

PHOTOGRAPHS OF OSCILLOSCOPE RECORDINGS
OF CYLINDER PRESSURE VERSUS CRANK ANGLE
FOR THE SPU-2A-3 ENGINE AT ALL TEST CONDITIONS

COMPARISON OF CYLINDER PRESSURE vs. CRANK ANGLE AND PRESSURE vs. VOLUME INDICATOR DIAGRAMS

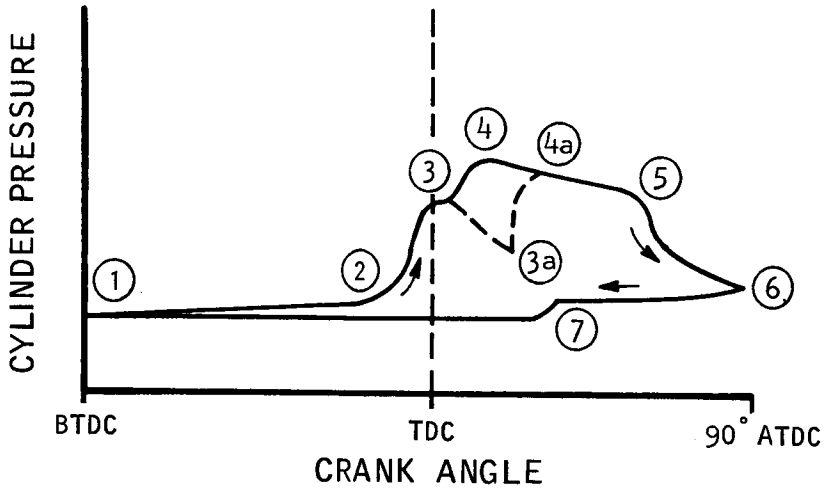

KEY

1 - 2 RECOMPRESSION OF RESIDUALS 2 - 3 H_2 ADMISSION 3 - 4 O_2 INJECTION AND COMBUSTION 4 - 7 EXPANSION 7 - 1 BLOWDOWN	WITH O_2 INJECTION IMMEDIATELY FOLLOWING H_2 ADMISSION
3 - 3a H_2 EXPANSION 3a - 4a O_2 INJECTION AND COMBUSTION	WITH DELAYED O_2 INJECTION

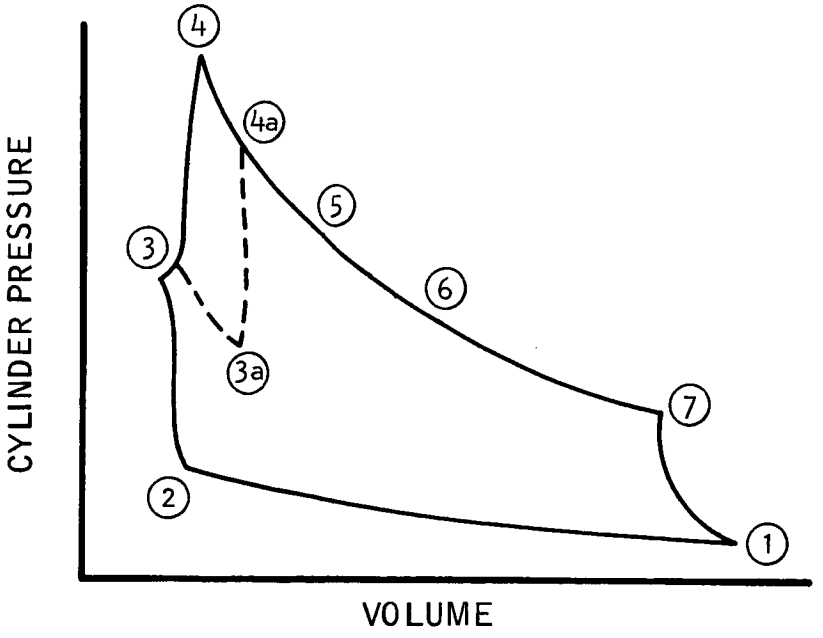

287-83

FIGURE B-1

DISCUSSION OF OSCILLOSCOPE RECORDINGS

Indicator Diagram	Comments
5149-8-3-1	The performance of the engine as an H_2 expander was studied. No O_2 admitted. Ample H_2 valve area was indicated by rapid rise of pressure at H_2 admission. Rise to full pressure in 10° crank rotation. No wire drawing should have been present until a speed of 6000 rpm was reached. Analysis of the expansion process indicates a polytropic exponent of 1.2 which indicates cyclic heat transfer into the gas. No leakage was indicated. Very retarded injection timing.
5149-8-3-2	Pressure rise in about 7° noted. Same conclusions as above.
5149-8-3-3	H_2 and O_2 injection but no combustion observed. Expansion work accelerates engine to speed faster than normal starting speed of 700 rpm.
5149-8-3-4	More expansion work than in 5149-8-3-3 because of higher H_2 and O_2 pressure - hence higher rpm. No combustion observed.
5149-8-5-1	Increasing exhaust temperature and speed indicate small degree of combustion.
5149-8-5-2	Two distinct cycles were observed. One cycle shows a detonation occurring about 30° BTDC. This preignition is attributed to excess O_2 in the residuals and O_2 valve leakage. The second exposure illustrates a good H_2 filling and smooth combustion occurring at about 35° ATDC.
5149-8-5-3	Sporatic combustion with indication of preignition.
5149-9-3-1 -2	H_2 dwell reduced to 32.5° with injection beginning at 21° BTDC. O_2 injection began at 20° ATDC and ended at 35° ATDC. Thus 10° "underlap" between H_2 valve closure and O_2 valve opening occurred. H_2 expansion before O_2 injection noted. Smooth even combustion. Low exhaust temperature indicates low combustion efficiency. Higher efficiency noted at higher speed.

Indicator Diagram	Comments
5149-9-3-3	Double exposure of two firing sequences. The most prominent trace indicates smooth filling and combustion. The "ghost" trace indicates preignition about 35° BTDC. The detonation pressure appears to be sufficiently high to prevent a fresh charge of H_2 from entering the cylinder and thus no normal firing was observed at about 20° ATDC.
5149-9-4-1 -2 -3 -4 -5	Propellant injection advanced 10° with no change in valve dwells. Smooth combustion. Inspection of the sequence from point 1 to point 4 indicates an increase in O/F ratio and an increase in BMEP. Comparison of point 3 and point 4 reveals consistent performance as O/F ratio was retained practically constant. Poor combustion firing shutdown (point 5) apparently caused by reduced O/F and lower engine speed which reduced turbulence.
5149-10-1 -2 -3 -4 -5 -6 -7 -8 -9 10	All traces except points 1 and 10 show smooth combustion. Low speed operation and/or low back pressure tends to promote preignition. During this series of tests, the propellant pressure was essentially constant. The tabulated O/F ratios are questionable; with constant supply pressures, the O/F should increase as rpm is reduced. Since BMEP rises with O/F (if combustion efficiency is constant) then BMEP should rise as speed is reduced. This is verified by the trace. Comparison of the pressure after combustion to that prior to combustion is indicative of the O/F ratio -- the higher the O/F, the higher the pressure ratio. A finite ignition delay on the order of 0.1 millisecond is noted by comparing the combustion location for points 7 and 9. At 5220 rpm, the combustion occurred 4 crank degrees later than when operating at zero rpm.
5149-10-2-1 -2 -3 -4 -5 -6 -7 -8 -9	Conclusions are the same as those drawn for the 5149-10-1 series. Smooth combustion in all diagrams except point 5. In the point 5 diagram, preignition was evident at 50° BTDC. Pressure appeared to decay early enough to permit H_2 to be admitted. Normal combustion also occurred. A "ghost image" is present which does not show combustion, so intermittent operation was certainly indicated. Low speed and high O/F are the probable cause of the roughness.

Indicator Diagram	Comments
5149-11-3-1 through -13	In this series, no precombustion or detonation was observable. Inability to obtain ignition at a back pressure of 1.4 psia is seen in point 4. Raising the back pressure to 10 psi produced smooth combustion as seen in point 5. BMEP is seen to decrease with increasing rpm with propellant supply conditions almost constant.
5149-11-8-1 through -14	The best performance (BSPC) was measured in this series. With fairly constant propellant supply, the back pressure is decreased from point 3 to point 10. Smooth combustion is observed until the back pressure reached 4.2 psi (point 8). Detonation began at this point, although it appeared to be sporatic. Further reduction in back pressure produced more regular detonation. Performance improved as back pressure was reduced. Comparison of point 11 and point 12 indicator diagrams reveals more violent detonation at 3000 rpm than at 6000 rpm. A higher O/F ratio at the lower speed point would explain this result. The effects of two other speeds are illustrated in points 13 and 14.

CYLINDER PRESSURE VS. CRANK ANGLE, SPU-2A-3 ENGINE

TEST 5149-8, RUN NO. 3

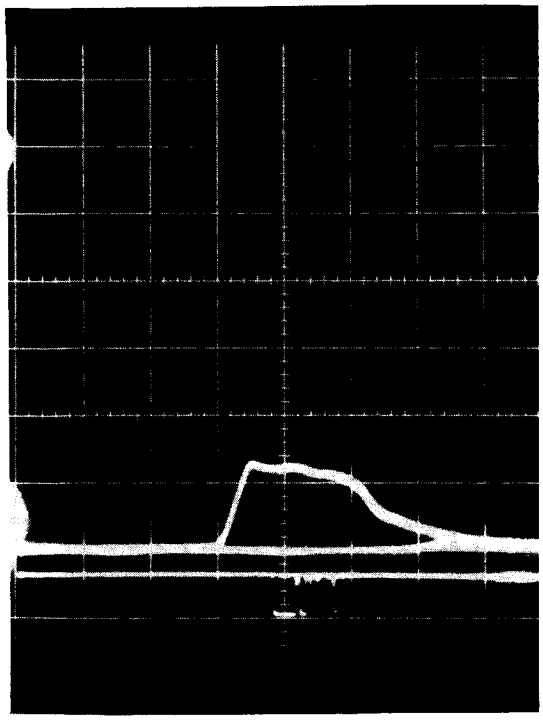

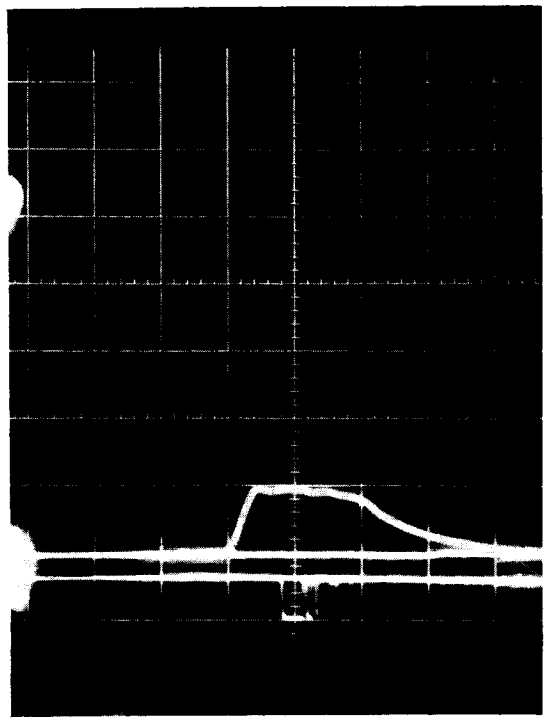

DATA POINT NO. 1

rpm = 1200

P_{0_f} = 0

P_{f_f} = 590 psi

P_{ex} = 1.8 psia

DATA POINT NO. 2

rpm = 795

P_{0_f} = 0

P_{f_f} = 370 psi

P_{ex} = 1.8 psia

NOTE: All visual data.

CYLINDER PRESSURE VS. CRANK ANGLE, SPU-2A-3 ENGINE

TEST 5149-8, RUN NO. 3

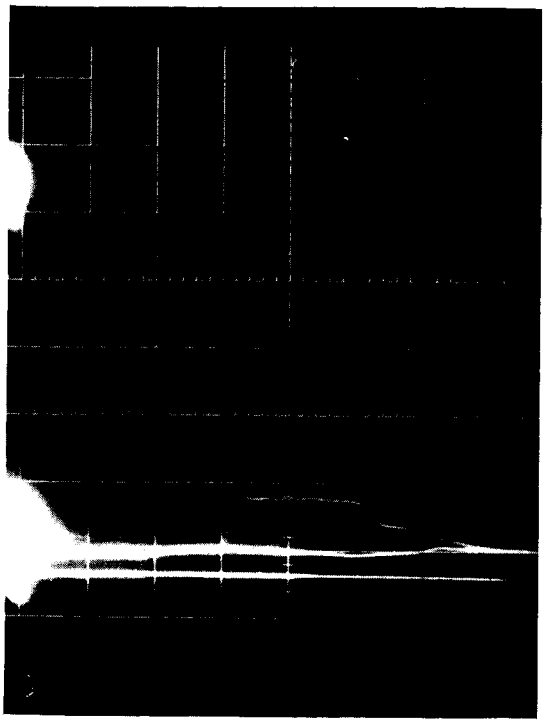

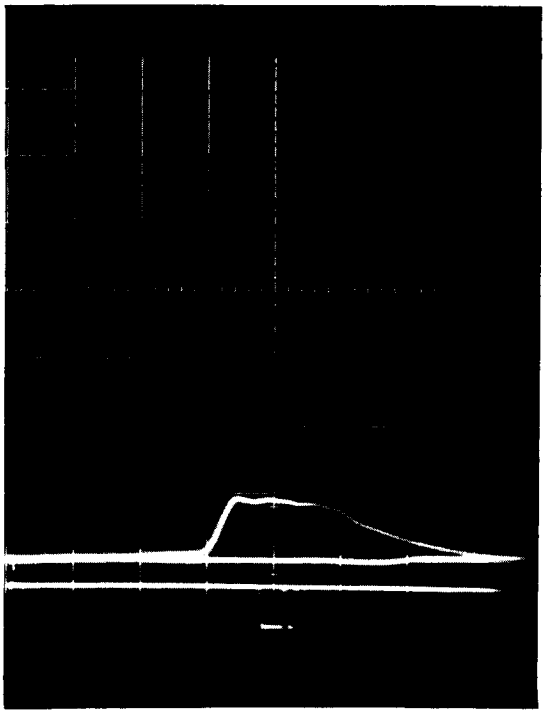

DATA POINT NO. 3

rpm = 1100

P_{O_1} = 270 psi

P_{f_1} = 450 psi

P_{ex} = 1.8 psia

DATA POINT NO. 4

rpm = 1350

P_{O_1} = 480 psi

P_{f_1} = 420 psi

P_{ex} = 1.8 psia

NOTE: All visual data.

CYLINDER PRESSURE VS. CRANK ANGLE, SPU-2A-3 ENGINE

TEST 5149-8, RUN NO. 5

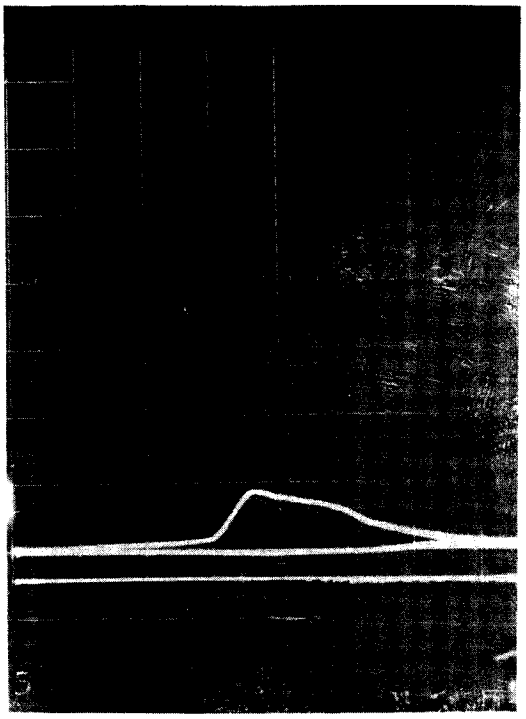

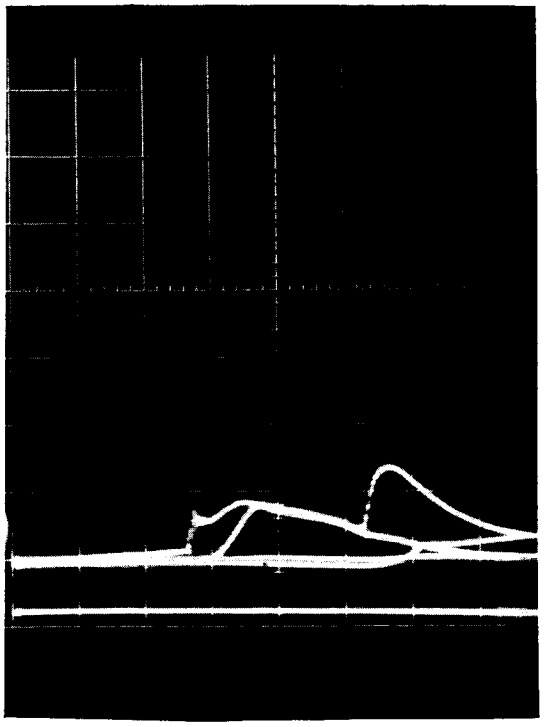

DATA POINT NO. 1

rpm = 2850

HP = 0.45

BMEP = 31.7 psi

O/F = N.A.

SPC = N.A.

P_{O_1} = 680 psi

P_{f_1} = 370 psi

P_{ex} = 3 psia

T_{ex} = 100°F

DATA POINT NO. 2

rpm = 2950

HP = 1.87

BMEP = 125.7 psi

O/F = N.A.

SPC = N.A.

P_{O_1} = 1110 psi

P_{f_1} = 375 psi

P_{ex} = 3 psia

T_{ex} = 310°F

CYLINDER PRESSURE VS. CRANK ANGLE, SPU-2A-3 ENGINE

TEST 5149-8, RUN NO. 5

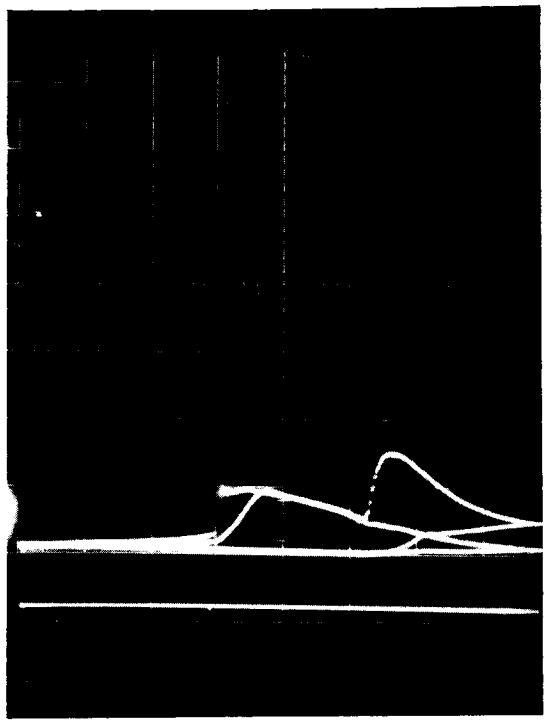

DATA POINT NO. 3

rpm = 3150

HP = 2.14

BMEP = 134.6 psi

O/F = 5.07

SPC = 3.68 lb HP-hr

P_{O_2} = 1275 psi

P_f = 375 psi

T_{ex} = 370° F

P_{ex} = 3 psia

CYLINDER PRESSURE VS. CRANK ANGLE, SPU-2A-3 ENGINE

TEST 5149-9, RUN NO. 3

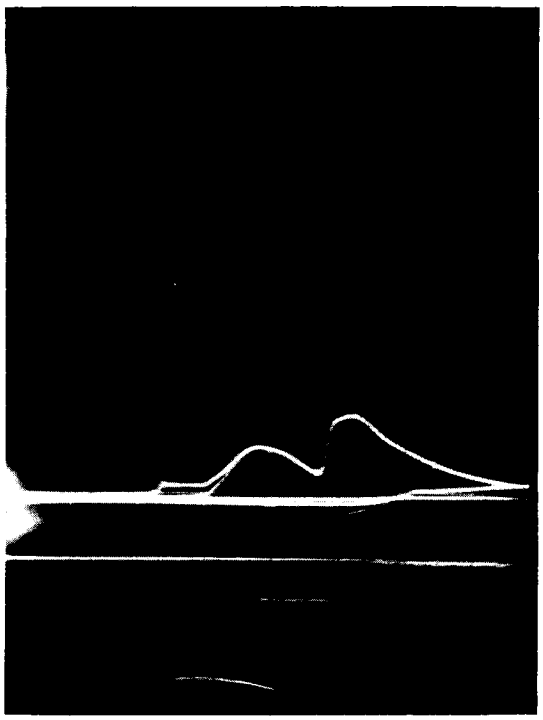

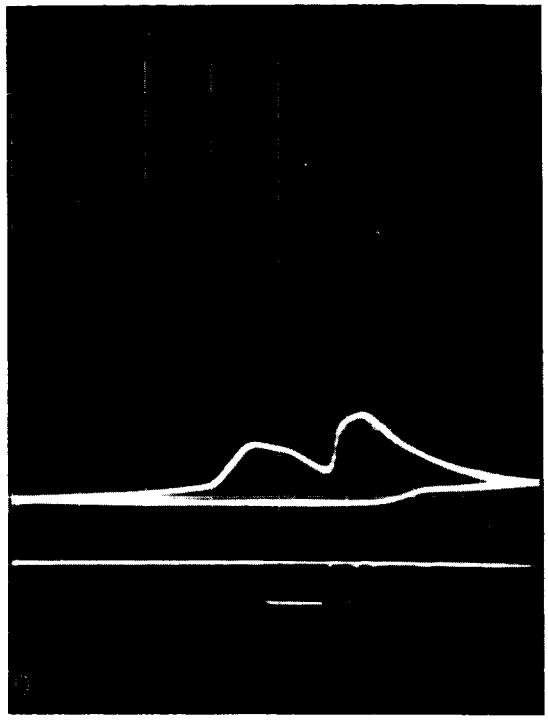

DATA POINT NO. 1

rpm = 2800

HP = 1.03

BMEP = 73.3 psi

O/F = 4.96

SPC = 8.1 lb/HP-hr

P_{O_1} = 1160 psi

P_{f_1} = 510 psi

P_{ex} = 9.6 psia

T_{ex} = 550°F

DATA POINT NO. 2

rpm = 3200

HP = 1.92

BMEP = 119 psi

O/F = 5.7

SPC = 4.04 lb/HP-hr

P_{O_2} = 1200 psi

P_{f_2} = 500 psi

P_{ex} = 6.0 psia

T_{ex} = 1350°F

CYLINDER PRESSURE VS. CRANK ANGLE, SPU-2A-3 ENGINE

TEST 5149-9, RUN NO. 3

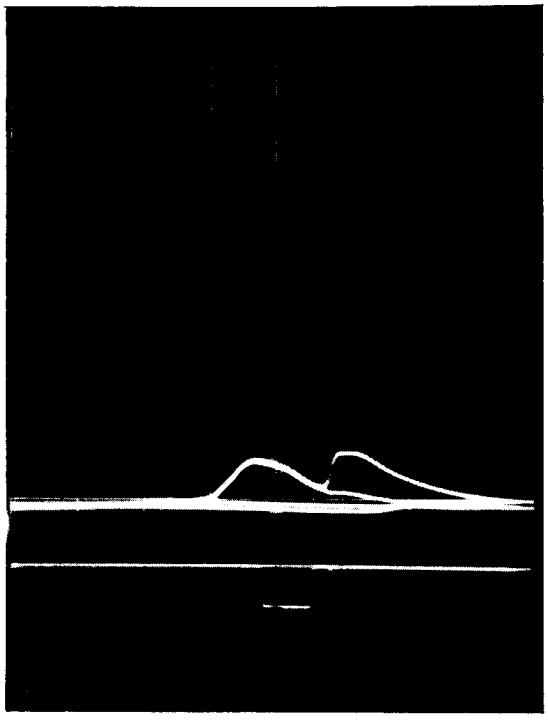

DATA POINT NO. 3

RPM = 3140

HP = 0.57

BMEP = 35.6 psi

O/F = 1.62

SPC = 3.12 lb/hr-hp

P_0 = 800 psia

P_f = 480 psia

P_{ex} = 5.6 psia

T_{ex} = 610°F

CYLINDER PRESSURE VS. CRANK ANGLE, SPU-2A-3 ENGINE

TEST 5149-9, RUN NO. 4

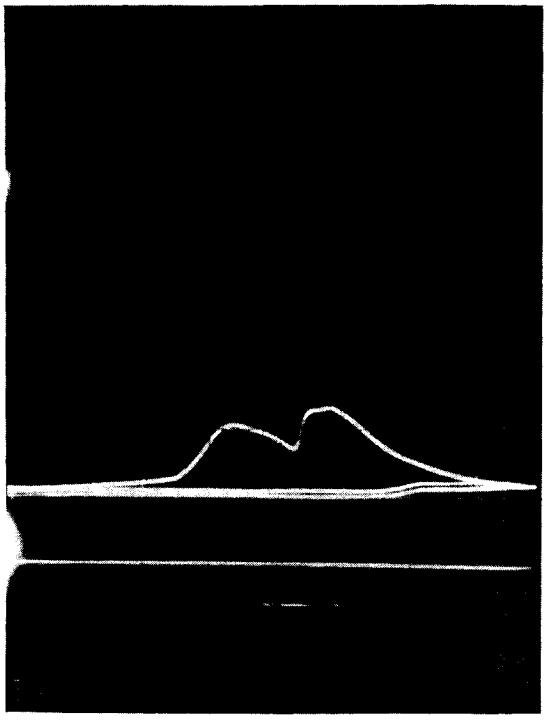

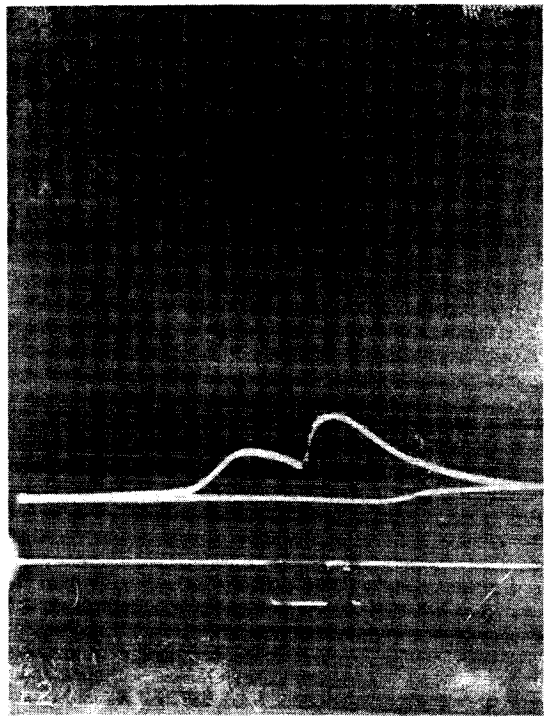

DATA POINT NO. 1

rpm = 2600

HP = 1.30

BMEP = 99 psi

O/F = 3.7

SPC = 5.2 lb/HP-hr

P_{O_1} = 1000 psi

P_{f_1} = 480 psi

P_{ex} = 7.4 psia

T_{ex} = 970°F

DATA POINT NO. 2

rpm = 3000

HP = 1.23

BMEP = 81.3 psi

O/F = 4.92

SPC = 5.5 lb/HP-hr

P_{O_1} = 1000 psi

P_{f_1} = 360 psi

P_{ex} = 5.5 psia

T_{ex} = 700°F

CYLINDER PRESSURE VS. CRANK ANGLE, SPU-2A-3 ENGINE

TEST 5149-9, RUN NO. 4

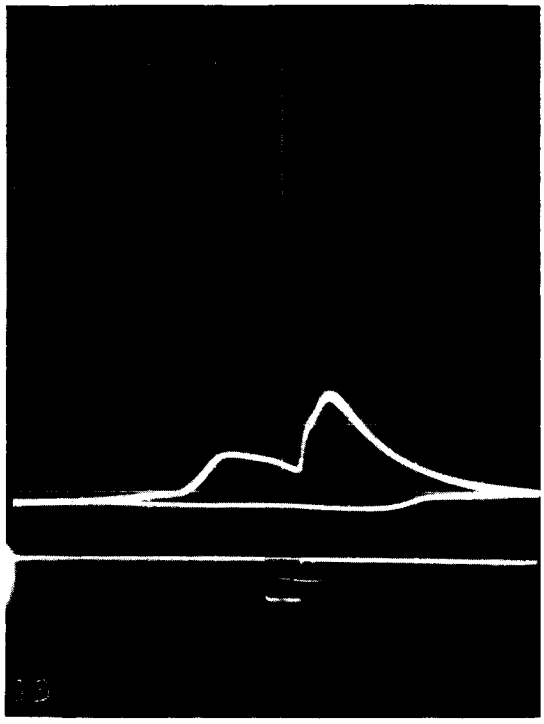

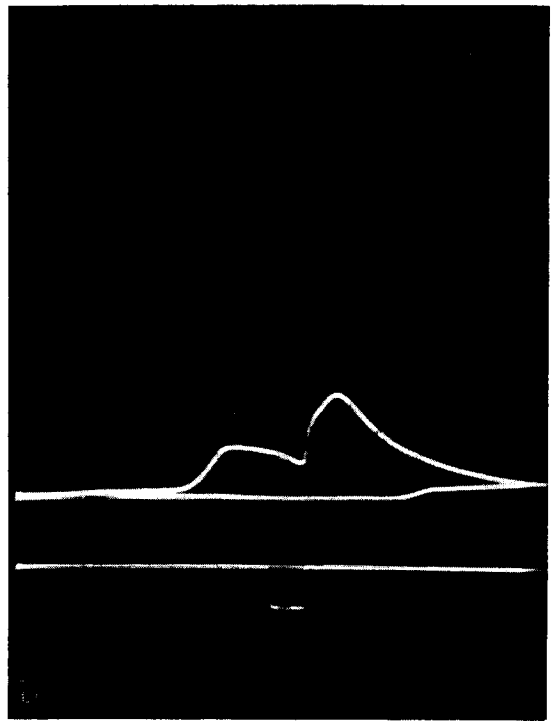

DATA POINT NO. 3

rpm = 2160

HP = 1.69

BMEP = 154 psi

O/F = 5.4

SPC = 4.4 lb/HP-hr

P_{O_I} = 1100 psi

P_{f_I} = 360 psi

P_{ex} = 4.9 psia

T_{ex} = 565°F

DATA POINT NO. 4

rpm = 2100

HP = 1.64

BMEP = 154 psi

O/F = 5.3

SPC = 4.2 lb/HP-hr

P_{O_I} = 1020 psi

P_{f_I} = 340 psi

P_{ex} = 5.3 psia

T_{ex} = 570°F

CYLINDER PRESSURE VS. CRANK ANGLE, SPU-2A-3 ENGINE

TEST 5149-9, RUN NO. 4

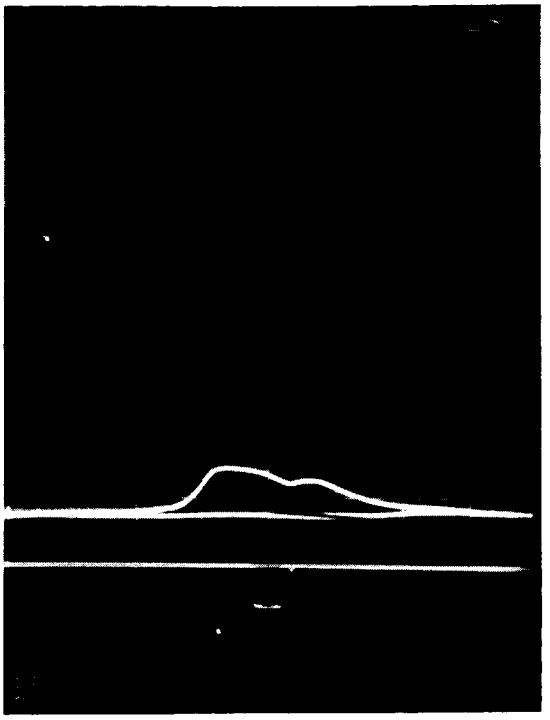

DATA POINT NO. 5

rpm = 1840

HP = 0.92

BMEP = 99 psi

O/F = 4.5

SPC = N.A.

P_{0_2} = 910 psi

P_{f_2} = 360 psi

P_{ex} = 4.7 psia

T_{ex} = 505°F

NOTE: Data point taken during controlled shutdown.

CYLINDER PRESSURE VS. CRANK ANGLE, SPU-2A-3 ENGINE

TEST 5149-10, RUN NO. 1

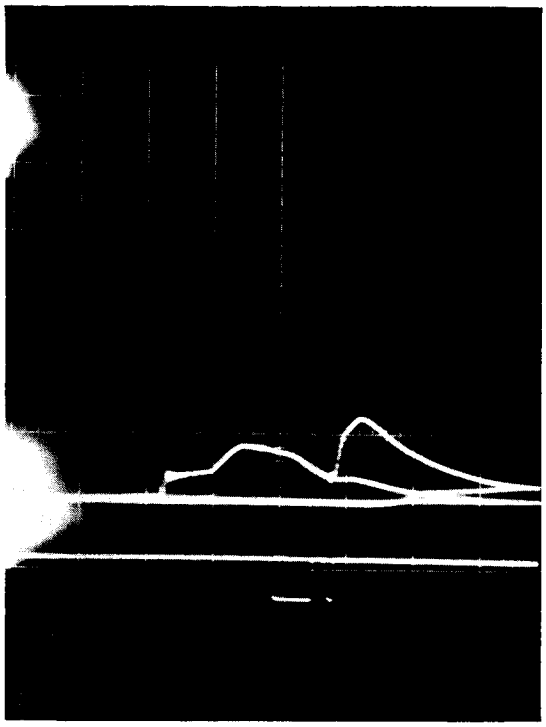

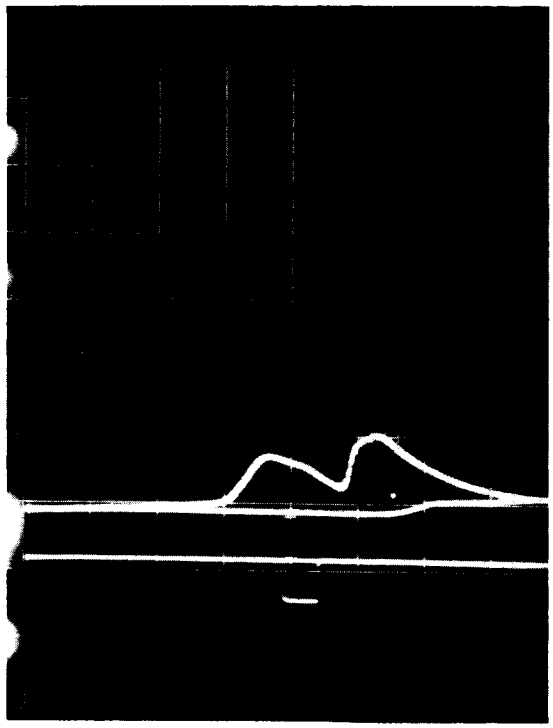

DATA POINT NO. 1

rpm = 2420

HP = 0.75

BMEP = 61.5 psi

O/F = 4.62

SPC = 10.8 lb/HP-hr

P_{O_i} = 960 psi

P_{f_i} = 440 psi

P_{ex} = 3.0 psia

T_{ex} = 650°F

DATA POINT NO. 2

rpm = 2940

HP = 1.70

BMEP = 115 psi

O/F = 5.36

SPC = 4.6 lb/HP-hr

P_{O_i} = 940 psi

P_{f_i} = 440 psi

P_{ex} = 5.4 psia

T_{ex} = 1400°F

CYLINDER PRESSURE VS. CRANK ANGLE, SPU-2A-3 ENGINE

TEST 5149-10, RUN NO. 1

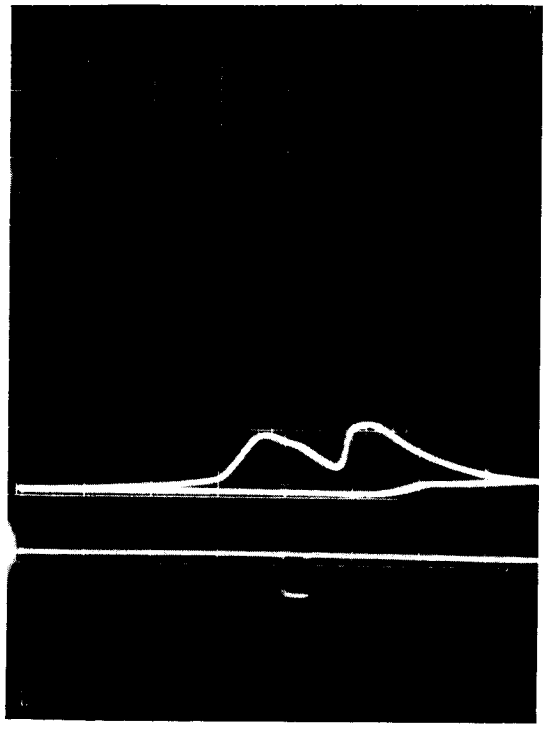

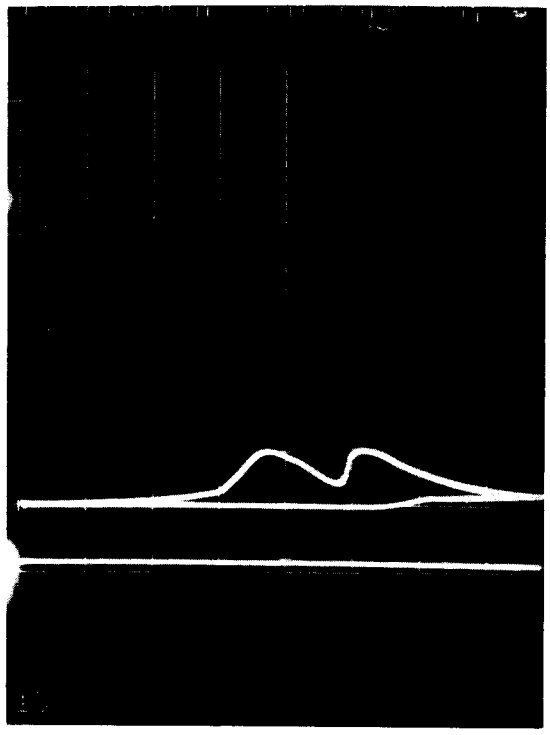

DATA POINT NO. 3

rpm = 3240

HP = 1.97

BMEP = 120 psi

O/F = 4.5

SPC = 4.06 lb/HP-hr

P_{O_I} = 980 psi

P_{f_I} = 440 psi

P_{ex} = 7.4 psia

T_{ex} = 1530°F

DATA POINT NO. 4

rpm = 4000

HP = 1.92

BMEP = 95 psi

O/F = 4.2

SPC = 3.96 lb/HP-hr

P_{O_I} = 980 psi

P_{f_I} = 440 psi

P_{ex} = 7.6 psia

T_{ex} = 1550°F

CYLINDER PRESSURE VS. CRANK ANGLE, SPU-2A-3 ENGINE

TEST 5149-10, RUN NO. 1

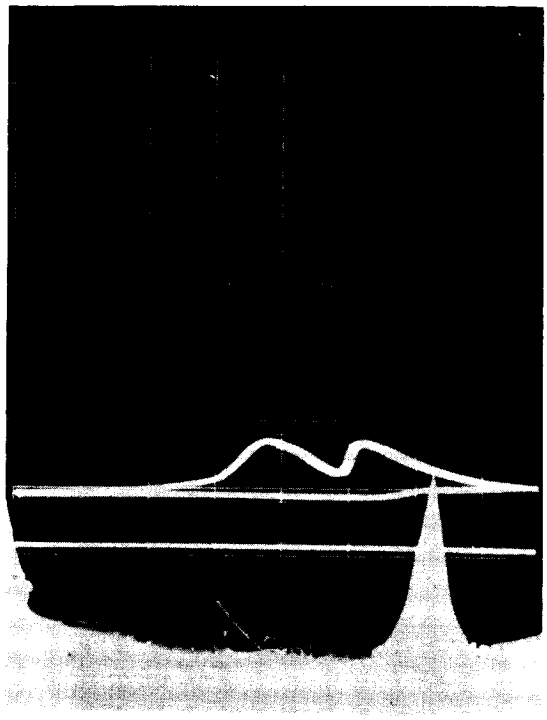

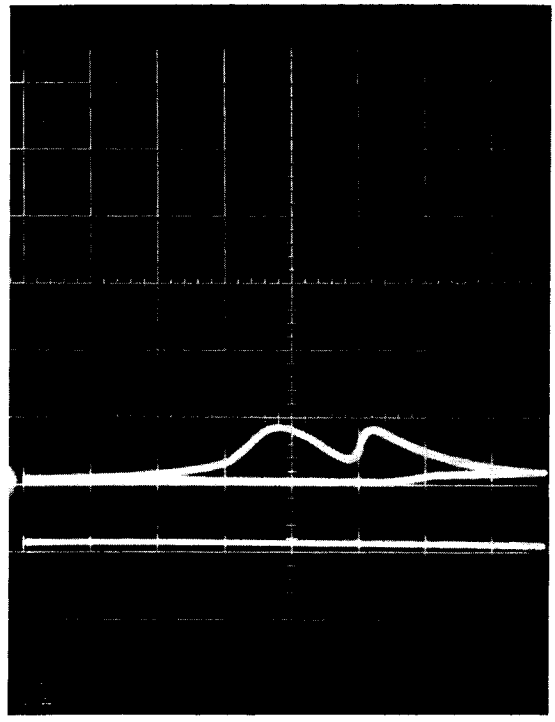

DATA POINT NO. 6

rpm = 4800

HP = 1.97

BMEP = 81 psi

O/F = 4.4

SPC = 3.99 lb/HP-hr

P_{O_I} = 980 psi

P_{f_I} = 440 psi

P_{ex} = 7.4 psia

T_{ex} = 1490°F

DATA POINT NO. 7

rpm = 5220

HP = 1.89

BMEP = 71 psi

O/F = 4.2

SPC = 4.01 lb/HP-hr

P_{O_I} = 980 psi

P_{f_I} = 440 psi

P_{ex} = 7.4 psia

T_{ex} = 1440°F

CYLINDER PRESSURE VS. CRANK ANGLE, SPU-2A-3 ENGINE

TEST 5149-10, RUN NO. 1

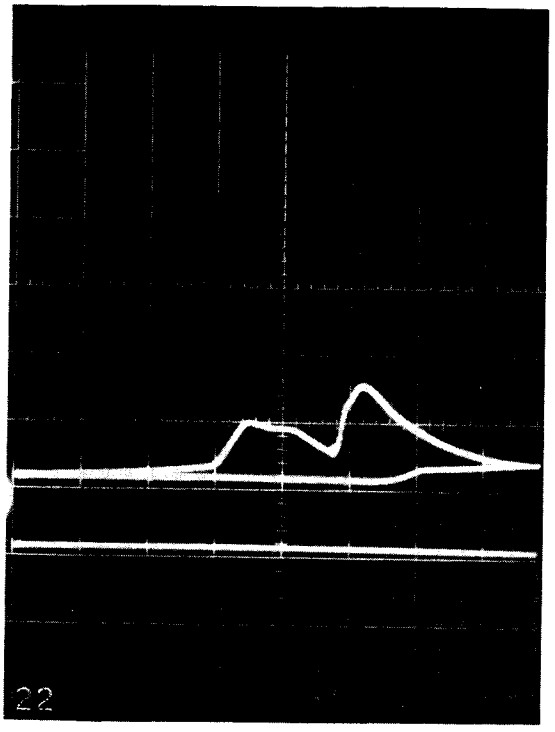

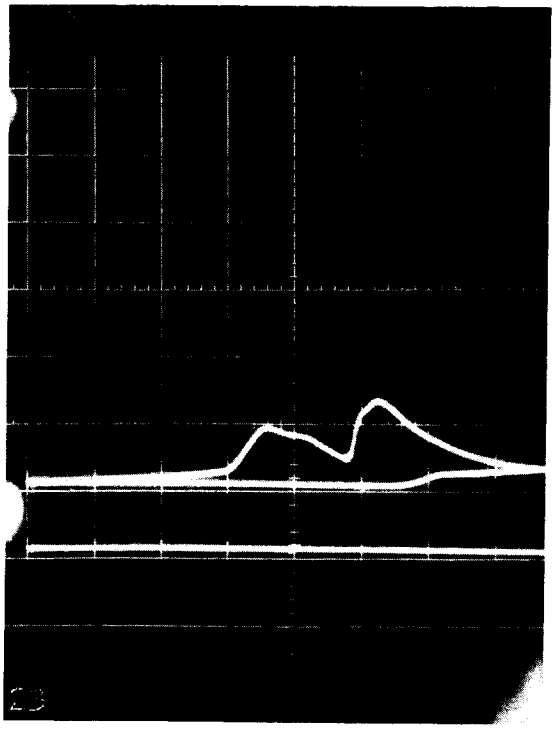

DATA POINT NO. 8

rpm = 2200

HP = 1.76

BMEP = 158 psi

O/F = 5.2

SPC = 4.6 lb/HP-hr

P_{O_l} = 980 psi

P_{f_l} = 440 psi

P_{ex} = 7.6 psia

T_{ex} = 1490°F

DATA POINT NO. 9

rpm = 2620

HP = 1.92

BMEP = 144 psi

O/F = 5.2

SPC = 4.1 lb/HP-hr

P_{O_l} = 960 psi

P_{f_l} = 420 psi

P_{ex} = 7.2 psia

T_{ex} = 1470°F

CYLINDER PRESSURE VS. CRANK ANGLE, SPU-2A-3 ENGINE

TEST 5149-10, RUN NO. 1

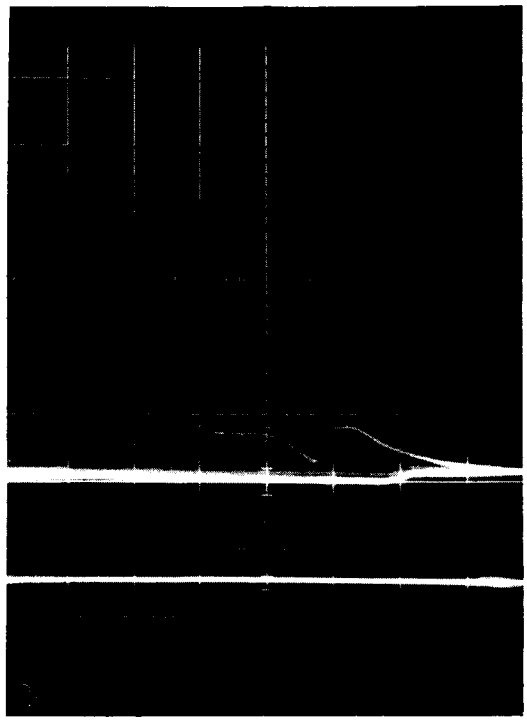

DATA POINT NO. 10

rpm = 7100

P_{O_l} = 420 psia

P_{i_l} = 420 psia

P_{e_x} = 7.5 psia

T_{e_x} = 390°F

NOTE: Data point taken during shutdown.

CYLINDER PRESSURE VS. CRANK ANGLE, SPU-2A-3 ENGINE

TEST 5149-10, RUN NO. 2

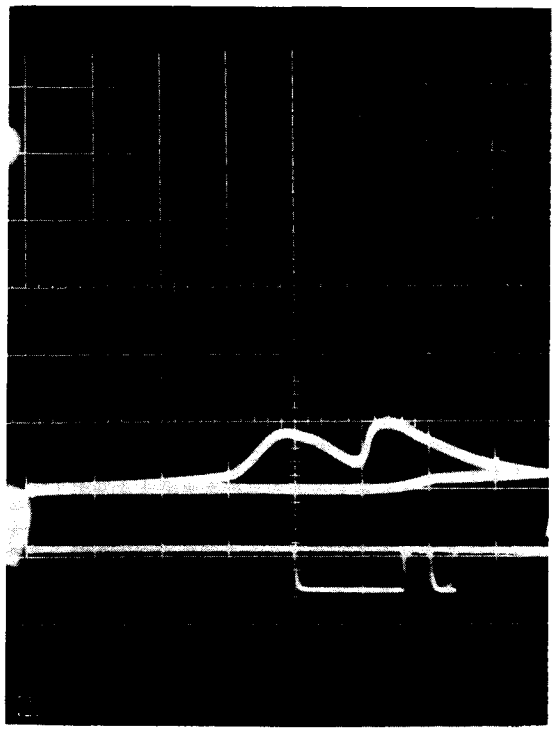

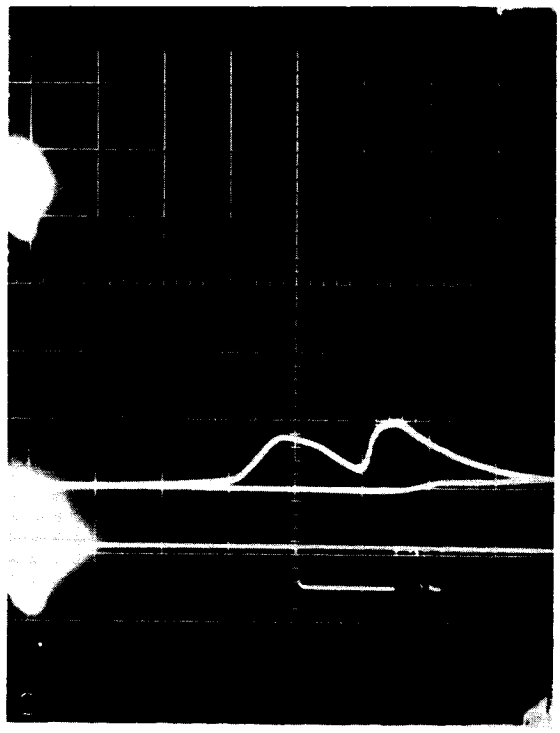

DATA POINT NO. 1

rpm = 4150

HP = 2.07

BMEP = 99 psi

O/F = 5.2

SPC = 3.96 lb/HP-hr

P_{O_1} = 1040 psi

P_{f_1} = 380 psi

P_{ex} = 5.5 psia

T_{ex} = 1550°F

DATA POINT NO. 2

rpm = 3600

HP = 2.16

BMEP = 119 psi

O/F = 4.9

SPC = 3.63 lb/HP-hr

P_{O_2} = 1020 psi

P_{f_2} = 380 psi

P_{ex} = 5.4 psia

T_{ex} = 1620°F

CYLINDER PRESSURE VS. CRANK ANGLE, SPU-2A-3 ENGINE

TEST 5149-10, RUN NO. 2

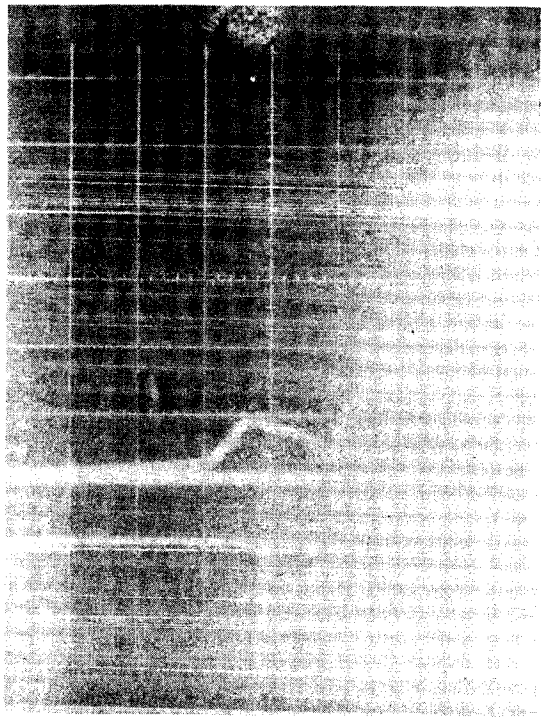

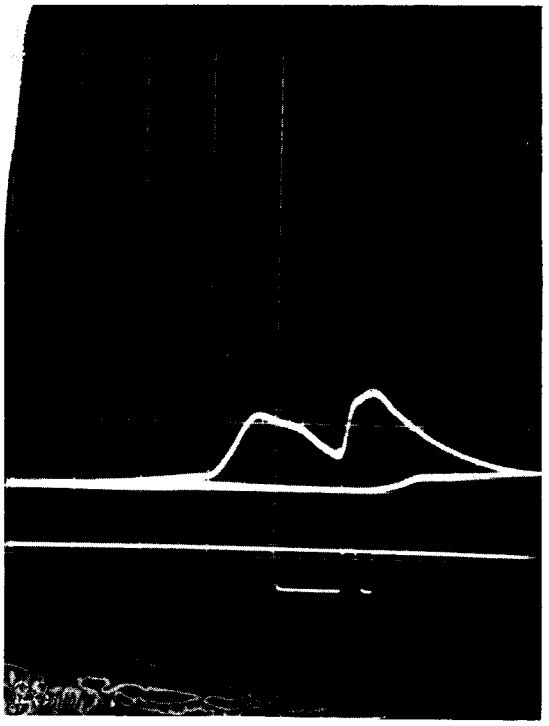

DATA POINT NO. 3

rpm = 2760

HP = 1.82

BMEP = 130 psi

O/F = N.A.

SPC = N.A.

P_{O_I} = 1030 psi

P_{f_I} = 380 psi

P_{ex} = 6.0 psia

T_{ex} = 1490°F

DATA POINT NO. 4

rpm = 2780

HP = 2.52

BMEP = 178 psi

O/F = 4.5

SPC = 3.29

P_{O_I} = 1000 psi

P_{f_I} = 480 psi

P_{ex} = 5.6 psia

T_{ex} = 1430°F

CYLINDER PRESSURE VS. CRANK ANGLE, SPU-2A-3 ENGINE

TEST 5149-10, RUN NO. 2

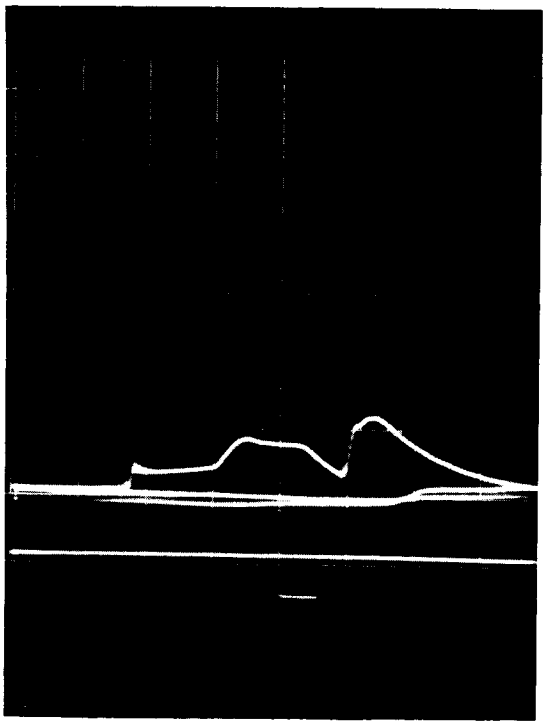

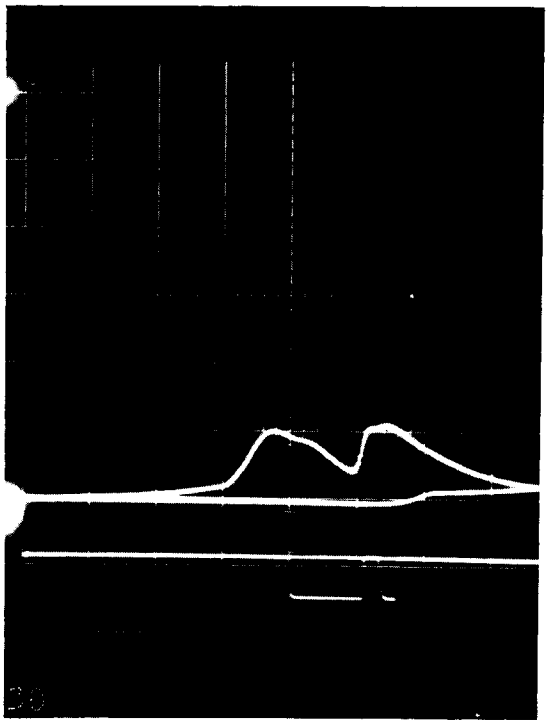

DATA POINT NO. 5

rpm = 2060

HP = 0.91

BMEP = 87 psi

O/F = 5.0

SPC = 8.4 lb/HP-hr

P_{O_I} = 900 psi

P_{f_I} = 480 psi

P_{ex} = 5.7 psia

T_{ex} = 870°F

DATA POINT NO. 6

rpm = 2960

HP = 2.22

BMEP = 148 psi

O/F = 4.2

SPC = 3.4 lb/HP-hr

P_{O_I} = 900 psi

P_{f_I} = 460 psi

P_{ex} = 8.0 psia

T_{ex} = 1570°F

CYLINDER PRESSURE VS. CRANK ANGLE, SPU-2A-3 ENGINE

TEST 5149-10, RUN NO. 2

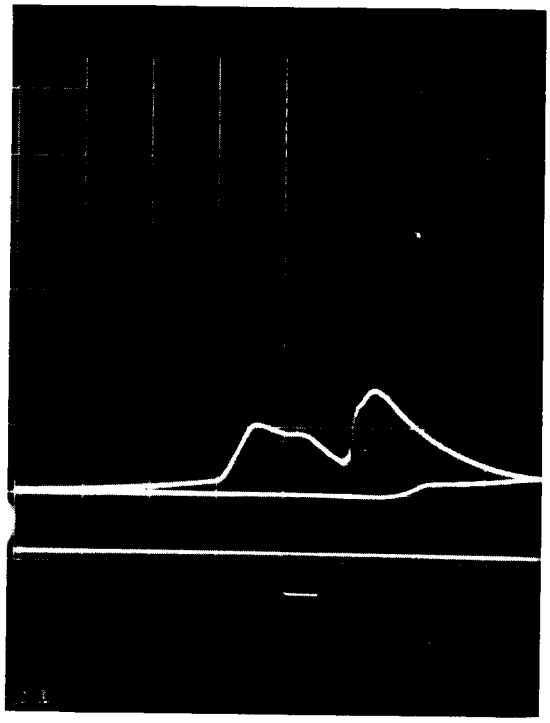

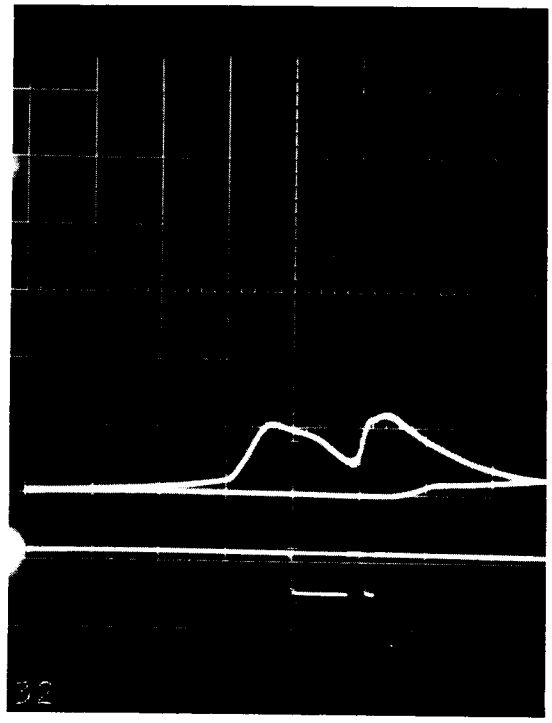

DATA POINT NO. 7

rpm = 2040

HP = 2.0

BMEP = 194 psi

O/F = 50

SPC = 4.1

P_{O_1} = 1000 psi

P_{f_1} = 480 psi

P_{ex} = 8.4 psia

T_{ex} = 1470°F

DATA POINT NO. 8

rpm = 2560

HP = 2.1

BMEP = 162 psi

O/F = 4.6

SPC = 3.7

P_{O_2} = 900 psi

P_{f_2} = 440 psi

P_{ex} = 8.2 psia

T_{ex} = 1520°F

THE Marquardt CORPORATION VAN NUYS, CALIFORNIA

CYLINDER PRESSURE VS. CRANK ANGLE, SPU-2A-3 ENGINE

TEST 5149-10, RUN NO. 2

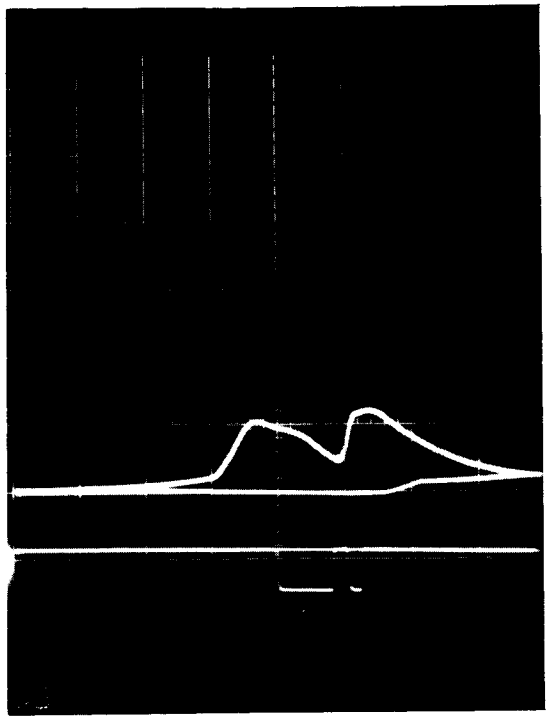

DATA POINT NO. 9

rpm = 2540

[illegible] = 2.06

BMEP = 160 psi

O/F = 4.4

SFC = 3.7 lb/[illegible]

P_D = 880 psi

P_f = 480 psi

P_{ex} = 9.5 psia

T_{ex} = 1550°F

CYLINDER PRESSURE VS. CRANK ANGLE, SPU-2A-3 ENGINE

TEST 5149-11, RUN NO. 3

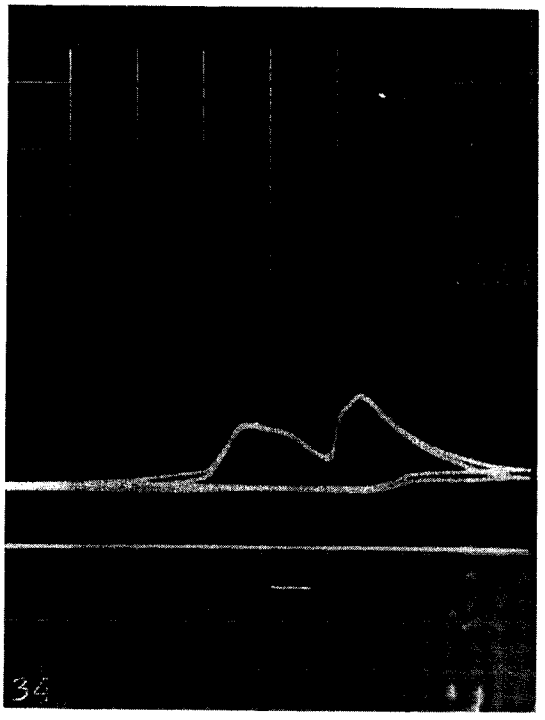

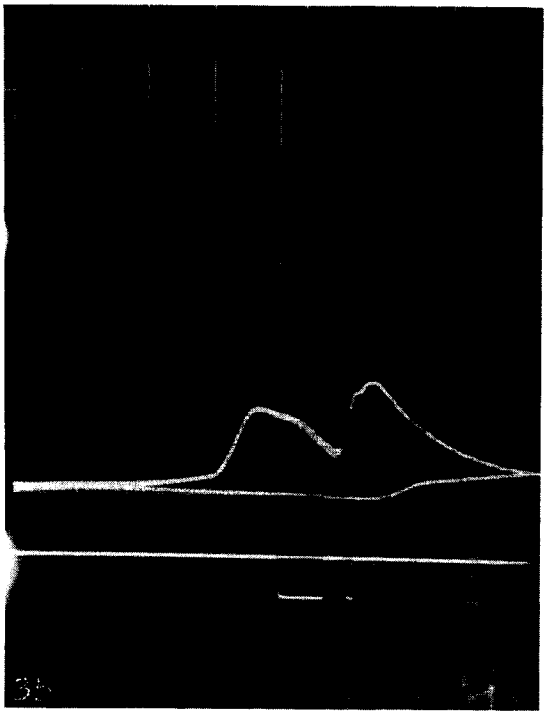

DATA POINT NO. 1

rmp = 2370

HP = 1.82

BMEP = 152 psi

O/F = 5.9

SPC = 4.5 lb/HP-hr

P_{O_1} = 1030 psi

P_{f_1} = 420 psi

P_{ex} = 7.3 psia

T_{ex} = 1850°F

DATA POINT NO. 2

rpm = 2470

HP = 2.40

BMEP = 192 psi

O/F = 4.5

SPC = 3.6 lb/HP-hr

P_{O_2} = 1060 psi

P_f = 520 psi

P_{ex} = 7.5 psia

T_{ex} = 1760°F

CYLINDER PRESSURE VS. CRANK ANGLE, SPU-2A-3 ENGINE

TEST 5149-11, RUN NO. 3

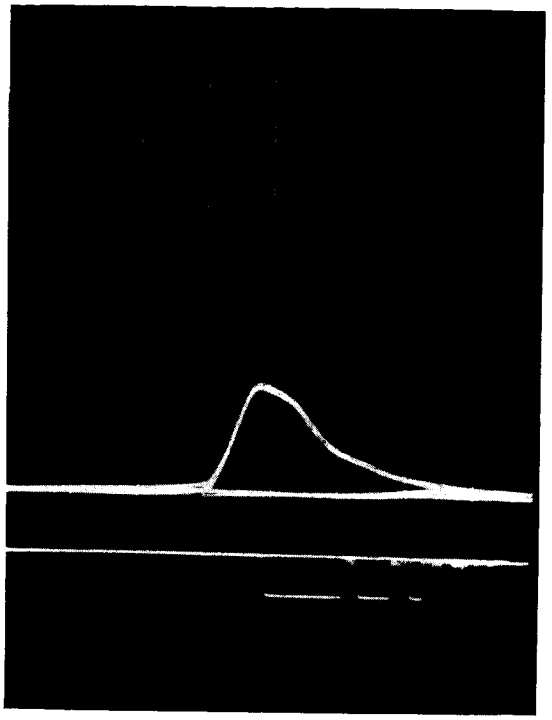

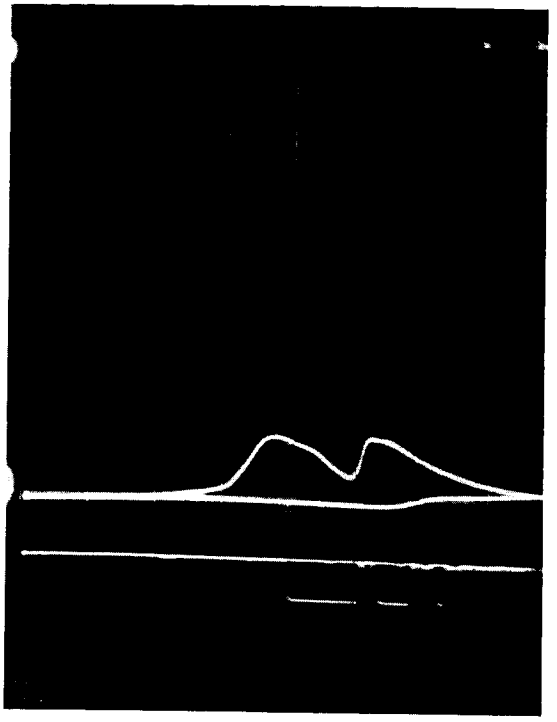

DATA POINT NO. 4

rpm = 2900

HP = 0.55

BMEP = 37.6 psi

O/F = N.A.

SPC = N.A.

P_{0_i} = 800 psi

P_{f_i} = 780 psi

P_{ex} = 1.4 psia

T_{ex} = 0°F

DATA POINT NO. 5

rpm = 3400

HP = 2.11

BMEP = 123 psi

O/F = 3.6

SPC = 3.5 lb/HP-hr

P_{0_i} = 870 psi

P_{f_i} = 520 psi

P_{ex} = 10.0 psia

T_{ex} = 1440°F

Expansion operation, no ignition

CYLINDER PRESSURE VS. CRANK ANGLE, SPU-2A-3 ENGINE

TEST 5149-11, RUN NO. 3

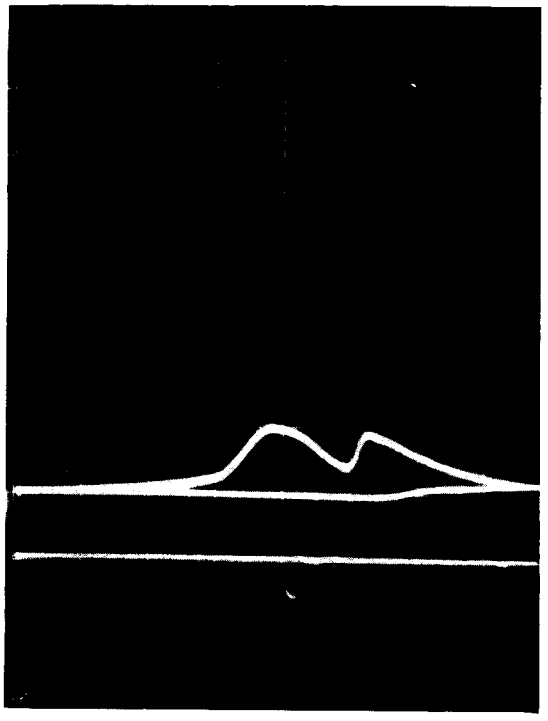

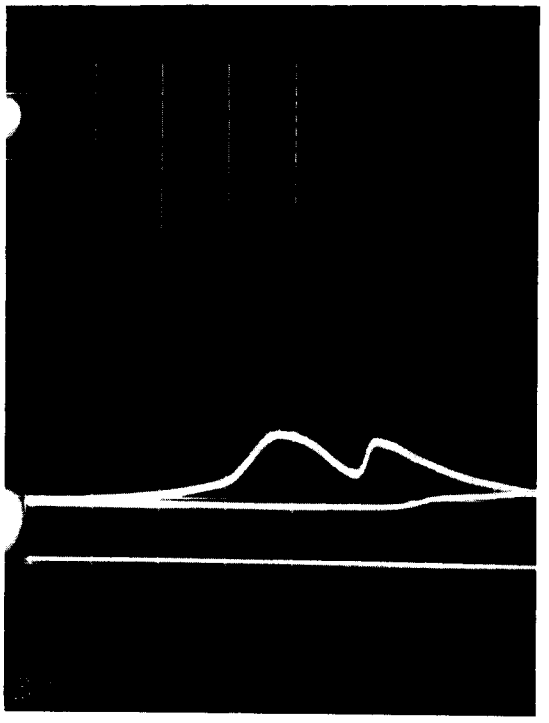

DATA POINT NO. 6

rpm = 4370

HP = 2.41

BMEP = 109 psi

O/F = 3.5

SPC = 3.0 lb/HP-hr

P_{O_2} = 870 psi

P_{f_2} = 500 psi

P_{ex} = 10.5 psia

T_{ex} = 1370°F

DATA POINT NO. 7

rpm = 4100

HP = 2.09

BMEP = 101 psi

O/F = 3.3

SPC = 3.3 lb/HP-hr

P_{O_2} = 880 psi

P_{f_2} = 520 psi

P_{ex} = 7.8 psia

T_{ex} = 1550°F

CYLINDER PRESSURE VS. CRANK ANGLE, SPU-2A-3 ENGINE

TEST 5149-11, RUN NO. 3

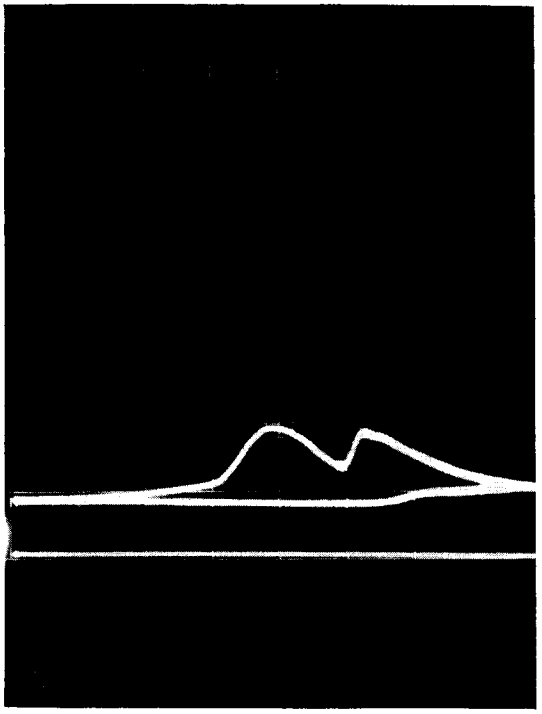

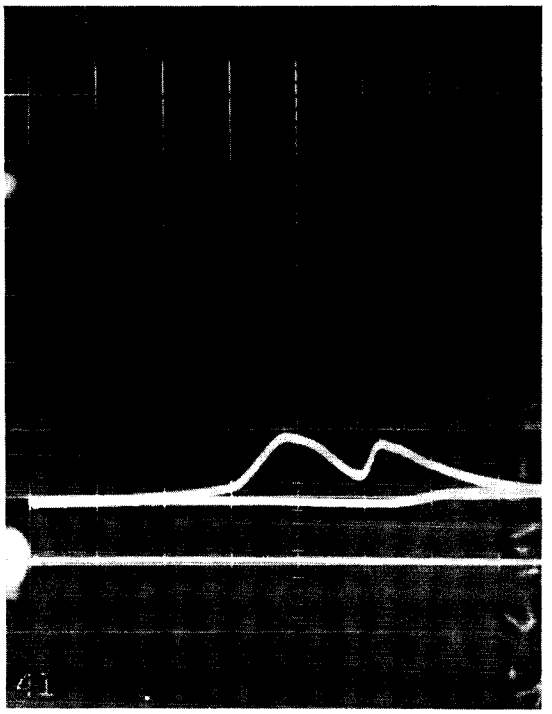

DATA POINT NO. 8

rpm = 4100

HP = 2.09

BMEP = 101 psi

O/F = 3.5

SPC = 3.5 lb/HP-hr

P_{O_i} = 870 psi

P_{f_i} = 520 psi

P_{ex} = 8.1 psia

T_{ex} = 1280°F

DATA POINT NO. 9

rpm = 4450

HP = 2.36

BMEP = 105 psi

O/F = 3.6

SPC = 3.1 lb/HP-hr

P_{O_i} = 870 psi

P_{f_i} = 520 psi

P_{ex} = 10.8 psia

T_{ex} = 1460°F

CYLINDER PRESSURE VS. CRANK ANGLE, SPU-2A-3 ENGINE

TEST 5149-11, RUN NO. 3

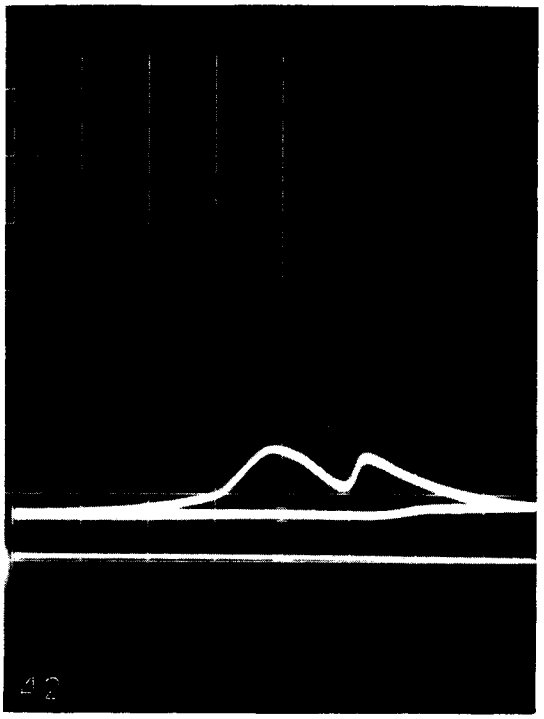

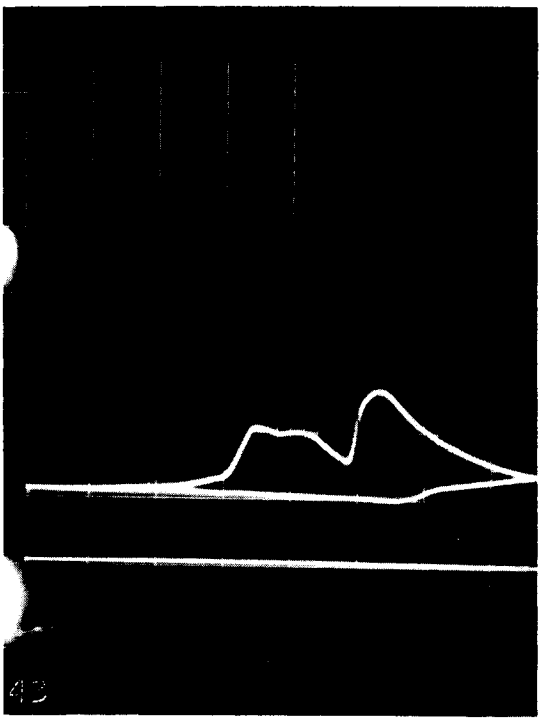

DATA POINT NO. 10

rpm = 5200

HP = 2.13

BMEP = 81 psi

O/F = 3.6

SPC = 3.4 lb/HP-hr

P_{0_i} = 890 psi

P_{f_i} = 500 psi

P_{ex} = 9.8 psia

T_{ex} = 1250°F

DATA POINT NO. 11

rpm = 1600

HP = 1.55

BMEP = 192 psi

O/F = 5.0

SPC = 4.8 lb/HP-hr

P_{0_i} = 840 psi

P_{f_i} = 480 psi

P_{ex} = 9.9 psia

T_{ex} = 1020°F

CYLINDER PRESSURE VS. CRANK ANGLE, SPU-2A-3 ENGINE

TEST 5149-11, RUN NO. 3

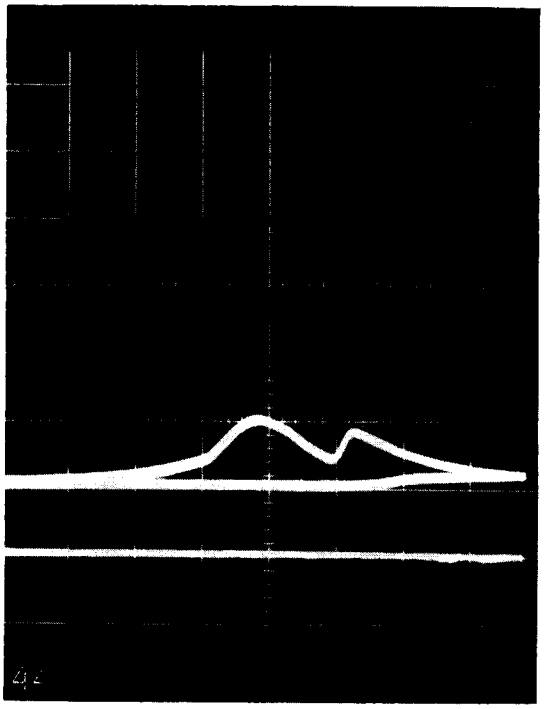

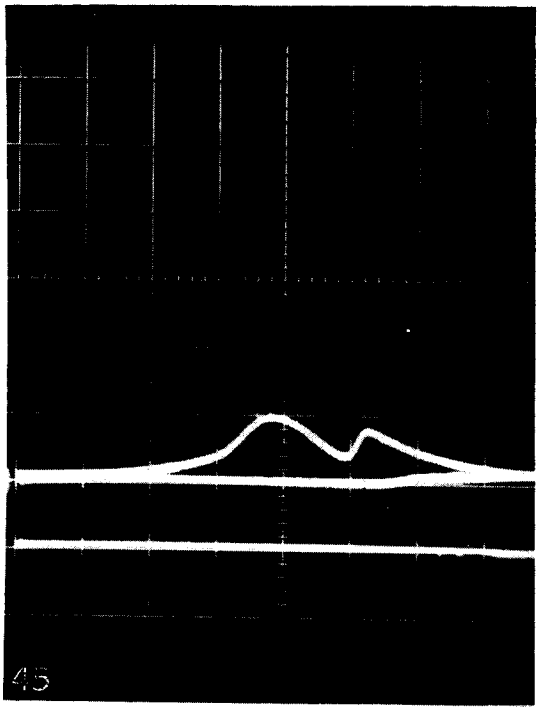

DATA POINT NO. 12

rpm = 5400

HP = 1.40

BMEP = 51.5 psi

O/F = 3.7

SFC = 5.0 lb/HP-hr

P_{O_2} = 810 psi

P_{f_2} = 460 psi

P_{ex} = 12.7 psia

T_{ex} = 1310°F

DATA POINT NO. 13

rpm = 5600

HP = 1.20

BMEP = 41.6 psi

O/F = 3.6

SFC = 5.8 lb/HP-hr

P_{O_2} = 840 psi

P_{f_2} = 470 psi

P_{ex} = 13.0 psia

T_{ex} = 1320°F

CYLINDER PRESSURE VS. CRANK ANGLE, SPU-2A-3 ENGINE

TEST 5149-11, RUN NO. 8

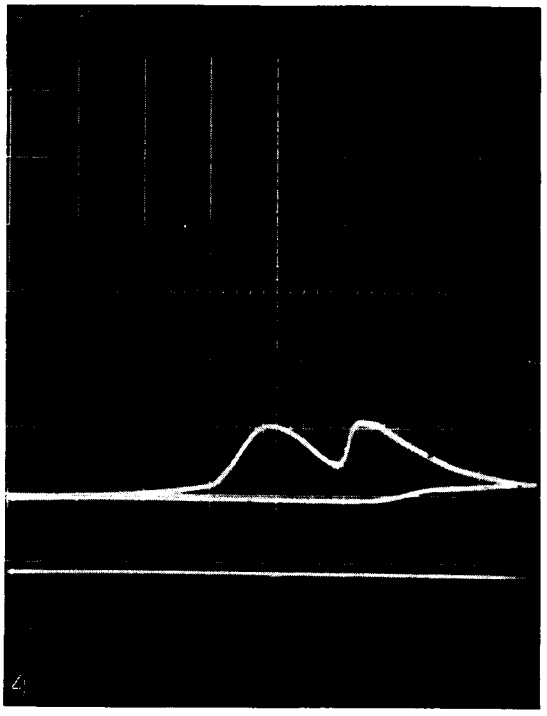

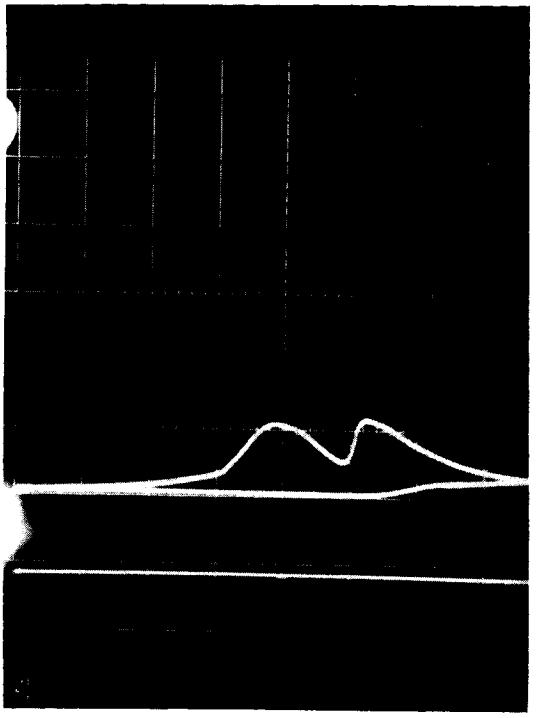

DATA POINT NO. 1

rpm = 4100

HP = 2.91

BMEP = 140 psi

O/F = 4.3

SPC = 3.1 lb/HP-hr

P_{O_1} = 1140 psi

P_{f_1} = 540 psi

P_{ex} = 7.5 psia

T_{ex} = 1420°F

DATA POINT NO. 2

rpm = 4850

HP = 3.15

BMEP = 129 psi

O/F = 4.6

SPC = 3.0 lb/HP-hr

P_{O_2} = 1290 psi

P_{f_2} = 540 psi

P_{ex} = 9.7 psia

T_{ex} = 1550°F

CYLINDER PRESSURE VS. CRANK ANGLE, SPJ-2A-3 ENGINE

TEST 5149-11, RUN NO. 8

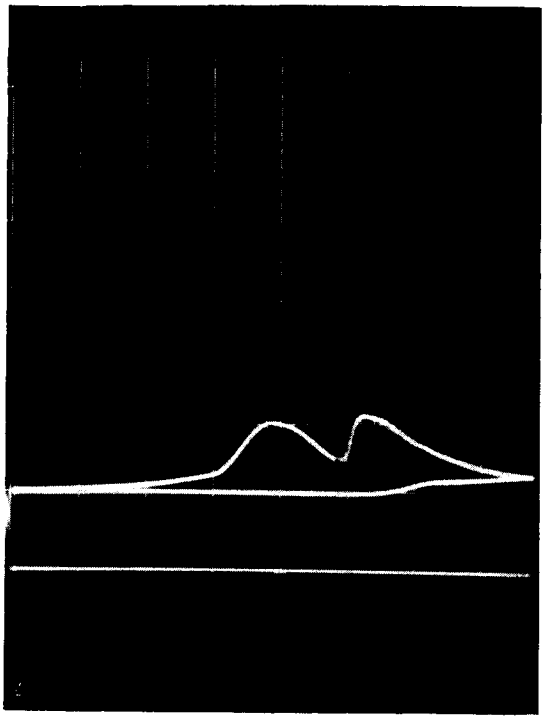

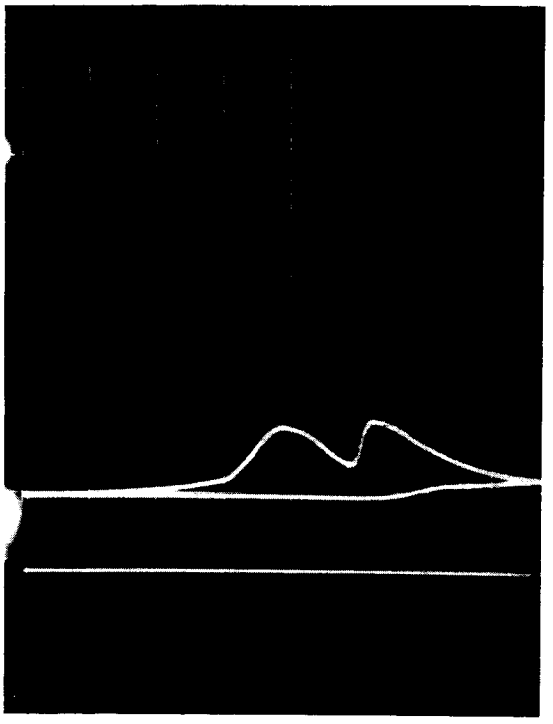

DATA POINT NO. 3

rpm = 4600

$\dot{w}_F$ = 3.36

BMEP = 144 psi

O/F = 4.7

SFC = 2.8 lb/$\dot{w}_F$-hr

P_{O_2} = 1280 psi

P_{f_2} = 540 psi

P_{ex} = 10.7 psia

T_{ex} = 1760°F

DATA POINT NO. 4

rpm = 4800

$\dot{w}_F$ = 3.50

BMEP = 144 psi

O/F = 4.6

SFC = 2.7

P_{O_2} = 1280 psi

P_{f_2} = 540 psi

P_{ex} = 8.0 psia

T_{ex} = 1520°F

CYLINDER PRESSURE VS. CRANK ANGLE, SPU-2A-3 ENGINE

TEST 5149-11, RUN NO. 8

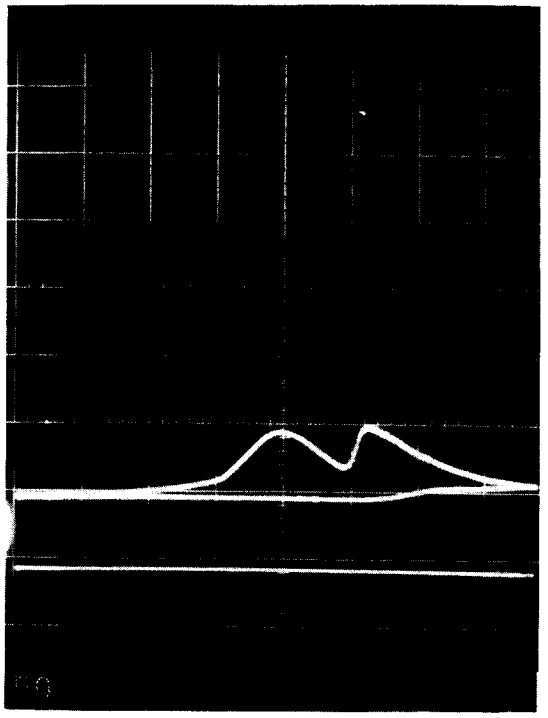

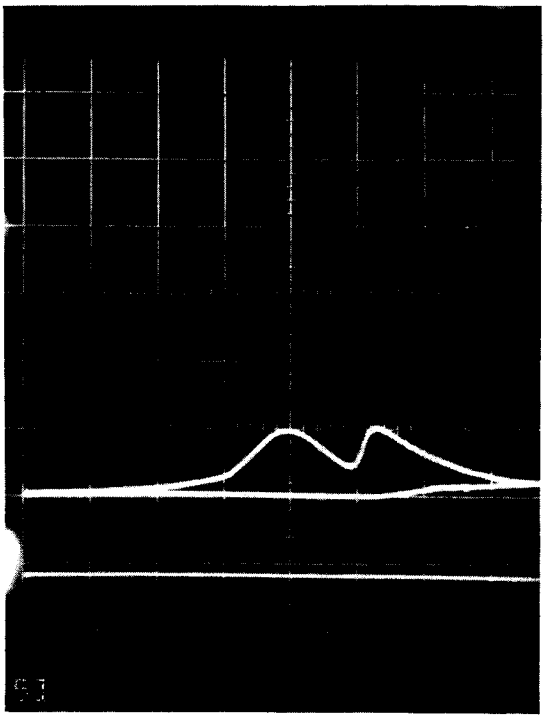

DATA POINT NO. 5

rpm = 5650

HP = 3.50

BMEP = 123 psi

O/F = 4.6

SPI = 2.7 lb/HP-hr

P_{c_1} = 1290 psi

P_{f_1} = 540 psi

P_{ex} = 7.4 psia

T_{ex} = 1540°F

DATA POINT NO. 6

rpm = 5900

HP = 3.24

BMEP = 109 psi

O/F = 4.6

SPI = 2.9 lb/HP-hr

P_{c_2} = 1280 psi

P_{d_2} = 540 psi

P_{ex} = 8.0 psia

T_{ex} = 1580°F

CYLINDER PRESSURE VS. CRANK ANGLE, SPU-2A-3 ENGINE

TEST 5149-11, RUN NO. 8

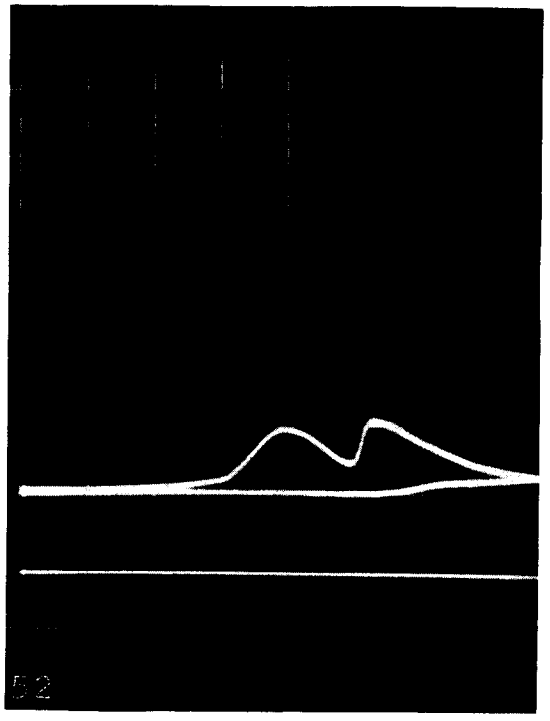

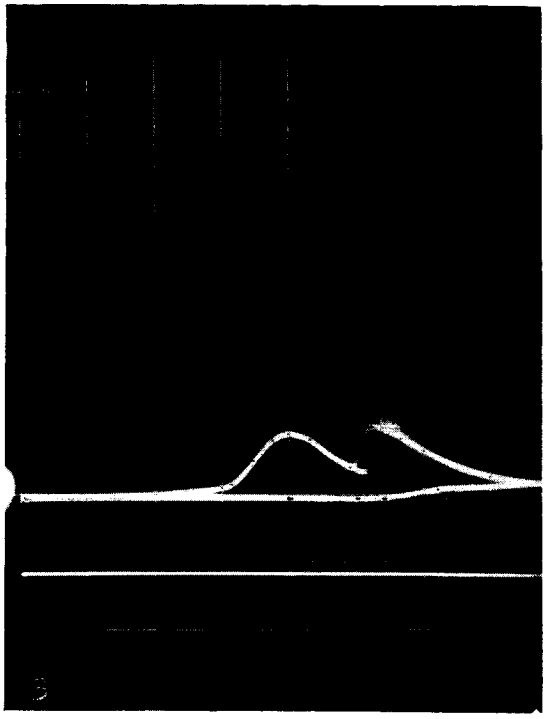

DATA POINT NO. 7

rpm = 5100

HP = 3.62

BMEP = 140 psi

O/F = 4.6

SFC = 2.6 lb/HP-hr

P_{O_1} = 1280 psi

P_{f_1} = 500 psi

P_{ex} = 5.5 psia

T_{ex} = 1450°F

DATA POINT NO. 8

rpm = 5200

HP = 3.79

BMEP = 144 psi

O/F = 4.6

SFC = 2.5 lb/HP-hr

P_{O_1} = 1280 psi

P_{f_1} = 500 psi

P_{ex} = 4.2 psia

T_{ex} = 1260°F

CYLINDER PRESSURES VS. CRANK ANGLE, SPU-2A-3 ENGINE

TEST 5149-11, RUN NO. 8

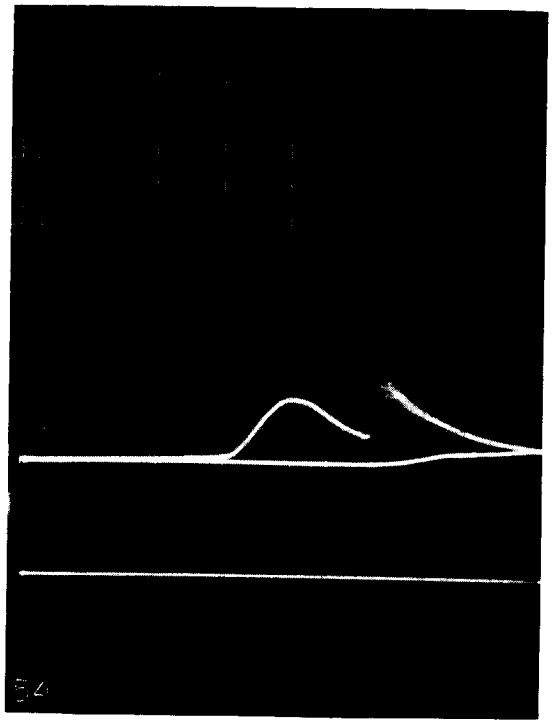

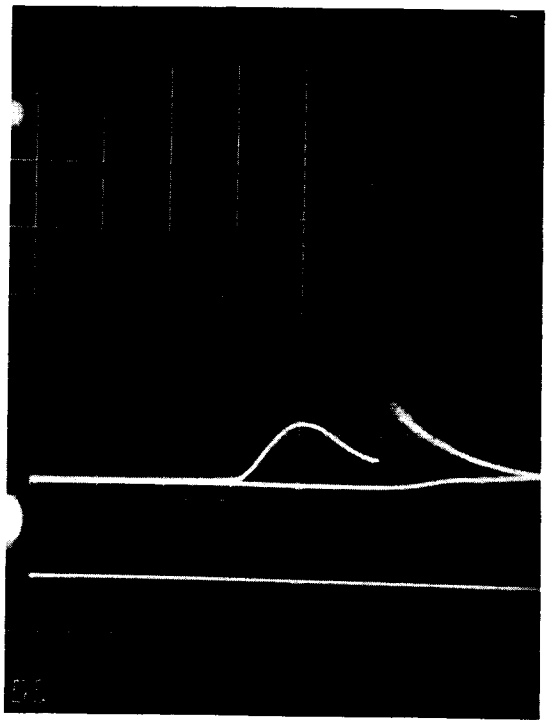

DATA POINT NO. 9

rpm = 5150

HP = 3.86

BMEP = 148 psi

O/F = [illegible]

SFC = 2.[illegible] lb/HP-hr

P_{0_3} = 1200 psi

P_{f_3} = [illegible]C psi

P_{ex} = 1[illegible] psia

T_{ex} = 1100 F

DATA POINT NO. 10

rpm = 5150

HP = 3.80

BMEP = 146 psi

O/F = 4.6

SFC = 2.5 lb/HP-hr

P_{0_3} = 1280 psi

P_{f_3} = 480 psi

P_{ex} = 0.9 psia

T_{ex} = 1230 F

CYLINDER PRESSURE VS. CRANK ANGLE, SPU-2A-3 ENGINE

TEST 5149-11, RUN NO. 8

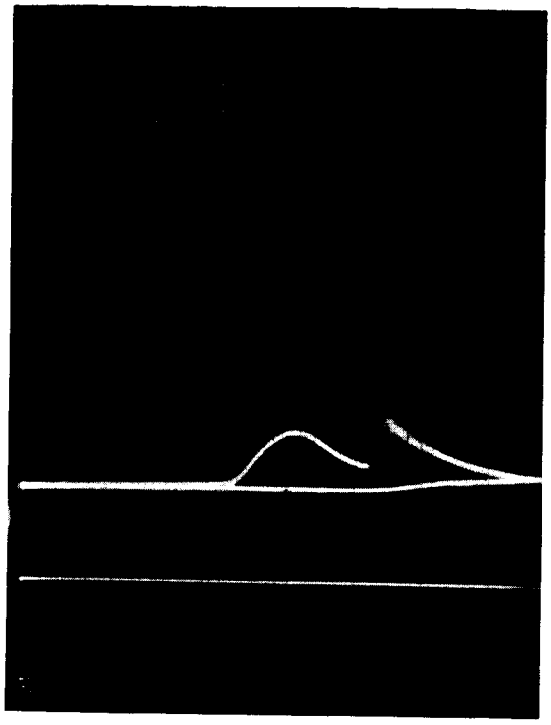

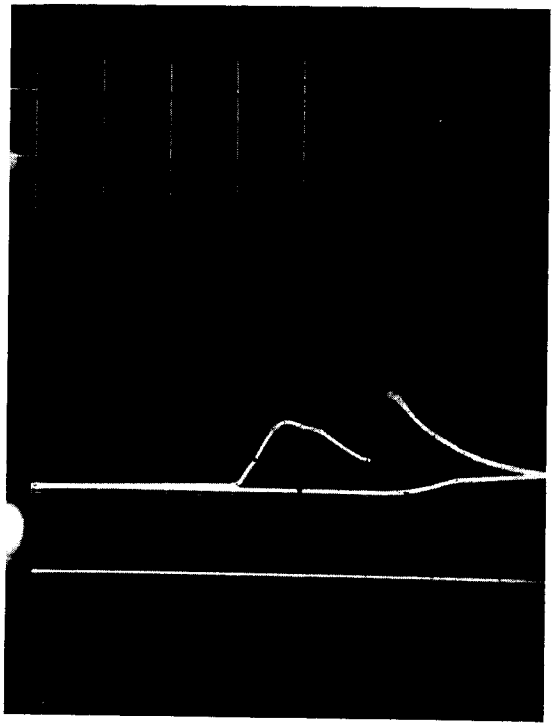

DATA POINT NO. 11

rpm = 6000

HP = 3.66

BMEP = 121 psi

O/F = 4.6

SPC = 2.6 lb/HP-hr

P_{0_1} = 1280 psi

P_{f_1} = 460 psi

P_{ex} = 0.6 psia

T_{ex} = 1190°F

DATA POINT NO. 12

rpm = 3000

HP = 2.85

BMEP = 188 psi

O/F = 4.6

SPC = 3.2 lb/HP-hr

P_{0_2} = 1280 psi

P_{f_2} = 460 psi

P_{ex} = 0.5 psia

T_{ex} = 1120°F

CYLINDER PRESSURE VS. CRANK ANGLE, SPU-2A-3 ENGINE

TEST 5149-11, RUN NO. 8

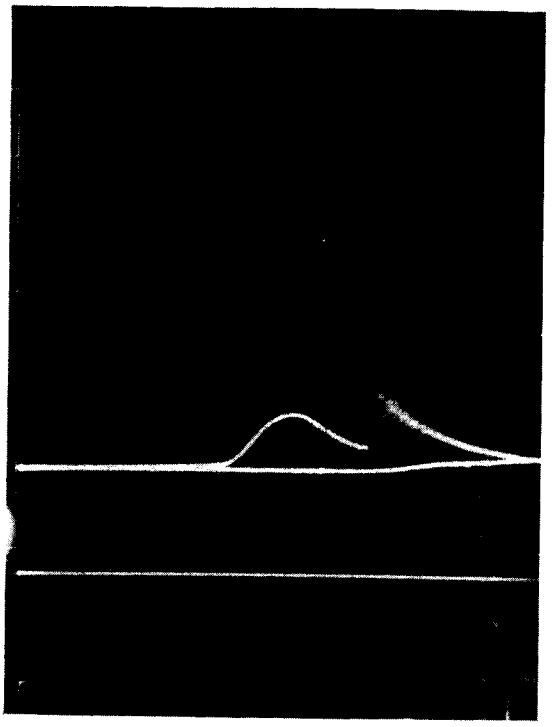

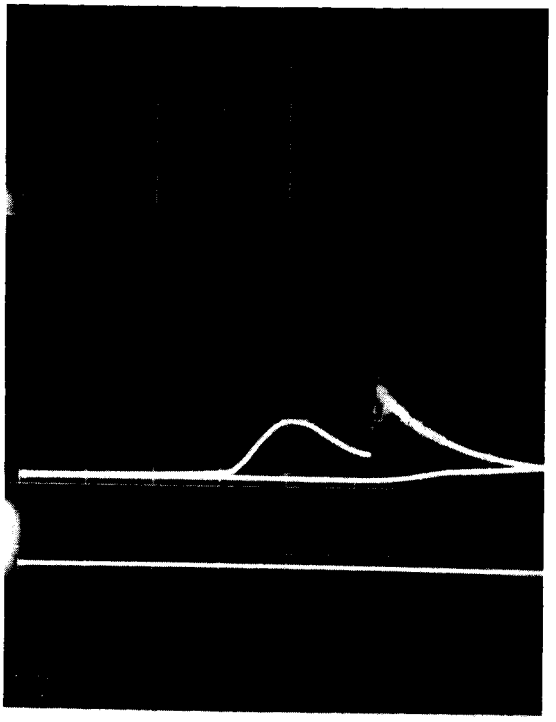

DATA POINT NO. 13

rpm = 6200

HP = 3.41

BMEP = 109 psi

O/F = 4.6

SPC = 2.8 lb/-P-hr

P_{0_i} = 1280 psi

P_{f_i} = 450 psi

P_{ex} = 1.1 psia

T_{ex} = 1040°F

DATA POINT NO. 14

rpm = 4900

HP = 3.48

BMEP = 140 psi

O/F = 4.6

SPC = 2.7 lb/-P-hr

P_{0_i} = 1290 psi

P_{f_i} = 410 psi

P_{ex} = 1.3 psia

T_{ex} = 1270°F

DISTRIBUTION

Copy No.	Transmitted to
1 to 9 and Reproducible.	NASA Manned Spacecraft Center Power Generation Branch, PPD 2101 Webster-Seabrook Road Houston, Texas 77058 Attn: Mr. C. D. Haines Contract NAS 9-857
10.	NASA Manned Spacecraft Center General Research Procurement Office 2101 Webster-Seabrook Road Houston, Texas 77058 Attn: Mr. John W. Twohig Contract NAS 9-857
11, 12.	NASA Headquarters Washington, D. C. 20546 Attn: Chief, Dynamic Systems, Code RNW Mr. Bernard Reznick
13, 14.	NASA Lewis Research Center 21000 Brookpark Road Cleveland, Ohio 44135 Attn: Solar and Chemical Power Branch Mr. Harry M. Cameron